NASA CR-
160457

PEP SOLAR ARRAY DEFINITION STUDY

FINAL TECHNICAL REPORT

31 DECEMBER 1979

NAS 9-15870

Prepared For
National Aeronautics and Space Administration
Lyndon B. Johnson Space Center
Houston, Texas

TRW

DEFENSE AND SPACE SYSTEMS GROUP

ONE SPACE PARK • REDONDO BEACH, CALIFORNIA 90278

PEP SOLAR ARRAY DEFINITION STUDY

FINAL TECHNICAL REPORT

31 DECEMBER 1979

TRW 35515-6001-RU-00

NAS 9-15870

DRL MA183TFA

Prepared For
National Aeronautics and Space Administration
Lyndon B. Johnson Space Center
Houston, Texas

By

TRW

DEFENSE AND SPACE SYSTEMS GROUP

ONE SPACE PARK • REDONDO BEACH, CALIFORNIA 90278

FOREWORD

This document is submitted in accordance with Article XI
of Contract NAS9-15870 and represents the deliverable under
Line Item 2 (MA183 TFA) of the Data Requirements List.

The data presented here completes the activities of Task 1
and ECP 1 under the Power Extension Package (PEP) Solar Array
Definition Study. Included are a system description, solar
array electrical design trades, a solar array mechanical design,
weight summary, loads and frequency analysis, a thermal analysis
summary, and results of the thermal cycling test on a solar cell
panel.

PEP SOLAR ARRAY DEFINITION STUDY

Final Technical Report

TABLE OF CONTENTS

TABLE OF CONTENTS - CONT.

TABLE OF CONTENTS - CONT.

PEP SOLAR ARRAY DEFINITION STUDY

Final Technical Report

LIST OF FIGURES

PEP SOLAR ARRAY DEFINITION STUDY

Final Technical Report

LIST OF TABLES

1.0 INTRODUCTION

This report presents the TRW conceptual design of a large, flexible, lightweight solar array that meets the requirements of the Power Extension Package (PEP) system. PEP is a proposed auxiliary power system for the Space Transportation System (STS) that will augment the power and permit longer duration missions of the Orbiter vehicle.

The conceptual design activity has focused on four major items in the design process. These are: 1) the solar array overview assessment, 2) the solar array blanket definition, 3) the structural-mechanical systems definition, and 4) the launch/re-entry blanket protection features. The overview assessment included a requirements and constraints review, the thermal environment assessment on the design selection, an evaluation of blanket integration sequence, a conceptual blanket/harness design, and a hot spot analysis considering the effects of shadowing and cell failures on overall array reliability. The solar array blanket definition included the substrate design, hinge designs and blanket/harness flexibility assessment. Also included in the blanket definition were solar cell trade studies, cover glass trade studies, solar cell layout evaluations and interconnector selection studies.

The structural/mechanical systems definition included an overall loads and deflection assessment, a frequency analysis of the deployed assembly and a components weights estimate. This task also included design of the blanket housing and definition of the blanket tensioning mechanism. The launch/re-entry blanket protection task included assessment of solar cell/ cover glass cushioning concepts during ascent and re-entry flight condition. An evaluation of stack height and container lid preload was made to determine clearances between adjacent panel solar cells in the stowed configuration. Excluded from the solar array design study was the deployment mast and canister, which were added to the PEP System contractor's responsibility.

A description of the PEP system and solar array requirements and interfaces is presented in Section 2. Discussions of the design trades and selection process for both the electrical and mechanical features of the solar array are presented in Section 3. The baseline PEP solar array design and an alternate configuration using large solar cells are summarized in Section 4. In addition to the solar array design tasks, effort was also devoted to definition of programmatic planning and costing activities. A program plan and manufacturing facility plan were written to develop, verify and deliver flight-qualified solar arrays. The estimated costs and risks for the selected designs are summarized in Reference 1.

2.0 PEP SYSTEM

2.1 System Description

The Power Extension Package (PEP) is a modular, photovoltaic, power package that is used on the Shuttle Orbiter vehicle to provide additional power and to permit longer duration missions. This added power and duration is only required for specific Orbiter missions, hence the package is designed for easy installation and removal from the cargo bay of the vehicle. Upon reaching orbit, the remote manipulator system (RMS) is used to extract the solar array module from the vehicle and orient it properly for deployment. Once the solar array is extended and aligned to the sun, it is ready for operational use to provide about 32 kilowatts of total power (BOL). A gimbal device and sun sensors are used to maintain the proper orientation of the solar cell panels relative to the sun vector. A harness attached to the RMS carries the power from the solar array to the cargo bay where it is regulated, processed, and distributed to the Orbiter load buses. Upon completion of the mission the array is folded back into its containers and restowed within Orbiter for return to earth.

Essential elements of the PEP system are illustrated in Figure 1. It consists of four assemblies; the ADA, the PRCA, the interface kit and the displays and controls. The Array Deployment Assembly (ADA) includes a core structure with special end fittings to attach to the Orbiter longerons, two lightweight, foldable solar array wings, two mast/canister deployment devices, two diode assembly interconnect boxes, a two-axis gimbal/slip ring assembly, and the canister support assembly. Each solar array wing consists of flexible, foldable blanket, a container box for the solar cell panel blanket, a blanket tensioning system and a guide wire system.

The Power Regulation and Control Assembly (PRCA) includes six pul e-width-modulated voltage regulators mounted to three cold plates, three shunt regulators and a power distribution and control box. All of these items are attached to a support structure which is mounted in the Orbiter cargo bay (Figure 2) and remains there during the operational phase of the mission.

POWER REGULATION/CONTROL ASSEMBLY

- REGULATORS, COLD PLATES
- POWER DISTRIBUTION
- SUPPORT STRUCTURE

DISPLAYS AND
CONTROLS

ARRAY DEPLOYMENT
ASSEMBLY

- ARRAYS
- ARRAY GIMBALS
- GIMBAL DRIVES
- SUN SENSOR
- INSTRUMENTATION
- MASTS

INTERFACE KIT

- RMS POWER CABLE
- ATTACHMENT FITTINGS
- ORBITER BAY PIPING
- ORBITER BAY WIRING

Figure 1. PEP System

-4-

ELECTRICAL HARNESSES
• POWER DISTRIBUTION
• INSTRUMENTATION
   AND CONTROL

POWER CABLE AND
RELEASE MECHANISM

MILTIPLEXER, DEMULTIPLEXER
AND CONTROL ASSEMBLY

DATA BUS COUPLER

VOLTAGE REGULATORS (6)

STRUCTURE
ASSEMBLY

POWER
DISTRIBUTION
BOX

SHUNT
REGULATORS
(3)

COLD-PLATE
ASSEMBLY (3)

PLUMBING
ASSEMBLY

Figure 2.   Power Regulation and Control Assembly

-5-

The PEP interface kit consists of a power cable that is attached to the RMS, electrical harnesses and a data bus cable that mates the PRCA and the Orbiter, and the structural attachment fittings and latches that connect the ADA and PRCA to the Orbiter longerons. Figure 3 illustrates the location and elements of the PEP interface kit. The final group of PEP hardware consists of the avionics equipment which is partly in the ADA and PRCA, and partly in the Orbiter crew compartment on the aft flight deck. These include the sun sensor, sensor processor and array pointing and control electronic assembly on the ADA; the multiplexer/demultiplexer (MDM) and data bus couplers on the PRCA; and the multifunction CRT display system (MCDS), the systems management computer, switch box and standard switch panel on the Orbiter aft flight deck. Key elements of the avionics assembly are schematically shown in Figure 4. The entire PEP system in the stowed configuration for launch or re-entry flight conditions is illustrated in Figure 5. Information on the PEP system was provided by the System Study Contractor in References 2 and 3.

2.2 Solar Array Requirements

The conceptual design of a PEP solar array must initially evolve from a general set of requirements, hence at the beginning of this study the requirements as listed in Table 1 were used. These requirements were jointly formulated by the System Study Contractor and JSC. Since it is recognized that the requirements are derived by a combination of factors, not all of which are technical, this initial set of requirements was considered preliminary and subject to change as the solar array design evolved.

Only a limited number of the requirements, however, have a direct impact on the design. The orbital altitude and inclination have a strong affect on the thermal and radiation environments and the total number of thermal cycles. These in turn have a direct bearing on the selection of solar cell type and interconnectors. The electrical power requirement affects the choice of solar cell and the size of the array. The array voltage and modularity requirements affect the number of cells and panels in series and the power harness design. The total power requirements were
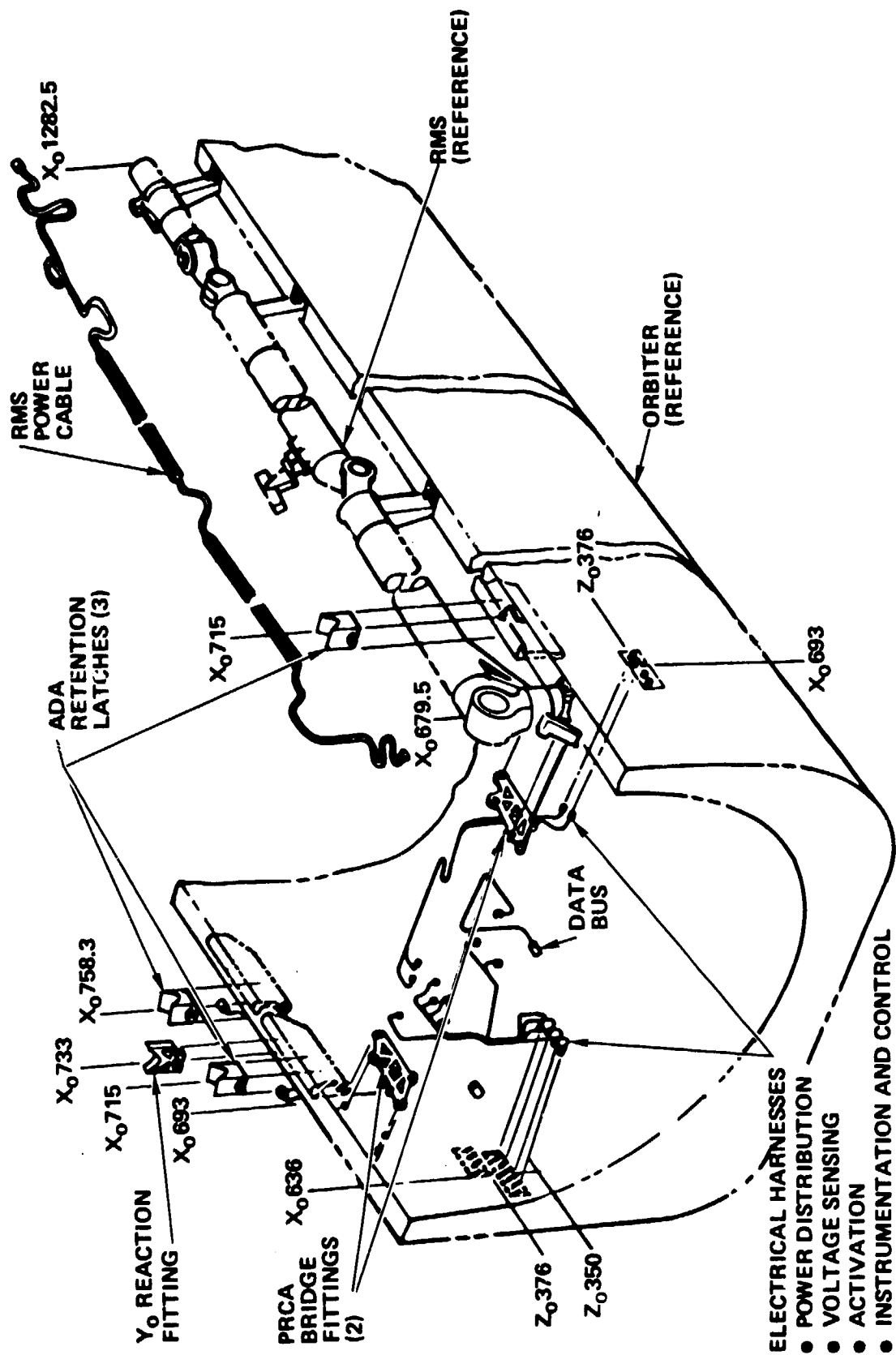
Figure 3. PEP Interface Kit
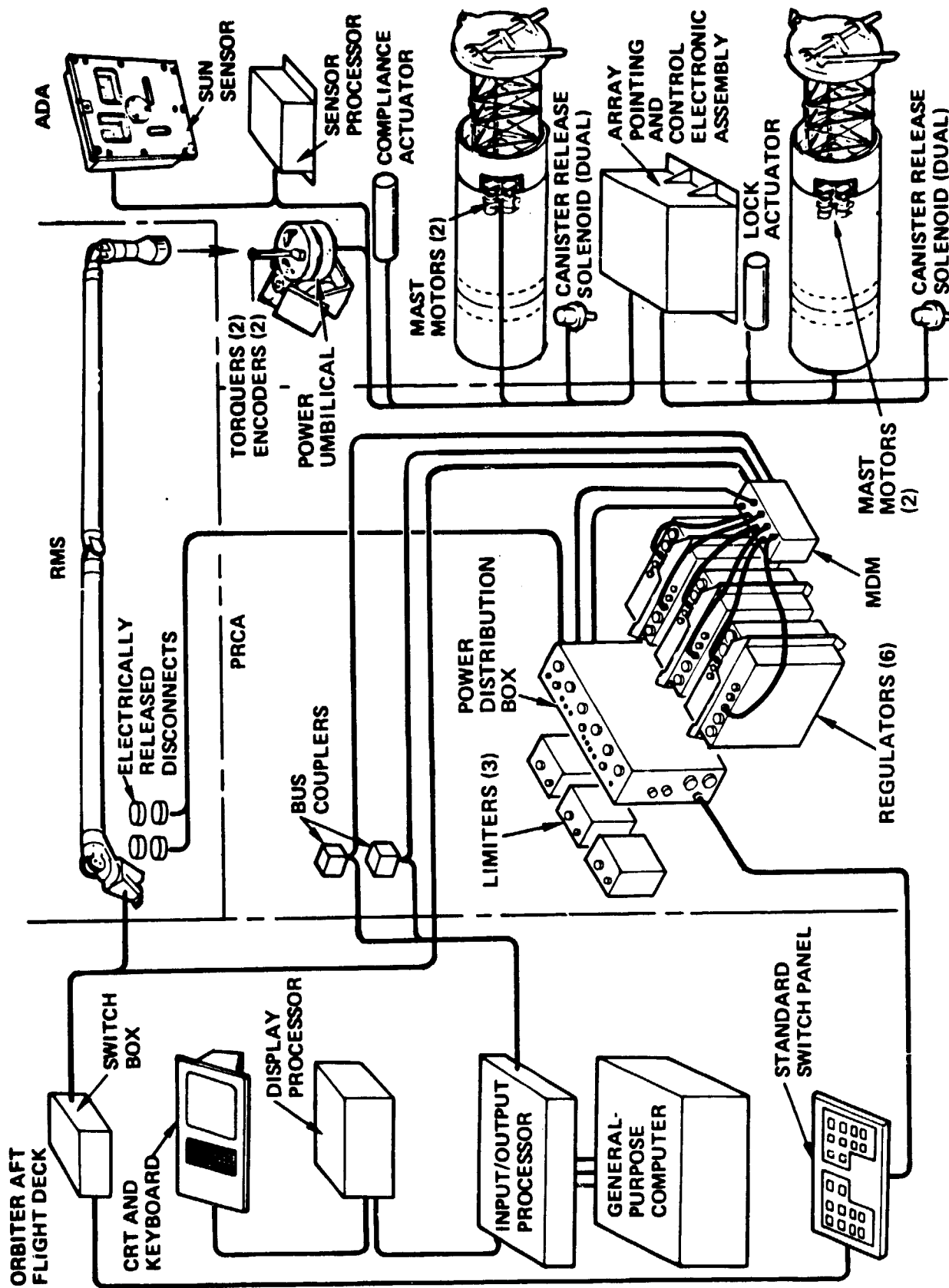
Figure 4. PEP Avionics Components

ARRAY DEPLOYMENT ASSEMBLY

POWER REGULATION & CONTROL ASSEMBLY

FWD
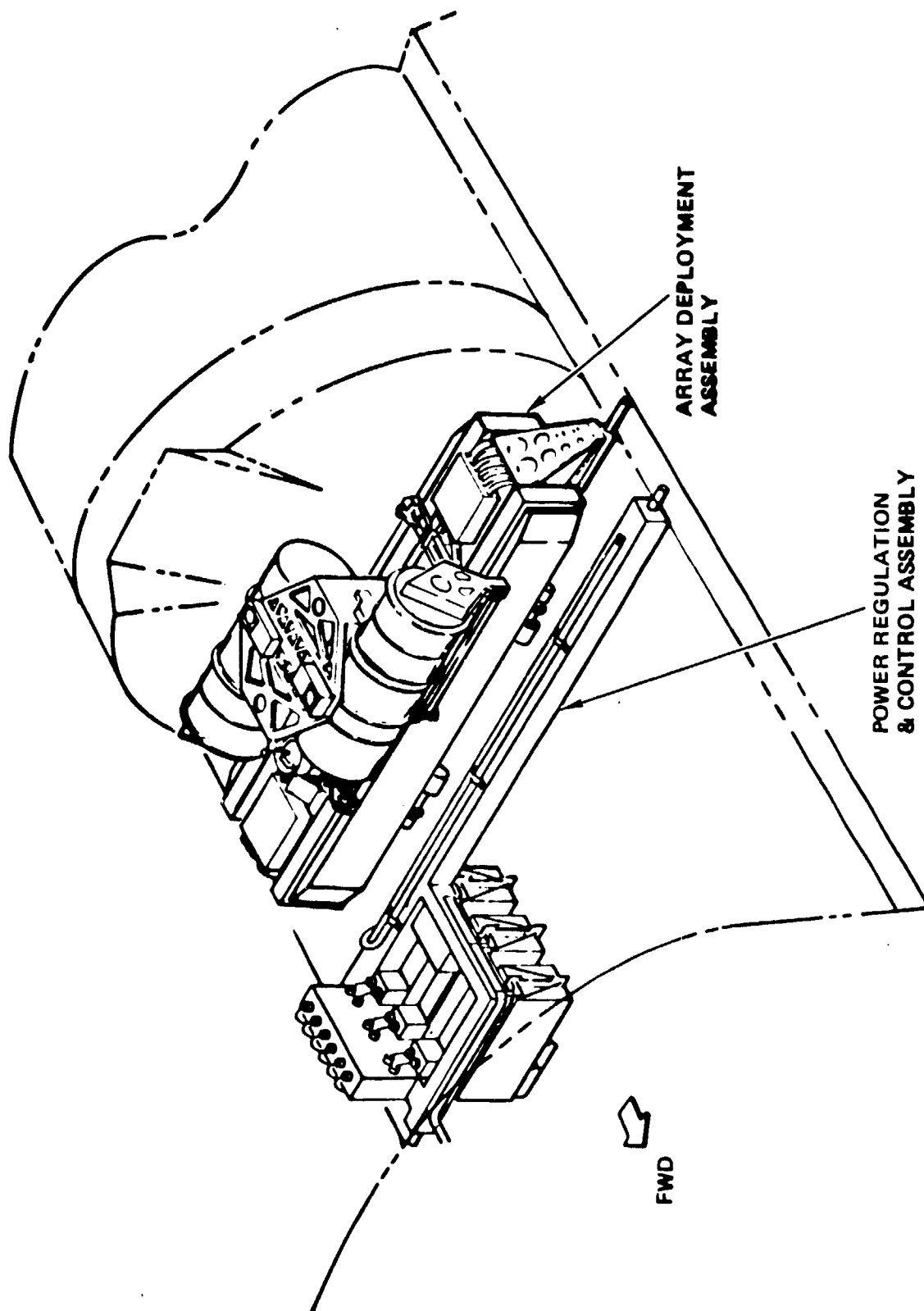
Figure 5. PEP System Stowed in Orbiter

-9-

Table 1. PEP Solar Array Design Requirements

DESIGN PARAMETER	CURRENT BASELINE		ALTERNATES/REMARKS
	NOMINAL	RANGE	
1. APPLICATION/MISSION REQTS.			
1.1 ORBITAL ALTITUDE (KM) (NMI)	407 (220)	185-1111 (100-600)	
1.2 ORBIT INCLINATION, DEG.	28.5 55.0 90-105	28.5-104	ETR MISSIONS - 78% ETR MISSIONS - 22% WTR MISSIONS - 100%
1.3 SOLAR VECTOR/ORBIT PLANE ANGLE (B), DEG.	50	±127.5	
1.4 ARRAY SHADOWING	NO	OCCASIONAL	DUE TO ORBIT, RMS, PAYLOAD. SHADOWS OCCUR AT ORBITAL RATES (~ 4 DEG'MIN.)
1.5 ARRAY ORIENTATION	NORMAL TO SOLAR VECTOR	ALL ATTITUDES	
1.6 LAUNCH VEHICLE	SHUTTLE ORBITER		MUST BE COMPATIBLE WITH ANY LOCATION IN PAYLOAD BAY TO STA. 1180
2. SYSTEM PERFORMANCE AND DESIGN REQTS. PER EACH OF TWO WINGS			
2.1 OUTPUT POWER-KW BOL EOL	16.4 DEFINE		AT ARRAY/PEP INTERFACE UNDER NOMINAL CONDITIONS (B = 50°)

Table 1. PEP Solar Array Design Requirements (cont'd)

DESIGN PARAMETER	CURRENT BASELINE		ALTERNATES/REMARKS
	NOMINAL	RANGE	
2.2 BOL OUTPUT VOLTAGE			
V_{MP} VOLTS	125	100-125	
V_{OC} VOLTS	<250		
2.3 BOL OUTPUT CURRENT		131-164	FOR REFERENCE ONLY; UNDER NOMINAL CONDITIONS
I_{MP} AMPS			
I_{SC} AMPS	>1.1 I_{MP}		
2.4 OPERATIONAL USAGE			
2.4.1 TIME PERIOD-YRS	10		
2.4.2 MISSION FREQUENCY	8 PER YEAR		
2.4.3 MISSION DURATION, DAYS	14	7-48	
2.4.4 DEPLOY/RETRACT CYCLES			
ON-ORBIT	?		
ON GROUND	CONTRACTOR DEFINE		
2.4.5 STORAGE TIME			
ON-ORBIT-YRS	3.07		
PAYLOAD BAY-KSC-HRS	50		
VAB-HRS	960		
OTHER-YRS	7		
STORAGE-YRS	7		
3. ENVELOPE CONSTRAINTS			
3.1 CONTAINER			
LENGTH - M (IN)	3.88 (152.8)		LOCAL WIDTH AND DEPTH FOR ATTACHMENTS AND LINKAGES EXTEND ENVELOPE TO 20.5 IN (WIDTH) AND 20 IN (DEPTH)
WIDTH - M (IN)	.43 (17)		
DEPTH - M (IN)	.30 (12)		
3.2 DEPLOYED LENGTH M (IN)	38.1 (1500)		

Table 1. PEP Solar Array Design Requirements (cont'd)

DESIGN PARAMETER	CURRENT BASELINE		ALTERNATES/REMARKS
	NOMINAL	RANGE	
4.0 LOADS AND STIFFNESS			
4.1 STRUCTURAL LOADS	PEP ENVIR.SPEC		
4.2 BLANKET TENSION - LBS	20		FULLY DEPLOYED ONLY
4.3 GUIDE WIRE TENSION - LBS	2		
4.4 MINIMUM FREQ. - HZ	.088		FIRST FREQ. OF MAST AND BLANKET ABOVE ISOLATION FREQUENCY
5.0 MASS PROPERTIES PER WING WING BOX/BLANKET KG(LBS)	164(361)		GOALS (MAST/CANISTER NOT INCLUDED)
6.0 RELIABILITY A. ORBITER/CREW SAFETY	0.9999		
B. RETURN FROM ORBIT	TBD		
C. MISSION COMP.	TBD		

initially specified only for beginning of life (BOL) but late in the
design phase, an end of life (EOL) power requirement was also defined.
Therefore, the selection of solar cell type was based on the BOL power
requirements; however, once the EOL requirement is specified for worst
case altitude and orbit inclination then trade studies considering radiation
degradation and solar cell efficiency would be performed to ensure that
the initial selection is still valid.

The envelope dimensions and weight allowance have a direct impact
on the solar panel size and the materials selection used throughout the
design. The envelope requirements are discussed in more detail in Section
2.4. It should be noted that the deployment/retraction device was not
included as a part of the solar array in the TRW definition study. It
was included as part of the system contractor's responsibility, hence the
discussions on requirements do not address this item. If a subsequent
phase of study or development should make this a part of the solar array
then requirements related to structural rigidity, extension and retraction
rates, and mast design loads would also become important.

2.3 PEP Power System - Solar Array Interfaces

The electrical and mechanical interfaces between the solar array and
the other PEP system hardware are illustrated in Figure 6. The array
blanket box assembly bolts to the ADA core structure at four locations
for each wing. There is one additional mechanical interface at the upper
end of the blanket where a linkage attaches to the tip fitting on the
deployment mast. The electrical interfaces are at the connector boxes
in the bottom, outboard ends of the blanket box assembly. The power
harnesses from the blanket and all instrumentation leads terminate at
these connector boxes. The system contractor supplies a harness from the
diode assembly to the solar array connector box.

2.4 Wing Container Envelope

The envelope available for the PEP solar array is determined from a
combination of constraints arising from Orbiter payloads, PEP system design
features and the solar array configuration. Assuming the Spacelab mission
is the most confining on available space, and working from preliminary
configurations of the ADA structure, the envelope presented in Figure 7
was allocated to the blanket container assembly for each wing in the PEP

-13-

DIODE ASSEMBLY

ARRAY BLANKET BOX ASSEMBLY

DIODE ASSEMBLY

CORE STRUCTURE

ELECTRICAL INTERFACES (2 PLACES/WING)

MECHANICAL INTERFACE (4 PLACES/WING)

MECHANICAL INTERFACE

ARRAY BLANKET BOX ASSEMBLY
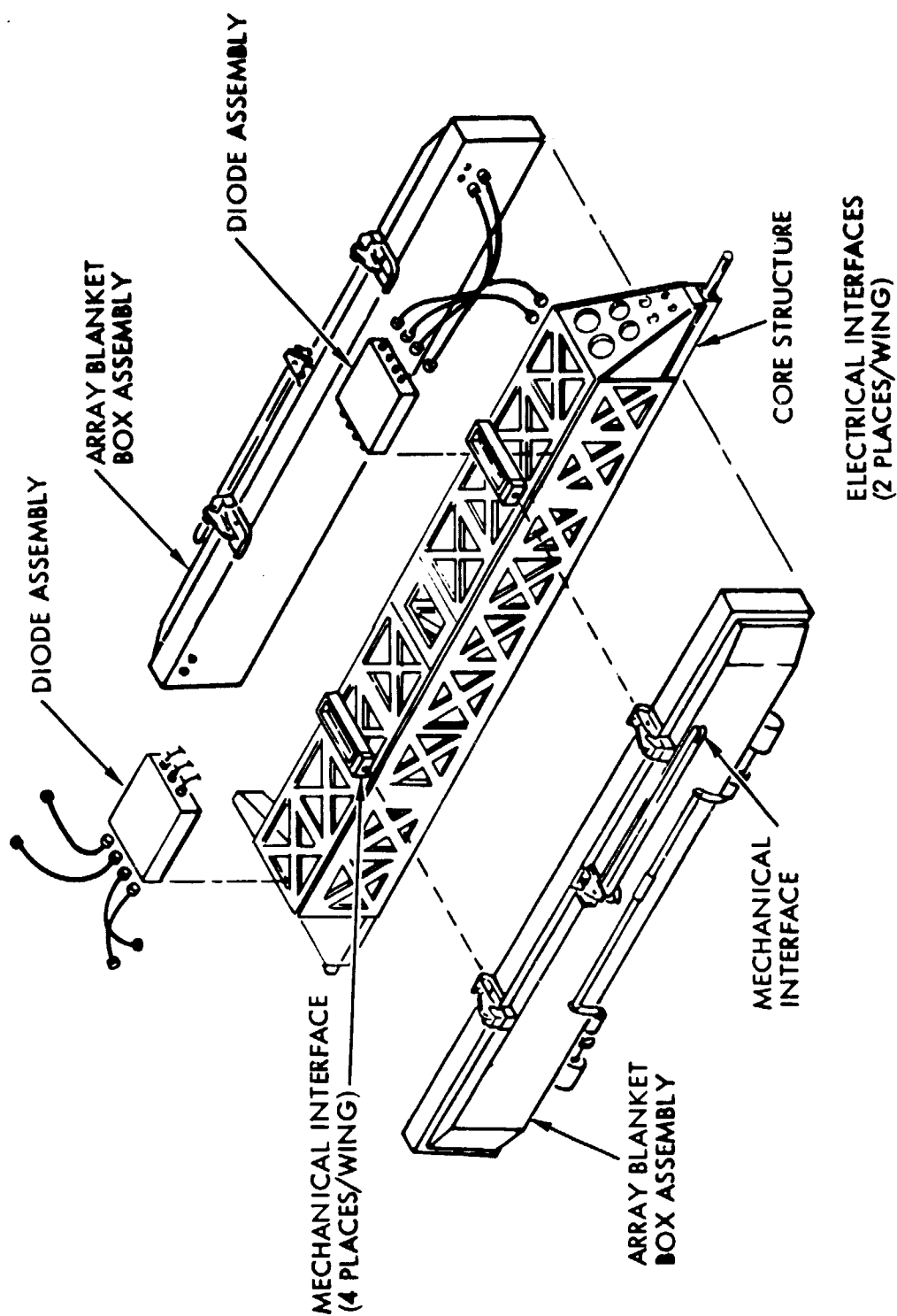
Figure 6. PEP System – Solar Array Interfaces

-14-

system. The principal dimensions are 3.88 meters (152.8 inches) in length, 0.43 meter (17 inches) wide, and approximately 0.30 meter (12 inches) in depth. These dimensions are considered applicable to the overall size of the wing container. By making appropriate allowances for the container structure and blanket restowing rattle space, the resulting dimensions dictate the solar cell panel size.

It is recognized that the volume available for the PEP system will permit some local protrusions of this volume. As the container latch mechanism and blanket tensioning mechanism designs evolve, revisions to the envelope may be required.

Figure 7. Solar Array Wing Envelope

UNITS: Inches

* 17.0 APPLIES TO ARRAY BOX. A LIP FLARE
  NOT TO EXCEED 0.25 PROTUSION MAY BE ADDED
Ⓐ INTERFACE WITH PEP STRONGBACK STRUCTURE
Ⓑ INTERFACE WITH MAST CANISTER EXTENSION LINK

3.0 DESIGN DEFINITION

3.1 General

The conceptual design of a large, lightweight, flexible solar array
requires an interaction of the electrical and mechanical features to
evolve a viable, cost effective configuration. To ensure that an inte-
grated design philosophy was used during the Phase B effort, a preferred
design approach was initially assumed and key design issues were addressed
before the trade studies were started. A discussion of these items is
presented in the following sections. An outline of the baseline and
alternate design configurations is then presented and the design de-
finition concludes with the in-depth discussions of the electrical and
mechanical trade studies.

3.1.1 Design Approach

The PEP Solar Array design and performance requirements are new
and unique with respect to existing solar array designs in several ways:
the BOL power level of 32.8 Kw and the specific power of 60-70 W/Kg at
BOL is significantly greater than those of any other array hardware design;
the array will be launched and returned to earth on a fairly periodic
basis; and the array will be used on a man-rated system, but can be re-
paired after returning from relatively short term space missions.

Investigations have shown that these new and unique requirements
could be met by either one of two approaches: one utilizing revolutionary
new (to the array industry) approaches, or evolutionary approaches that
are building on existing and proven technologies. Trade studies, however,
revealed that the remaining hardware acquisition and life cycle mainten-
ance costs for either approach could be identical, so that only initial
development cost and schedule risks are decision drivers. Therefore, TRW
has selected the much lower risk evolutionary approach to its version of
the PEP array design.

A major consideration in the design implemen tion has been the need
for automated array assembly operations. Even if large 5 x 5 or 6 x 6 cm
size solar cells were to be used instead of the more standard 2 x 4 cm

cells, the total number of parts to be handled and assembled would be a cost driver that mandates automated assembly processes.

In consideration of these factors, the principal approach selected by TRW for the PEP design is to make maximum use of existing flight-type hardware and to use existing manufacturing processes wherever possible. It is felt that the power level and performance requirements of PEP are so different from state-of-the-art arrays that the risks associated with scaling up to the large system should not be compounded by adding in new technology items unless it is absolutely necessary. Hence the baseline design will select, if possible, flight-proven type solar cells, cover glasses, and interconnectors in order to minimize performance and schedule risks. In addition, the solar cell sizes and cell stack processes will be selected to minimize risk and make maximum us   TRW's existing automated assembly line. By necessity the blanket substrate design will be new technology in order to meet the program weight goals; however, the substrate designs will be made compatible with the   mated assembly line.

Another fundamental approach is to make the PEP design sufficiently flexible to accommodate alternate lower cost approaches and new technologies if they should evolve within the PEP development phase. The large solar cell is one possible candidate in this category and the impact on the baseline design is assessed in the solar array design definition. A detail risk/cost trade study would be made before a new technology item would be selected over an existing, flight-proven element. Finally it should be noted that the TRW baseline design approach is to meet all the stated PEP requirements and to give top priority to crew safety. This is consistent with the system study contractor philosophy and is followed throughout the solar array trade studies.

3.1.2 Major Development Issues

The principal development issues seen for the PEP solar array design are summarized in Figure 8. The number one item is the solar cell selection and the issues related to cost, weight and solar array size. The solar cell protection feature during the launch and reentry environments is a second major item in recognition of the cell fragility and the compact storage requirements. The unique requirement to return the blanket to earth means

-18-

ITEM	ISSUES
SOLAR CELL SELECTION	• LOW COST • HIGH W/KG PERFORMANCE • BLANKET/MAST LENGTH
SOLAR CELL CUSHIONING	• CELL FRAGILITY • BLANKET SLIPPAGE
BLANKET RESTOWAGE	• PANEL STIFFNESS • THERMAL DISTORTIONS • DYNAMIC MOTION
HARNESS DESIGN	• LOW COST • LOW MASS • FLEXIBILITY AND FATIGUE
MANUFACTURING PROCESSES	• RISK AND COST OF NEW APPROACHES

Figure 8. Key Development Issues

that it must refold and restow in the container in a positive and reliable manner. To achieve this, the blanket without the tension pre-load must have inherent stiffness and be under control during dynamic and thermal environments. Another potential major problem item is the solar array harness. The harness will run the length of the blanket and therefore must have flexibility and low mass like other blanket components. It is desired to have the harness folded stack height less than the blanket height and to have a high fatigue resistance to survive the many folding and unfolding operations. The final potential development issue is the manufacturing processes required for the PEP solar array. It is antici-pated that significant risks and costs are associated with the substrate manufacturing, hence early confirmation of their producibility should be demonstrated.

3.1.3 Solar Array Elements for Definition Study

The solar arrays are a part of the PEP system as described in Section 2.1. The elements that make up the solar array are dependent upon the interface definition between the system and solar array contractor's hard-ware. For the purpose of this study, the deployment/retraction device of the solar array blankets relative to the blanket container is included on the system contractor's side of the interface. Therefore the items that make up the solar array are as follows:

- Blanket
  - Solar Cells, Covers and Interconnects
  - Substrate
  - Hinges
  - Harness

- Blanket Housing
  - Container and Lid
  - Lid Latching Mechanism
  - Blanket Tension Mechanism
  - Guide Wire System

- Spreader Bar and Linkage

These elements are illustrated for a partially-deployed wing in Figure 9 and in Figure 10 for the fully deployed wing with the extendable mast. The blanket overall length is 36.98 meters (1456 inches), consisting of 102 solar cell panels and a substrate leader at the forward and aft ends. Each panel is 3.81 meters (150 inches) long and .36 meters (14 inches) wide. Details of the electrical and mechanical design features and the rationale for the selection are covered in the next two sections.

3.2 Solar Array Electrical Design

3.2.1 Solar Array Sizing

Preliminary trade-offs indicated the desirability of minimizing the blanket length and mass, for given stowage volume constraints. Thus the highest practical cell output per unit blanket area, i.e., the highest practical in-orbit cell efficiency was baselined as described in Section 3.2.5. Figure 11 illustrates the impact on array system power output (for a fixed number of panels per wing) as the cell efficiency is varied. Figure 11 also shows how the number of required active panels per wing for constant array output (32.8 Kw)varies as a function of cell efficiency. For example, a change from the baselined 14% cell to a more commonly used 12.8% cell would increase the number of panels from 102 to 112. This 10% increase in the number panels is equivalent to a 140 inch (11.7 feet) increase in mast length and about 65 lb increase in the weight for two blankets (weights are summarized in Figure 39).

The overall solar array is sized to meet the specified 32.8 Kw BOL power output requirement. The array is composed of two wings and each wing is assembled from a group of identical panels. The panel geometry is sized on the basis of the available envelope with appropriate allowances for container, hinge, and rattle space. Once the panel size is established and the solar cell arrangement per panel is formulated then the power for each can be determined. The appropriate number of panels are then selected to meet the wing power output requirements. There are no other inherent panel or array limitations which constrain the array size. A larger or smaller number of panels may be assembled into the blankets. Solar cell sizes may be varied to make the panel output voltage a desirable fraction of the bus voltage, and to maximize the packing density of the cells on

-21-
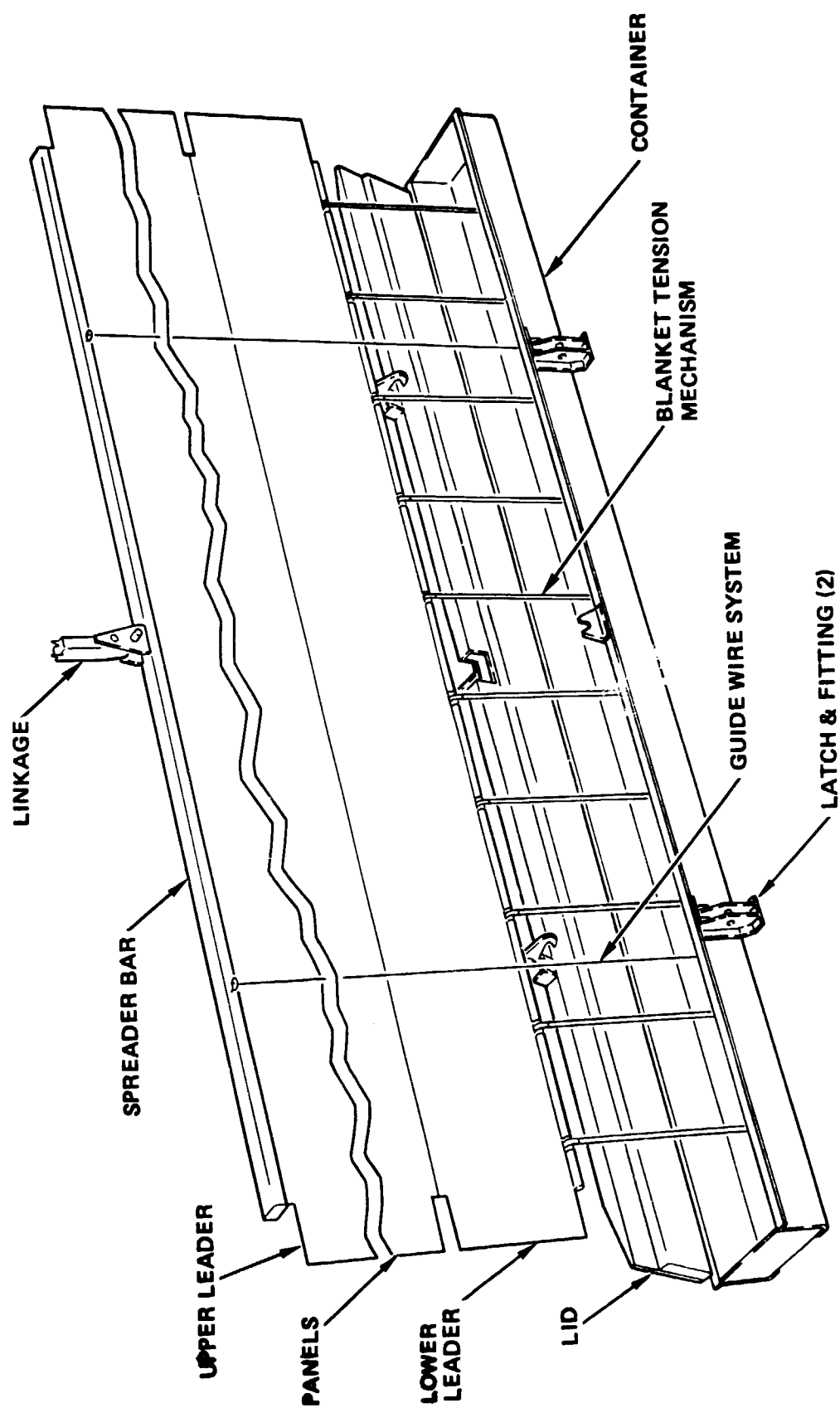
Figure 9. PEP Solar Array - Partially Deployed

BLANKET HOUSING

EXTENDABLE MAST

1453.00"

150.00"

150.00"

137.60"

14.00"

ARRAY PANEL (CELL SIDE)
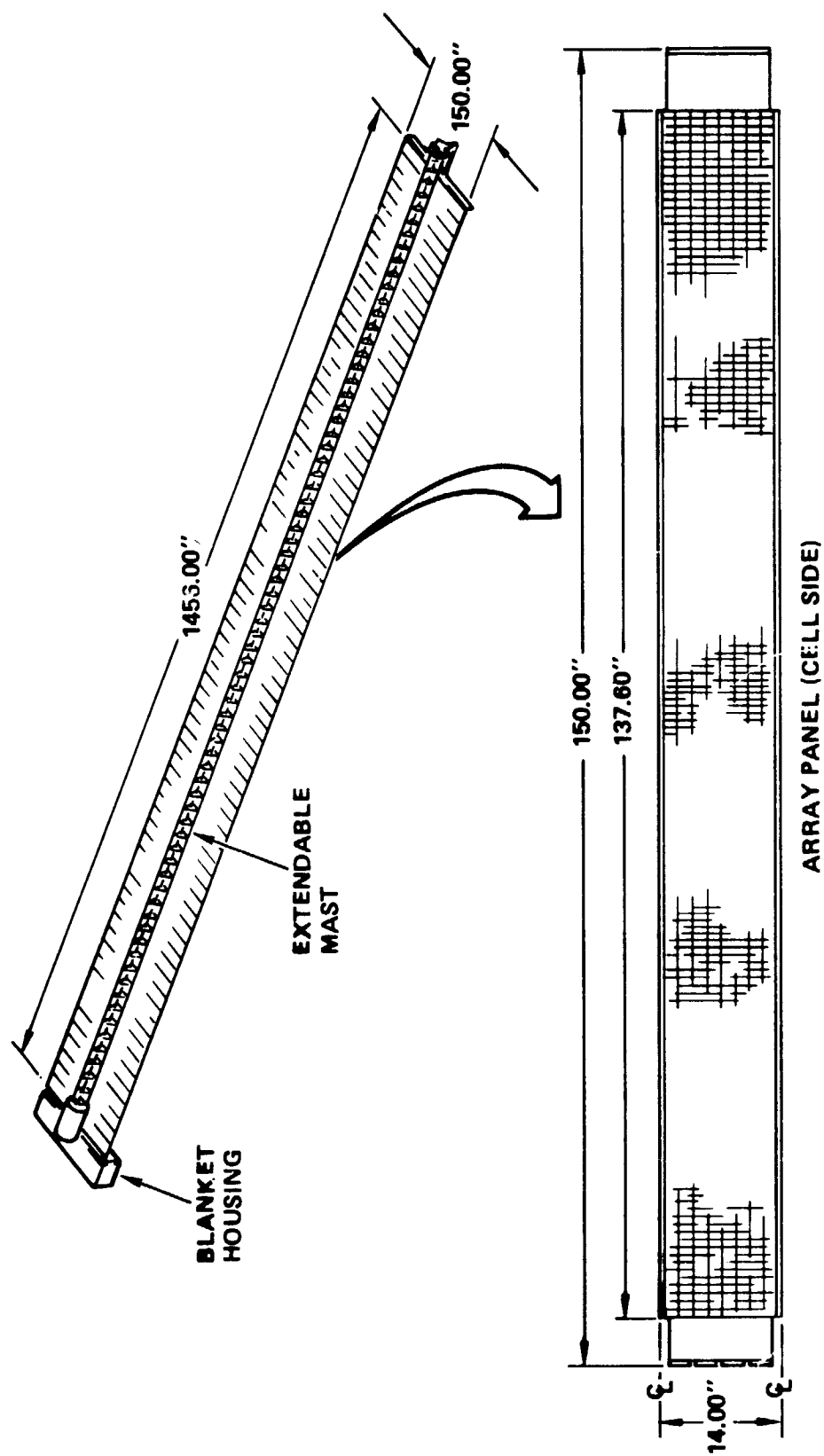
Figure 10. PEP Baseline Solar Array - Fully Deployed
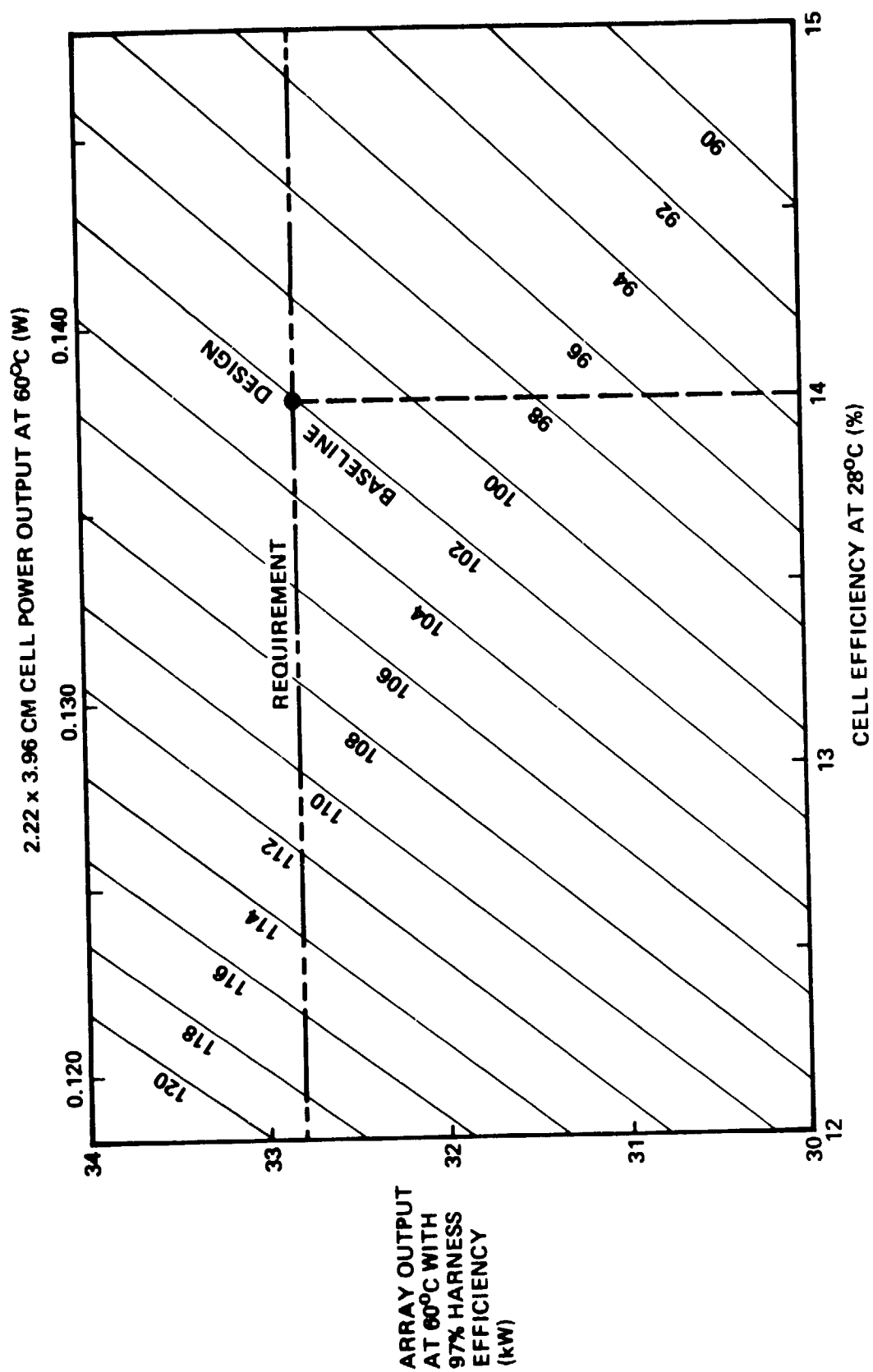
Figure 11. Solar Array Sizing

the panel. The solar cell efficiency determines the power output per
panel and the number of required panels is readily adjustable to ac-
commodate cells of any efficiency. Other factors such as cost and weight
become important as solar cell efficiencies vary.

3.2.2 Array Performance

Each of the two wings of the baseline solar array system is comprised
of 102 active solar cell panels. Each panel carries 1,200 solar cells
of 2.22 x 3.96 cm size and produces an output of 165.5W at 63V at 60°C,
nominally. Panels are series-connected in pairs into electrical modules
to produce a nominal bus voltage of 126V at the module level, and 122 V
at the wing output connector. Each wing (122,400 solar cells) produces
16.4 KW, and the array provides 32.8 KW, at 60°C operating temperature,
at beginning of life (BOL), at the array output connectors.

The alternate array design uses 100 active panels per wing (36,000
cells). Each panel carries 360 cells of 5.7 x 5.3 cm size. Panels, pro-
ducing 25V output nominally, are connected into modules in groups of five
for 122 V nominal bus voltage and 32.8 KW array power output at the array
output connectors.

The mechanical design details for both the 2.22 x 3.96 cm cell base-
line and the 5.7 x 5.3 cm cell alternate wing designs are summarized in
Table 2. The corresponding electrical performance details are given in
Table 3.

3.2.3 Solar Cell Layout Design Trades

Solar cell circuit can be layed out on the panel in essentially two
different ways as illustrated in Figure 12. In the upper view, rectan-
gular cells are shown positioned on the panel with their long dimension
parallel to the hinge line, while in the lower view they are positioned
perpendicular to the hinge line. In the first case, the string of cells
"snakes" up and down from the left toward the right, while in the latter
case the strings reach from panel end to panel end. Similar layouts are
also possible with the larger solar cells. With either approach, suscepti-
bility to hot spot effects can be reduced and magnetic field cancellation
can be achieved. Because of somewhat lower manufacturing complexity and
slightly higher solar cell packing density, the selected approach depicted
in the lower view was selected. A summary of the design features for the

-25-

| | WING CONFIGURATION | |
PARAMETERS	2.22 x 3.96 CM SOLAR CELL	5.70 x 5.30 CM SOLAR CELL
PANEL WIDTH – IN. ($\mathrm{\mathcal{C}}$ TO $\mathrm{\mathcal{C}}$)	14.00	14.00
PANEL LENGTH – IN.	150.00	150.00
NO. OF PANELS	102	100
NO. OF LEADERS	2	2
BLANKET LENGTH – IN.	1456.00	1428.00
CELL THICKNESS – MILS	8	8
COVER THICKNESS – MILS	6	6
NO. OF CELL/PANEL	1200	360
TOTAL NO. OF CELLS (10^3)	122.4	36.0
WEIGHT (LBS)	355	357

Table 2. Wing Design - Solar Cell Comparison

LEVEL	TEMPERATURE (°C)	LOSS	VOLTAGE (V)	POWER* 2.22 x 3.96	POWER* 5.7 x 5.3
CELL	28	1.00	0.485	0.166W	0.570W
	60	1.00	0.419	0.138W	0.470W
PANEL	60	1.00	63 (25)	165.5W	169.0W
MODULE	60	1.00	126	331W	845W
	60	0.97	122	321W	820W
WING	60	0.97	122	16.4 KW	
ARRAY	60	0.97	122	32.8 KW	

*14% CELL AT 28°C

Table 3. Array Electrical Performance - Beginning of Life
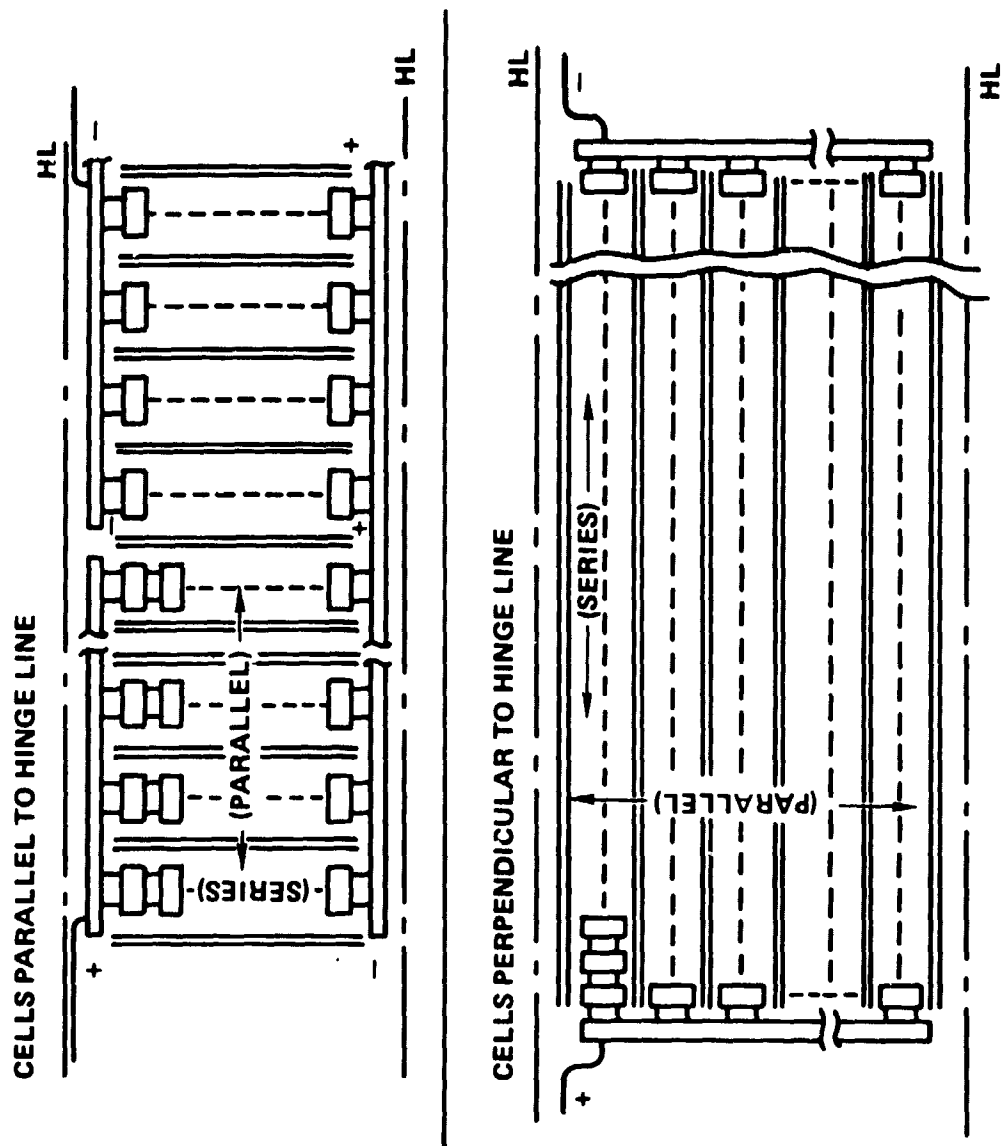
Figure 12. Solar Cell Layout Trade Study

baseline configuration using 2.22 x 3.96 cm cells and an alternate configuration using 5.7 x 5.3 cm cells is presented in Figure 13.

3.2.4   Reliability and Hot Spot Considerations

There are several unique solar array design requirements to be met by the PEP array that have heretofore not been encountered:

- The array produces relatively high output voltage (100-150 V) and is subject to shadowing, making the hot spot phenomenon more critical.

- The thin Kapton solar cell substrate possesses negligible lateral heat conduction capability, thereby amplifying the array's susceptibility to hot spot effects.

- The solar cells, interconnectors, and interconnector-to-cell joints will be exposed repeatedly to vibrational and other mechanical loads after increasing accumulated thermal cycling exposure.

Recoganizing that the PEP array is designed for Sortie missions and that the power is not essential to crew safety, the opportunity exists to provide a low cost design that could be inspected and repaired as needed between missions. However when considerations for operational costs are included it is not deemed practical for economic reasons to perform extensive rework after each mission. Therefore, the selected approach for the array is to possess inherently high reliability and longevity, requiring little rework after a number of missions. This approach encompasses the number of cells connected in parallel, the cell-to-substrate mounting technique, the interconnector design, and the cell cushioning concept. Related to it also are the interconnector-to-cell joining method, and the solar cell size selection.

For given array shadowing patterns and other constraints, the number of cells connected in parallel determines the severity of hot spot effects. Generally, hot spot effects are minimized by either utilizing single-cell strings ("one cell in parallel"), or by connecting many cells in parallel. Extrapolation of the data generated for the Skylab Orbital Workshop solar array system indicated, however, that single-cell strings would be ruled

-29-

PARAMETER	BASELINE	ALTERNATE	RATIONALE
(SOLAR CELL SIZE)	(2.22 x 3.96 CM)	(5.70 x 5.30 CM)	(REFERENCE)
NUMBER OF CELLS IN PARALLEL	8 PER PANEL	6 PER PANEL	• MINIMIZES HOT SPOT EFFECTS
NUMBER OF CELLS IN SERIES	150 PER PANEL	60 PER PANEL	• MAXIMIZES CELL PACKING DENSITY
PANEL VOLTAGE	63 V	25 V	• PROPER FRACTION OF BUS VOLTAGE
NUMBER OF PANELS PER MODULE	2	5	• 125 V BUS VOLTAGE
NUMBER OF MODULES PER BLANKET	51	20	HIGHER CELL PACKING DENSITY OF LARGER (ALTERNATE) CELLS REDUCES BLANKET SIZE
NUMBER OF PANELS PER BLANKET	102	100	
CURRENT ROUTING	COUNTER FLOW	COUNTER FLOW	• MAGNETIC TORQUE CANCELLATION

Figure 13. Design Summary Solar Cell Layout

out for PEP due to the higher operating voltage. However, connecting 8 cells in parallel, in an arrangement as shown in Option B in Figure 14 would result in acceptable hot spot conditions of not more than 17 volts reverse bias and 170°C worst-case cell temperature. The assumed, hypothetical shadowing condition for this case was that cells would be shadowed by sharply defined shadows that would not permit the sharing of reverse bias and power dissipation that actually occurs with more diffuse shadow patterns that are caused by opaque objects that are several meters away from the solar cells. The estimated, hypothetical worst-case temperature of 170°C is sufficiently removed from the 183°C solder melting temperature so that hot spot effects do not mandate welded interconnectors.

Hot spot conditions can not only be caused by array shadowing, but also by broken solar cells and by failed interconnector/solar cell joints. Figure 15 identifies a number of such failures as they relate to various environmental stresses. Figure 16 illustrate a few key failure modes and their effect on array output for the baseline solar cell design.

3.2.5 Solar Cell Trade Studies

3.2.5.1 Design Constraints

The quantity, thickness and efficiency of the selected solar cell type has a significant impact on the blanket and mast lengths and on the array system weight. Primarily to minimize adverse impacts on the overall orbiter/RMS/array dynamics, solar cells were selected having the highest practical operating efficiency that can be expected to be in production at the space solar cell vendors by 1980/81.

The relationship between the number of panels required per wing (for constant array output) and the solar cell efficiency (at 28°C) is illustrated in Figure 11. An array, using the highest achievable cell efficiency without a P^+ field structure of approximately 12.8%, would require 112 panels per wing, thereby increasing the blanket and mast lengths by 140 inches (11.7 feet of 3.56 m) over the baseline wing of 102 panels.

SELECTED DESIGN

• SURVIVES SOLDER MELTING AT 183°C

• LOWER COST THAN TYPE C

ESTIMATED WORST-CASE HOT-SPOT*

	VOLTAGE (V)	POWER (W)	TEMPERATURE (°C)
A	30	5	270
B	17	2	170
C	10	2	170
D	28	9	340
E	22	9	340

OPTION

S = 1 2 3 4 5 6 7 8 9 10 11 12 13 14 300

TYPICAL SOLAR CELL

TYPICAL SHUNT DIODE
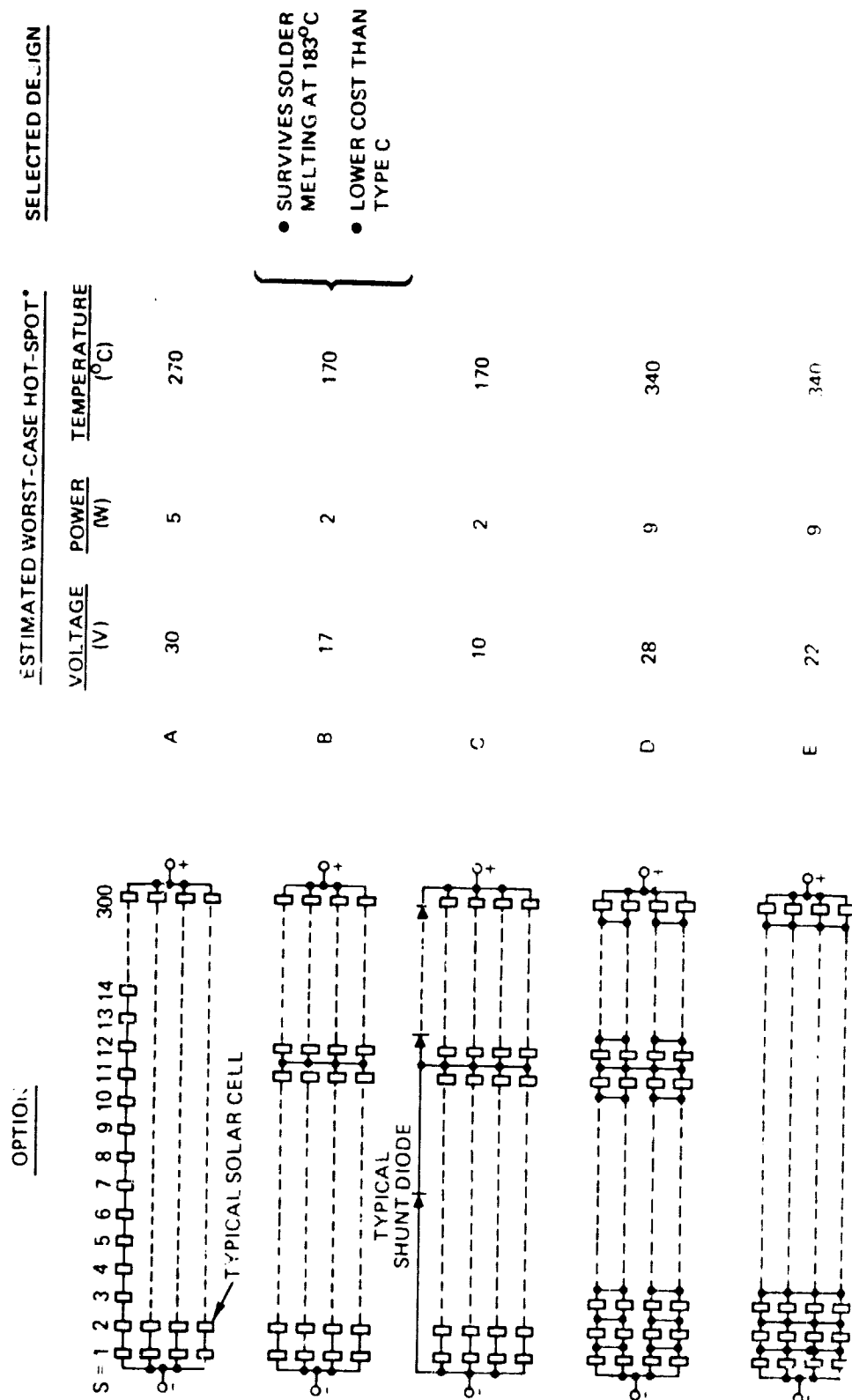
*EXTRAPOLATED FROM SKYLAB ORBITAL WORKSHOP SOLAR ARRAY SYSTEM Z-LOCAL VERTICAL STUDY

Figure 14. Cell Layout/Hot Spot Trade Study

ENVIRONMENT	SOLAR CELL	CELL/INTERCONNECT JOINT	INTERCONNECTOR LOOPS
TEMPERATURE CYCLING	PROPAGATION OF CRACKS (WELDED)	FATIGUE CRACKING	FATIGUE CRACKING
VIBRATION, ACOUSTIC, SHOCK	PROPAGATION OF CRACKS (WELDED)	FATIGUE CRACKING	FATIGUE CRACKING
DEPLOYMENT, RESTOWAGE	CELL CRACKING	STRESSES AIDING FAILURE	STRESSES AIDING FAILURE
SHADOWING	SHORT-CIRCUIT FAILURE	SOLDER MELTING AND OPEN-CIRCUIT FAILURE	—

Figure 15. Potential Failure Mechanisms

-33-

FAILURE MODE	FAILURE EFFECT ON OUTPUT OF A SINGLE MODULE (WORST CASE)	
	ON SAME CELL CONTACT	ON ANOTHER CELL CONTACT
OPEN JOINT OR INTERCONNECTOR LOOP	1ST JOINT: NONE 2ND JOINT: NONE 3RD JOINT: NONE 4TH JOINT: 30 W LOSS	NONE NONE NONE NONE
FRACTURED CELL	NONE – FRACTURED PORTIONS REMAIN IN CIRCUIT 10 W LOSS – SHADED AREA MAY BECOME DISCONNECTED 30 W LOSS – CELL MAY BECOME OPEN-CIRCUITED (WORST CASE)	
SHORTED CELL	8 PARALLEL-CONNECTED SHORTED CELLS IN A MODULE REDUCE ITS POWER OUTPUT BY 1 W	

Figure 16. Solar Cell Failure Modes and Effects

3.2.5.2 Available Solar Cell Types

For general space applications, essentially three different classes of solar cell types are available: 10 ohm-cm cells for high charged-particle radiation environments as found in the Van Allen belts and at synchronous altitude, 2 ohm-cm cells, and p^+ or field cells for low radiation environments as found in low earth (i.e., Shuttle) orbits and in interplanetary space. The p^+ or back surface field (BSF) cells provide approximately 10% more power at beginning of life than the 2 ohm-cm cells Beyond 1 Mev fluence levels of approximately 1×10^{14} e/cm^2 their advantage begins to diminish slowly. The 10 ohm-cm cells are of no interest to the PEP missions because of their initial low output, therefore a higher output p^+ cell type has been selected. This cell has been in production for several years at Applied Solar Energy Corporation (ASEC): formerly OCLI or Optical Coating Laboratory, Incorporated, and is flight-proven on many satellites. As presently developed, the average production yields approximately 13.8% efficiency at 28°C. Discussions held with two solar cell vendors indicated that 14% efficiency cells should be readily available for the PEP schedule needs. Thus 14% was selected as the baseline efficiency.

3.2.5.3 Thermophysical Characteristics

The selected 14% efficient baseline cell is an 8 mil (0.20 mm) thick p^+ field cell. The front surface is polished and coated with an optically highly efficient multi-layer anti-reflective coating. Together with a back surface reflector, the cell is expected to exhibit a solar absorptance of 0.75 as measured in the laboratory (non-operating). Under orbital operating conditions and maximum power extraction from the cell, the effective solar absorptance is diminshed to 0.63, resulting in an operating temperature as low as 58°C.

Figure 17 illustrates the interrelationships between the solar cell operating temperature and the effective solar absorptance for two substrate thicknesses. The baseline Kapton substrate is approximately 2 mil thick, being made of two plies of 1 mil each. The 1 mil Kapton line is shown for reference only. The higher cell operating temperature on thinner substrates arises from a decrease of the hemispherical emittance of the Kapton with decreasing material thickness as given in the small ta .e entitled
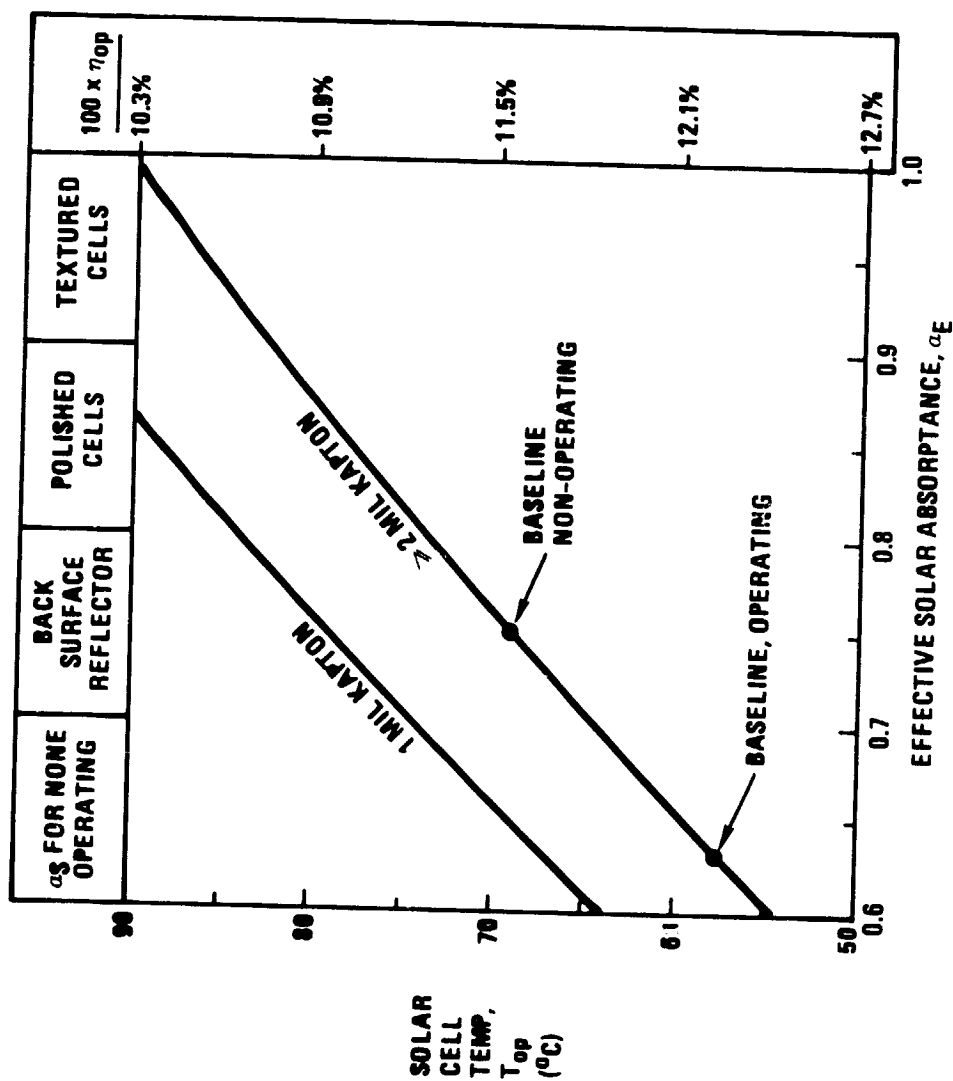
Figure 17. Solar Cell Estimated Operating Temperatures

"substrate" in Figure 17. Such relationship of emittance to thickness is observed on essentially all materials, even on thermal control paints.

The right-hand scale on the graph indicates the operating efficiency of the 14% (at 28°C) baseline cell at the corresponding operating temperatures given on the left-hand scale. Three of the four boxes at the upper end of the graph define the approximate range of the non-operating (measured) solar absorptance values for three distinct classes of solar cells: 0.7 to 0.8 for back surface reflector (BSR) types, 0.8 to 0.9 for polished cells without BSR, and 0.9 to 1 for textured, or non-reflective cells. The efficiency gain achieved by front surface texturing is essentially counteracted by the cell's higher operating temperature.

3.2.5.4 Solar Cell Size

Many different solar cell sizes can be used on the blankets as illustrated in Figure 18 without necessitating a change in the panel and blanket dimensions. Only the rib spacing needs to be modified to accommodate the different cell width dimensions. The impact of changing the cell size on the solar cell layout and the electrical blanket configuration is also shown in this table. The particular dimensions of the baseline and alternate, as well as the other cell sizes, were determined by maximizing the solar cell packing density within the fixed panel outside dimensions.

The selection of a nominal 2 x 4 cm size cell for the baseline design was based on low risk; this cell size has been in production at the vendors and in assembly at TRW for years. Automated production tooling and processes are in existence and are being used every day.

A larger, alternate nominal 5 x 5 cm solar cell size could be attractive for cost reasons The larger cell size would also permit a 2% higher cell packing density, thereby reducing the blanket size from 102 to 100 panels. However, since this cell size has never been fabricated in sufficient quantity and characterized by electrical and environmental testing, either individually or in an assembly, it could not be used for a production-ready baseline approach.

NUMBER OF CELLS IN SERIES	NUMBER OF PANELS/MODULE	CELL SIZES (IN CM) FOR NUMBER OF CELLS IN PARALLEL		
		8	6	5
150	2	2.22 x 3.96	2.22 x 5.30	2.22 x 6.30
100	3	—	3.38 x 5.30	—
75	4	4.55 x 3.96	4.55 x 5.30	—
60	5	—	5.70 x 5.30	5.70 x 6.30*

*CORNERS CROPPED

Figure 18. Solar Cell Size Trades

3.2.5.5 Solar Cell Thickness

Variations in the cell thickness has a large impact on the array blanket weight and cost, and has a mild impact on cell efficiency. The weight impact arises primarily from the fact that of the 353 lbs. blanket weight, 279 lbs (79%) are contributed by the solar cells. As cells are made thinner however, the breakage rate in cell manufacturing and assembly increases, also increasing the unit cell cost . The minimum practical thickness for large-scale, low-risk production is believed to be 8 mil (0.20 mm) as presently specified for the TDRSS project.

The effect of cell thickness variation on power output is somewhat contrary for p^+ field and non p^+ cells. For the non p^+ cells, the power output decreases as the thickness is decreased. However, the p^+ field effect tends to be enhanced as the cell thickness is reduced to less than the mean minority carrier diffusion length (about 12 mil). Thinner cells (< 8 mil) are expected to benefit greatly from the p^+ field structure as already demonstrated by the high efficiency and charged particle radiation resistance of many of the experimental 2 mil p^+ cells.

3.2.5.6 Contact Configuration

Primarily for low risk reasons, the flight proven conventional palladium-passivated titanium-silver contact type was selected. High-efficiency wrap-around contact cells, presently under development under NASA-LeRC sponsorship, are still not as efficient as the same size cells with conventional contacts and have not been environmentally tested yet. Inasmuch as the TRW automated interconnector handling equipment does not impose significant economic penalties on the array assembly, there is no incentive to use lower-output, higher-cost, wrap-around contact cells. The cost of wrap-around contact cells is estimated by the cell vendors to be in the vicinity of 20% higher than conventional cells while the power output is estimated at 2 to 3% less for the same cell size.

3.2.5.7 Temperature Coefficients

At the present time, the values of the p^+ field cell power output temperature coefficients are uncertain. For many of the newer, high-efficiency

-39-

solar cell types, for both p^+ and non p^+ types, and for thicker as well as thinner cells, temperature coefficients for maximum power of -4.6% per °C have been reported in the literature. It is not clear at this time where this deviation from the more typical -4.3% per °C for the older cell types arise from. In any case, for the trade studies presented here, both p^+ and non p^+ cells have been assumed to exhibit -4.6% per °C coefficients.

3.2.6 Cover Glass Trades

3.2.6.1 Available Cover-glass Types

The available solar cell cover materials include microsheet, ceria doped glass, and fused silica. The ceria glass inherently blocks the transmission of solar UV radiation to the cover adhesive, while microsheet and fused silica usually carry a UV reflective coating. Any of the covers may or may not have a front surface AR coating. Of the available materials, the lowest cost microsheet darkens most under heavy charged particle radiation, but this is of minor concern for the planned low-radiation PEP missions. Essentially all optical losses due to UV and charged particle radiation can be ascribed to the coverglass adhesive, estimated to be about 2% at EOL, independent of the cover material.

For the above stated reasons and cost, microsheet covers have been selected for the baseline design, having a highly reflecting 350 nm cut-on UV coating and a conventional MgF AR coating. Such microsheet covers have been successfully used on the Skylab Orbital Workshop Solar Array and on other arrays for military missions in geosynchronous orbit.

3.2.6.2 Cover Sizing

The covers are slightly larger than the solar cells, overlapping the interconnector-to-cell joints. Thus, perfect radiation shielding of the solar cells is achieved and a smooth front surface is provided that minimizes sharp edges at which snagging could occur.

3.2.6.3 Cover Thickness

A baseline cover thickness of nominally 6 mils (0.15 mm) was selected because of widespread existing experience. However, recent developments

-40-

have indicated that a reduction to 4 mils (0.10 mm) may be possible
in which case a weight reduction per array system of 61.2 lbs (27.8 kg)
could be realized.

3.2.7 Interconnector Selection

3.2.7.1 Design Requirements

The solar cell interconnector design is driven primarily by the
18,000 thermal cycles expected during three years of cumulative orbital
operation within the ten year program life of the array, and some additional
thermal cycles caused by array shadowing. The thermal cycle accumulation
will be interspersed with mechanical load applications due to deployment
and restowage, and with vibrational loads during ascent and descent of the
Shuttle Orbiter. Secondary design considerations include interconnector
electrical losses, weight, and assembly cost.

3.2.7.2 Material Selection

Of all known metals, Invar has a coefficient of linear thermal ex-
pansion that most closely matches that of silicon. Consequently, thermo-
mechanical stresses in the interconnector-to-solar cell joints are minimized
by using Invar, and thermal cycling life of the joints is maximized. Invar,
a low expansion alloy made primarily of 36.0% Nickel and about 63% Iron,
is a poor electrical conductor. A thin silver plating therefore provides
electrical conductivity as well as a solderable (or weldable) surface.

3.2.7.3 Fatigue Life Considerations

The thermal cycling fatigue life of welded or soldered joints is strongly.
but not solely, related to the coefficients of linear thermal expansion.
Other important parameters include material stiffness, ductility and
metallurgical effects. Theoretical analyses and thermal cycling testing
have shown that joints between silver plated Invar interconnectors and
silver plated solar cells have a significantly longer fatigue life than
those with silver plated Kovar, and even longer life than those with copper
or pure silver.

-41-

The results of one of the theoretical analyses for welded joints is depicted in Figure 19. This analysis showed a one order of magnitude improvement of Kovar over copper or silver, and another order of magnitude improvement of Invar over Kovar. The ordinate was not calculated, but was chosen to coincide with a set of reliable test data.
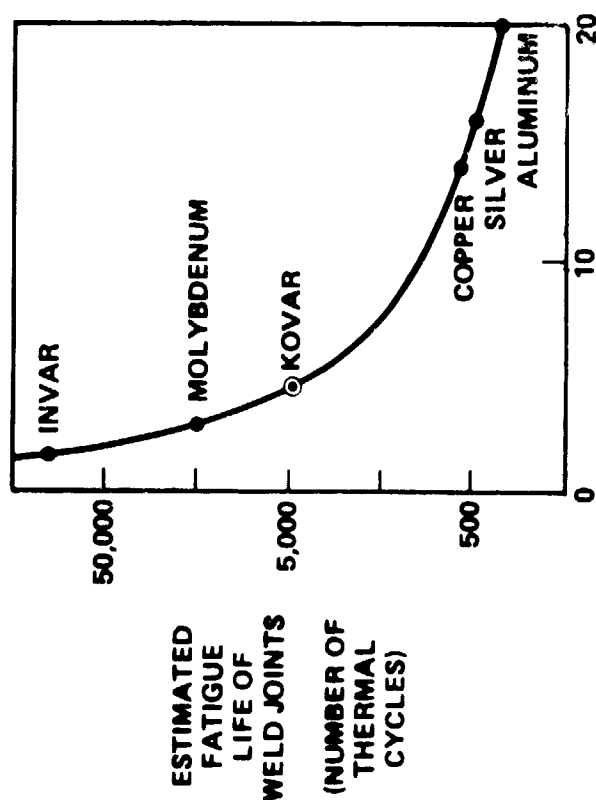
3.2.7.4 Configuration Selection

Invar interconnectors, silver plated on both sides, do not lend themselves to etched printed-circuit fabrication techniques. Therefore, discrete piece parts as illustrated in Figure 20 are utilized (the automatic handling of these parts in the array assembly is shown in Reference 1). For the baseline solar cells, two such interconnectors are used per cell, providing four-fold redundan' current paths and four joints on each of two solar cell contacts. For the larger 5.7 x 5.3 cm cells, three interconnectors per cell are planned. The corresponding electrical losses in the interconnectors are about 0.03% for the baseline cells and 0.1% for the alternate cells.

The out-of-plane expansion loops (Figure 20) effectively decouple any external forces and loads from the interconnector/cell joints, thereby enhancing their thermal cycling life. External loads are caused by blanket compression and tension during stowage and deployment, by vibration and shock, by thermal expansion differences between the solar cells and the blanket substrate, and by panel (blanket) curving and billowing during ground handling, testing, deployment, restowing, and in orbit during attitude changes and plume impingement. The loops do not protrude past the plane of the coverglasses, so that no interference exists in the stowed blanket condition. A significant factor in reducing the external forces on the joints is that the solar cells are permanently bonded with adhesive to the substrate. Thus, the joints support only the light interconnectors.

3.2.7.5 Joining Method

For the baseline approach, soldered interconnectors were selected rather than welded ones, primarily for cost and risk reasons. Analyses and preliminary tests indicate soldered joints will meet mission requirements. Soldering is a well-established, highly reliable technique whose

OPTION

SELECTED DESIGN

- INVAR SHOWS LONGEST LIFE

- SOLDERED KOVAR INTERCONNECTS PASSED 4800 THERMAL CYCLING TEST FOR SKYLAB OWS ARRAY; THIS DATA WAS USED TO CALIBRATE NORMALIZED STRAIN-RANGE CURVE

- SOLDERED JOINTS ARE NOT AS SENSITIVE TO $\Delta\alpha$ AS WELDED JOINTS, BUT ARE VERY SENSITIVE TO MECHANICAL FORCES FROM INADEQUATELY SIZED EXPANSION LOOPS

REF: A. KAPLAN, 10TH PHOTOVOLTAIC SPECIALISTS CONFERENCE

ESTIMATED FATIGUE LIFE OF WELD JOINTS

(NUMBER OF THERMAL CYCLES)

INVAR

MOLYBDENUM

KOVAR

COPPER
SILVER
ALUMINUM

50,000

5,000

500

0   10   20

DIFFERENCE IN THERMAL EXPANSION COEFFICIENTS

$\Delta\alpha = \alpha_{METAL} - \alpha_{SILICON}$
($^{\circ}C^{-1} \times 10^{-6}$)

Figure 19.   Interconnector Material Selection – Thermomechanical

- 25 μm THK Ag PLATED INVAR

- 2 U-SHAPED PARTS PER CELL (> 4 X REDUNDANCY)

- COMPLIANT EXPANSION LOOPS

- FRONT SOLDER (WELD) JOINT SANDWICHED BETWEEN CELL AND COVER
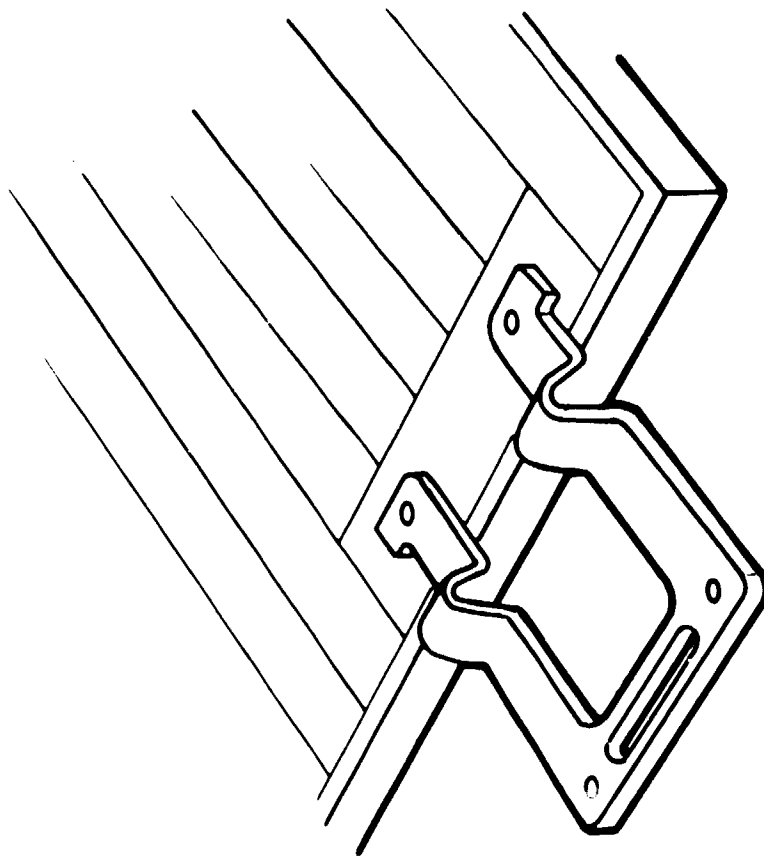
Figure 20. Interconnector Design

-44-

process control problems, both at the cell vendors and at TRW, are well understood. In addition to an automated soldering facility, TRW also has in place, a high-rate welding capability, complete with automated NDT (Non-Destructive Test) equipment, and many years of welding experience. However, the process control understanding for welding is not as complete as it is for soldering. There are many solar cell manufacturing process parameters and other environmental and metallurgical conditions that are unrelated to the assembler's welding schedule, but may significantly affect the thermal cycling life capability of joints. Welded joint pull strength has not been found to be a reliable indicator of thermal cycling life, everything else being constant (such as electrode foot print size, weld pulse power, etc.). Thus welding is not normally ultilized unless mission conditions dictates its need.

3.2.8 Harness Design

3.2.8.1 Requirements

The harnesses conducts the electrical power generated by the solar cell panels to the base of the array wings, terminating in array output connectors. The harnesses must be sized and designed for minimum system weight, adequate stand-off voltage between conductors of opposite polarity, high flexibility at the panel hinge lines, adequate hinge folding/unfolding flex cycling life, environmental stability, reliability, manufacturability, repairability, crew safety, and thermal and mechanical compatibility with the solar cell panel/blanket so as not to impede restowage in orbit. Not mandatory, but highly desirable for stowage container design reasons, is the desire for the folded (stowed) harness stack height not to exceed the folded stack height of the solar cell panel blanket. Further requirements call for instrumentation cables (6 to 12 per harness) and a minimum number of power circuits (50 per array) that can be connected into six groups of independent power sources.

The above stated requirements imply that the harness be as narrow as possible so as not to overly reduce the panel area on which solar cells could be mounted.

3.2.8.2 Configuration Options

The two possible harness design options are either flat photo-etched printed circuit type conductors, stacked into several layers inboard, or round conductors composed of stranded wires arranged in a single, flat layer. Each of these approaches has advantages and disadvantages. However, the stranded wire approach appears to offer greater mechanical flexibility at the hinges, better inspectability, and easier repairability.

Figure 21 illustrates in cross-section the round wire approach. Cross-sections for power conductors vary between 24 and 18 AWG gages. Where larger cross-sections are required, 18 AWG conductors are paralleled so that the folded stack height will not exceed the folded panel stack height. The number of runs and corresponding cross-sections, for both baseline copper-clad aluminum conductor and optional all-copper harnesses are presented in Figure 22. The copper-clad aluminum harness design features for both the baseline and alternate solar cell array designs are summarized in Figure 23.

3.2.8.3 Panel Connections

Termination of the harness runs at the solar cell panels is illustrated in Figure 24. Flat copper ribbons extend from the harness wires to the solar cell string termination strips such that no conductors cross over others. The series connection of panels is done similarly on the opposite side of the panels (not illustrated).

The connection of the panels to each other and the harnesses is schematically shown in Figure 25 for the baseline 2.22 x 3.96 cm cells and in Figure 26 for the alternate 5.7 x 5.3 cm cells. Both figures together confirm that any odd or even number of panels, electrically connected in series, can be accommodated with equal ease.

3.2.8.4 Conductor Selection

The available, practical conductor options include copper, copper-clad aluminum, and aluminum. For a given power loss, aluminum conductors would weight nearly one-half of copper conductors. However, the environmental stability of aluminum cables, especially their terminators, remains

TYPICAL RUN OF SINGLE POWER LEAD

TYPICAL RUN OF PAIRED POWER LEADS

6 RUNS 24 AWG INSTRUMENTATION

51 MODULES/WING BLANKET
2 HARNESS/BLANKET

1 MIL KAPTON SHEETS

SOLAR CELLS

PANEL SUBSTRATE

ALL WIRES STRANDED COPPER-CLAD ALUMINUM 36 AWG
18 AWG HAS 57 STRANDS
20 AWG HAS 37 STRANDS
24 AWG HAS 16 STRANDS
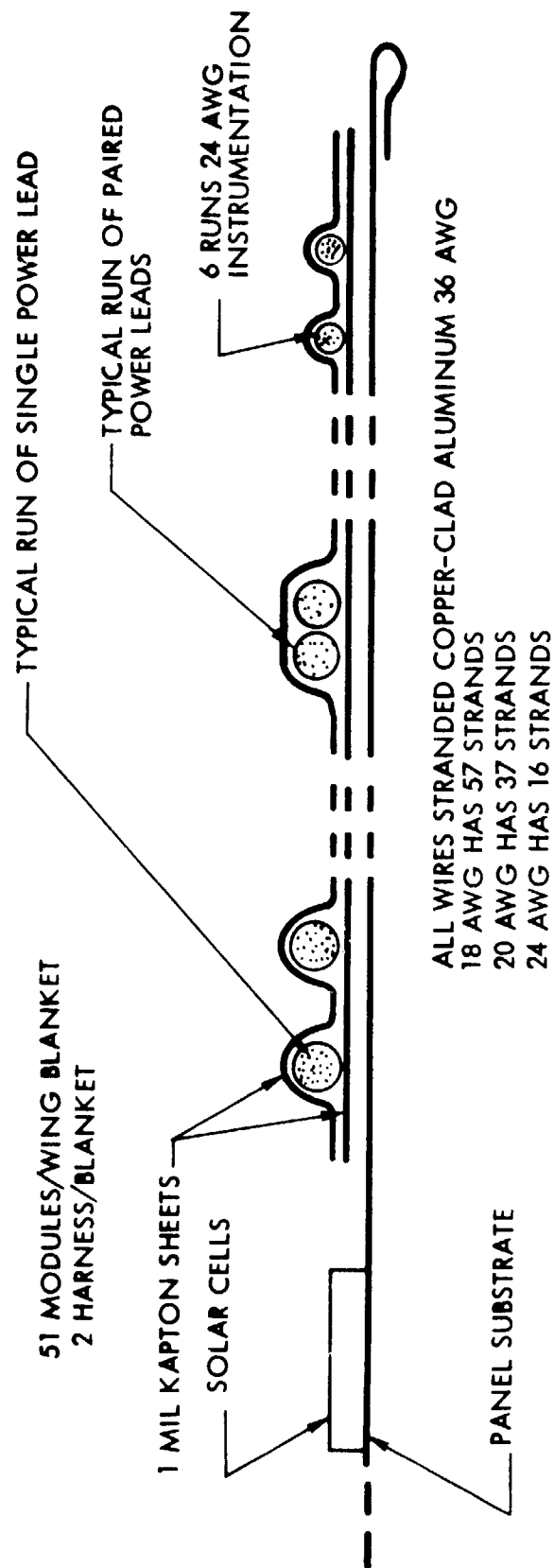
Figure 21. Harness Design Features

MODULE	NO. OF WIRES		AWG COPPER	BASELINE AWG ALUMINUM	TOTAL RUN LENGTHS(2)	
	LEFT	RIGHT			(FT)	(M)
1-11	12	10	24	22	364	111
12-21	10	10	22	20	844	257
22-33	12	12	20	2 x 21	1656	505[3]
34-51	18	18	2 x 21	2 x 19	2 x 3302	2 x 1159
INSTRUM	6	6	24	24	1518	463
TOTAL CONDUCTOR MASS[4]			26.2 KG	15.2 KG		

(1) EACH WING HAS A LEFT AND A RIGHT HARNESS
(2) PER WING, INCLUDING ONE INBOARD LEADER PANEL
(3) FOR ALUMINUM NEED TWICE THE STATED LENGTH
(4) FOR TWO WINGS

- MAXIMUM WIRE SIZE IS SELECTED TO MAKE STACKED HARNESS HEIGHT APPROXIMATELY EQUAL TO STACKED PANEL HEIGHT
- ALL POSITIVE AND NEGATIVE MODULE RUNS ARE CONTINUOUS TO WING TERMINATION STRIPS

Figure 22.   Summary of Harness Sizing

-48-

PARAMETER	BASELINE	ALTERNATE	RATIONALE
(SOLAR CELL SIZE)	(2.22 x 3.96 CM)	(5.70 x 5.30 CM)	(REFERENCE)
CONSTRUCTION	STRANDED WIRES IN A SINGLE FLAT LAYER	STRANDED WIRES IN A SINGLE FLAT LAYER	• FLEXIBILITY AT THE HINGES • INSPECTABLE AND REWORKABLE
NUMBER OF HARNESSES PER BLANKET	2	2	• ONE ON EACH SIDE FOR SYMMETRY
WIRE ROUTING	ANTI-PARALLEL	ANTI-PARALLEL	• MAGNETIC TORQUE CANCELLATION
NUMBER OF WIRES PER HARNESS • POWER • INSTRUMENTATION	51 6	20 6	• ALL MODULE POSITIVES AND RETURNS ARE BROUGHT TO WING BASE
CONDUCTORS	• Al CORE • 12% Cu JACKET	• Al CORE • 12% Cu JACKET	• LOW WEIGHT • Cu PROVIDES ENVIRONMENTAL PROTECTION AND SOLDER-ABILITY
CONDUCTOR SIZING	3% LOSS	3% LOSS	• MINIMUM ARRAY WEIGHT
INSULATION	• KAPTON • SPACING	• KAPTON • SPACING	• FLEXIBLE AND DURABLE • RADIATION RESISTANCE
HARNESS THICKNESS	0.05 INCH	0.05 INCH	• HARNESS FOLDS INTO SMALLER STACK HEIGHT THAN PANELS
CONNECTION TO SOLAR CELLS	RIBBON	RIBBON	• NO CROSSING OF CONDUCTORS • LOW STACK HEIGHT

Figure 23. Rationale for Harness Design
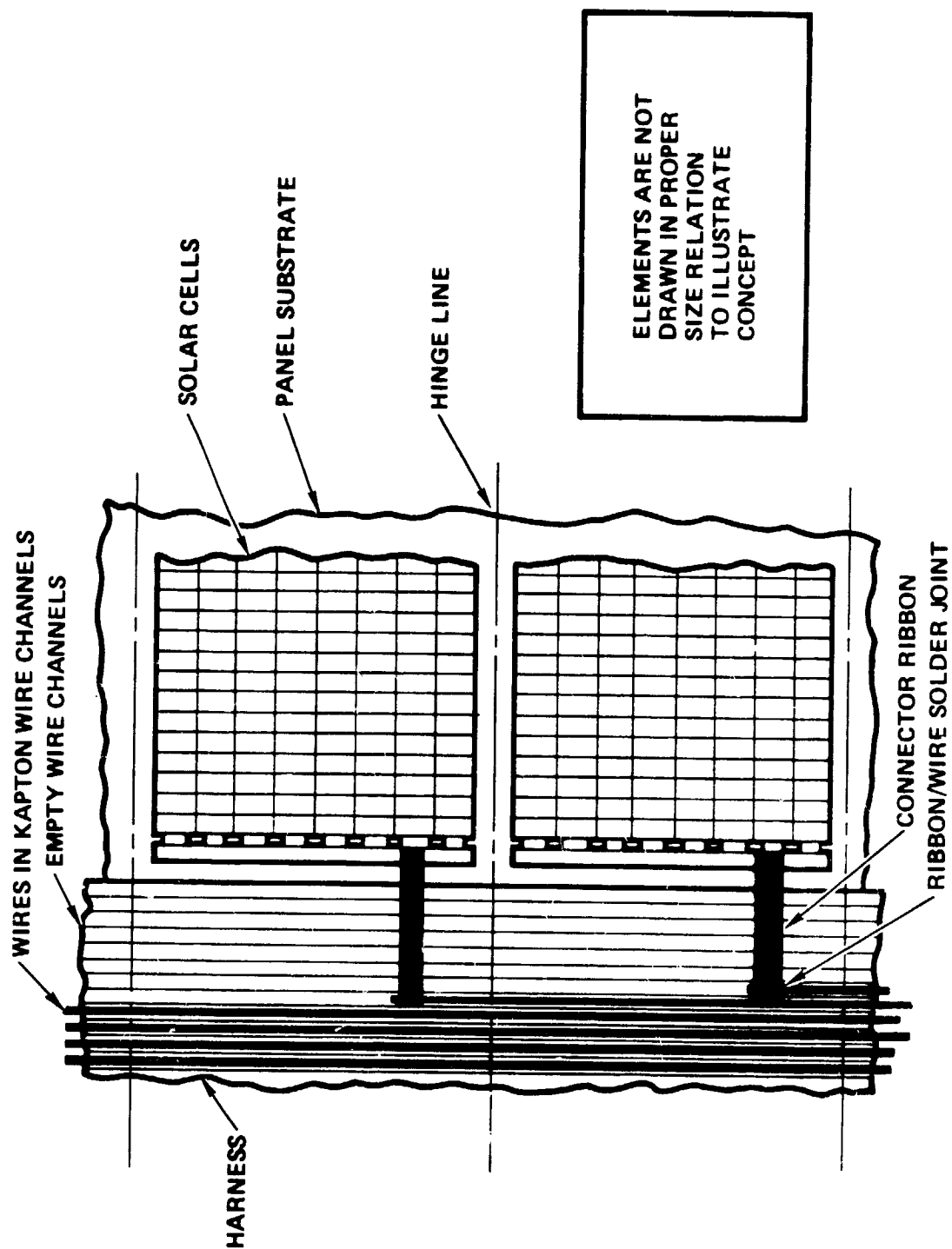
Figure 24. Harness Break-Out and Panel Termination Concept

Figure 25. Blanket/Harness Wiring Concept - Baseline Design

RIGHT HARNESS

LEFT HARNESS

PANEL SUBSTRATES

PANEL TYP

MODULE TYP

HINGE TYP

63V

PATTERN REPEATS
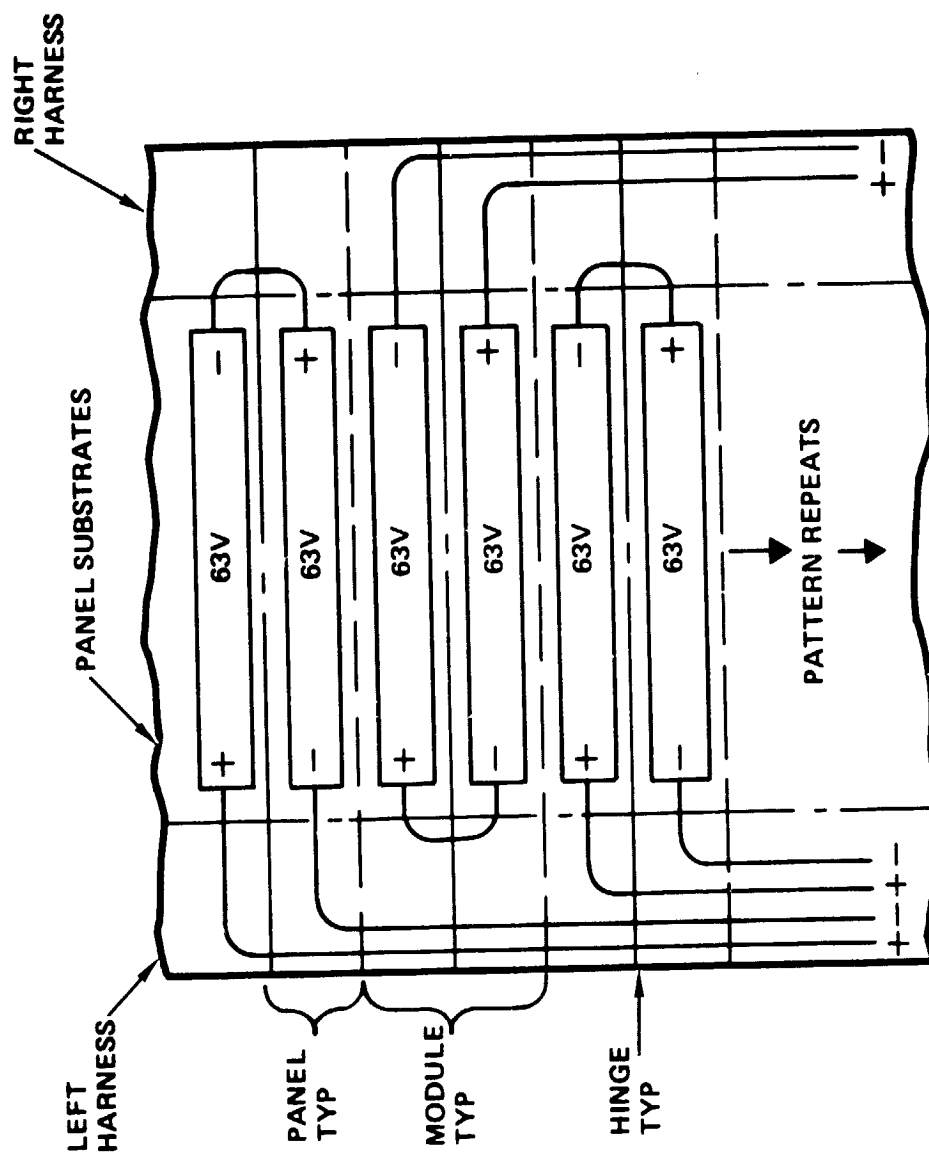
- ALL PANELS ARE IDENTICAL
- ALTERNATE POLARITIES CANCEL MAGNETIC TORQUES
- SINGLE-LAYER FLAT CABLE HARNESS IS EASY TO MANUFACTURE AND REPAIR
- 51 MODULES PER WING

SECOND MODULE

FIRST MODULE

● 20 MODULES PER WING

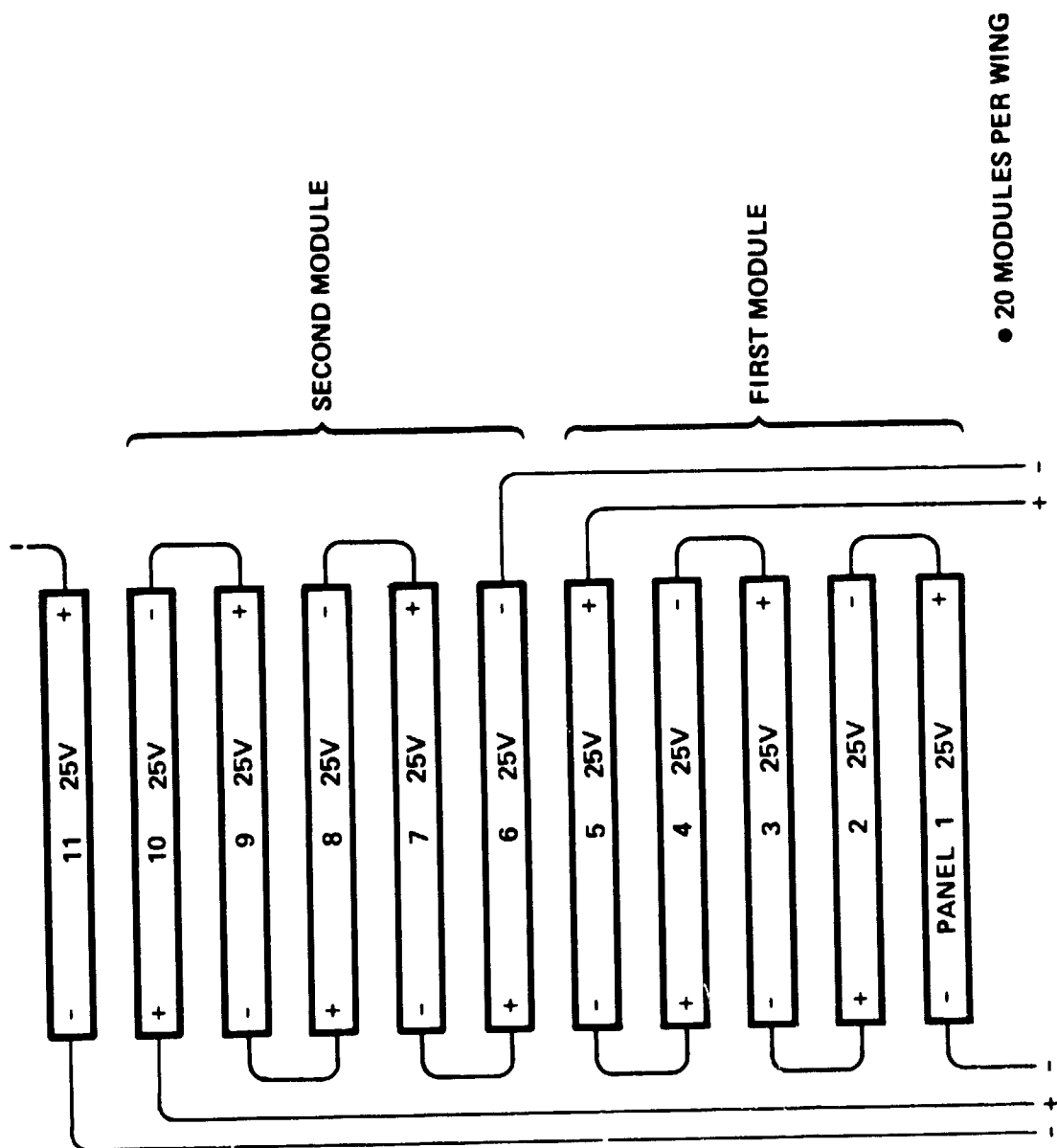| 11 25V | 10 25V | 9 25V | 8 25V | 7 25V | 6 25V | 5 25V | 4 25V | 3 25V | 2 25V | PANEL 1 25V |

Figure 26.   Blanket/Harness Wiring Concept - Alternate Design

somewhat of a technical challenge. Since shuttle flights will develop
elevated temperatures and humid conditions in the cargo bay, the use of
pure aluminum conductors probably constitutes an excessive corrosion risk.
Therefore copper-clad aluminum wires that are environmentally more stable
were selected as baseline.

The power conductor cross-sections were sized based on minimum
array system weight. Figure 27 depicts the trade study. A minimum weight
system is achieved with 3% power loss for the copper clad aluminum.
The actual minimum for copper, requiring more than 104 panels per wing,
was not calculated. The temperature coefficients of resistivity for copper
and aluminum are almosu identical, so that this trade study is applicable
for any reasonable temperatue range.

3.2.9 Cost Trade Studies in Solar Array Design

The dominant element in the solar array design from performance,
weight and cost view points is the solar cell. A series of trade studies
as identified in the previous section were performed to select the proper
solar cell for PEP based primarily on performance and producibility. In
order to perform solar cell trade studies based on costs, data was solicited
from several vendors to obtain unit costs as a function of size, efficiency,
thickness, quantity and certain other design features. Results of these
data are summarized in two charts.

As would be expected, the individual solar cells become more expensive
as the efficiency requirements increase. The compensating factors are that
less cells, covers, panels and labor are required as the efficiency increases,
hence the important information is on total program costs and not the cell
unit costs. Figure 28 summarizes the impact on total PEP solar array
costs as the solar cell efficiency is varied from the baseline 14% point.
Each data point breaks down the change in total costs in terms of solar cell
costs, cover glass, substrate, labor and miscellaneous material costs.
For example, at a cell efficiency level of 14.5% the cell unit cost is up
29% resulting in an overall program cost increase 3.3%. The number of solar
cell panels however are reduced from 102 to 98, requiring less cells,
covers, substrates, labor and other materials and bringing the overall pro-
gram costs to a point only 2.6% higher than the baseline. The interesting
point is that the inflection in the cost curve occurs at a solar cell

-53-

Figure 27. Harness Weight Trades
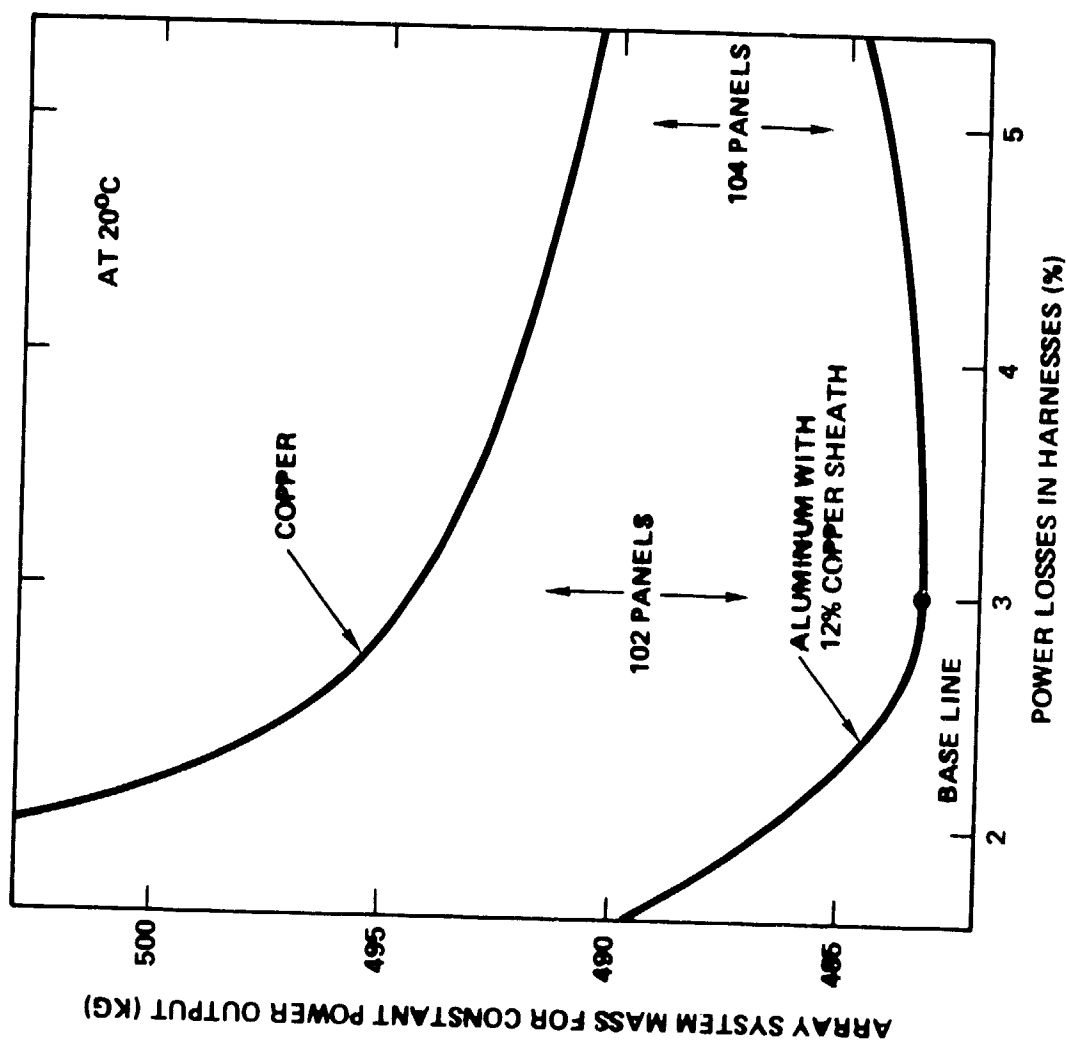
CONCLUSIONS

- ALUMINUM HARNESS SAVES 11 KG (24 LBS)

- MINIMUM SYSTEM MASS OCCURS WITH ALUMINUM HARNESS AND 3% LOSS

- ALUMINUM GAGES ARE 2 AWG SIZES LARGER THAN COPPER GAGES FOR POWER LEADS

- ACTUAL HARNESS MASS WILL INCREASE BY < 10% (< 1.5 KG FOR ARRAY) TO COMPENSATE FOR LOSSES AT WIRE TEMPERATURES BETWEEN 15°C AND 50°C, EST
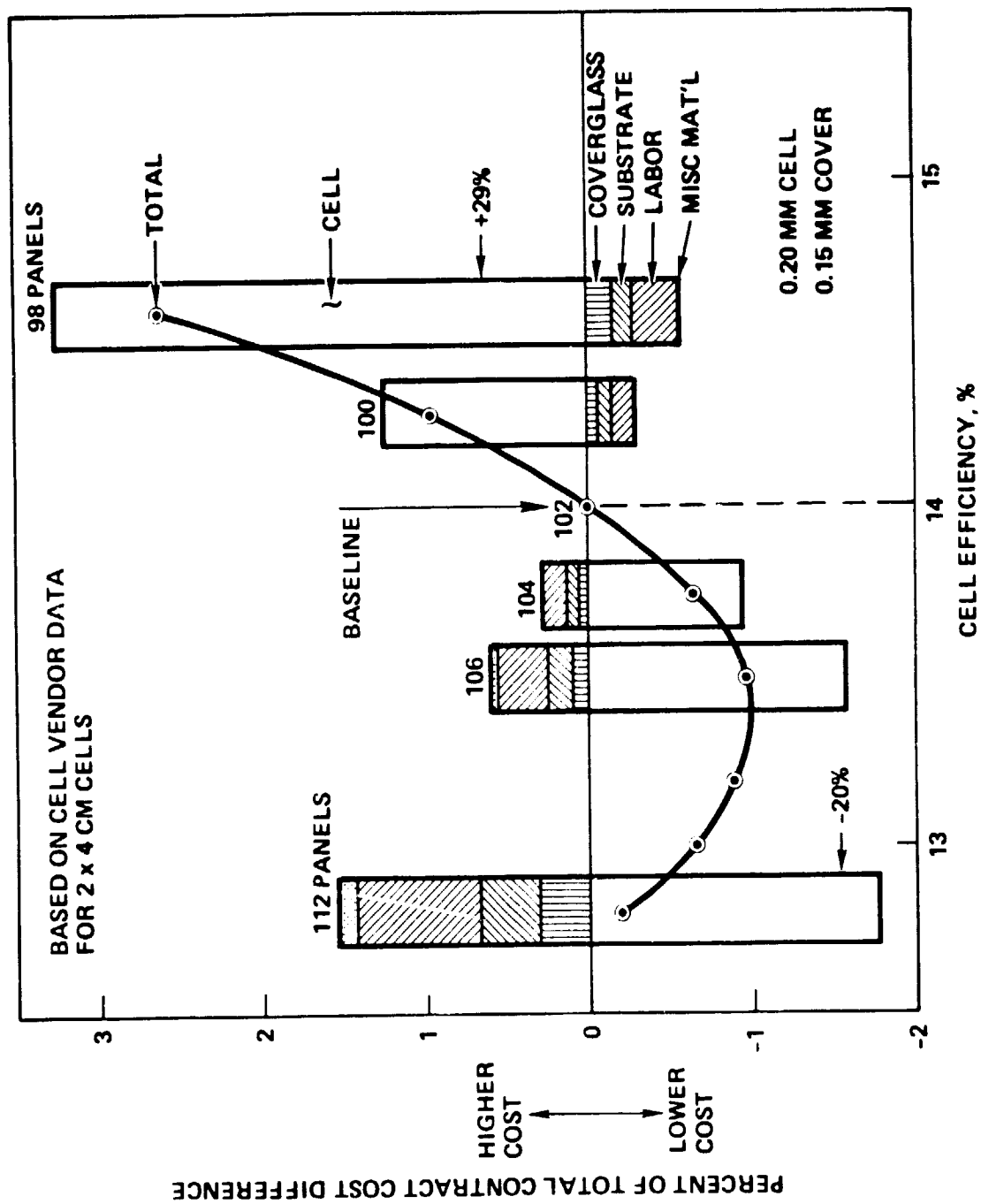
-54-

Figure 28. Cost/Efficiency Trade Study

efficiency of 13.5% but it shows only a 1% reduction from the baseline program costs. Since the uncertainty in the solar cell vendor cost data is greater than one percent the important results from the trade study is that solar cell efficiency is not a strong cost driver on the PEP solar array program.

Another aspect of solar cell efficiency not shown in Figure 28 is weight. It is evident that as the efficiency increases the weight will decrease, and for the PEP design, a $\pm$ 0.5 percent change in efficiency will have an increase or decrease of about 30 lbs. on the baseline design system weight. A more significant interaction of cost and weight is illustrated in Figure 29. The data plotted here is the change in total PEP solar array costs versus blanket and system weight for variations in solar cell thickness. Results are presented for both the baseline cells and the alternate design with the large 5.7 x 5.3 cm cells. It is evident that increasing the baseline solar cell thickness from 8 mil to 12 mil will reduce the program costs by 5% and increase the system weight by 50 Kg. The alternate large cell design shows a 9% lower cost for the 8 mil cell and somewhat less than that at the thicker cell gages. The cost differentials include different cell unit costs as well as different attrition rates and are based on a combination of solar cell vendor data and past experience from TRW hardware programs. It should be noted that the uncertainty in the curves at 2 mil thickness levels is large compared to the 8 mil and higher thicknesses because of the lack of production data.

3.3 Solar Array Mechanical Design

The mechanical design of the PEP solar array is concerned with all elements of the array that support and protect the solar cell strings and the electrical wiring. This consists of the substrates, hinges, and harness in the blanket assembly; and the container, lid, latches, tensioning mechanism, guide wire system and spreader bar in the blanket housing assembly.

3.3.1 Design Trades and Goals

Design studies were made for each major assembly to obtain the best possible configuration that was consistent with the design requirements
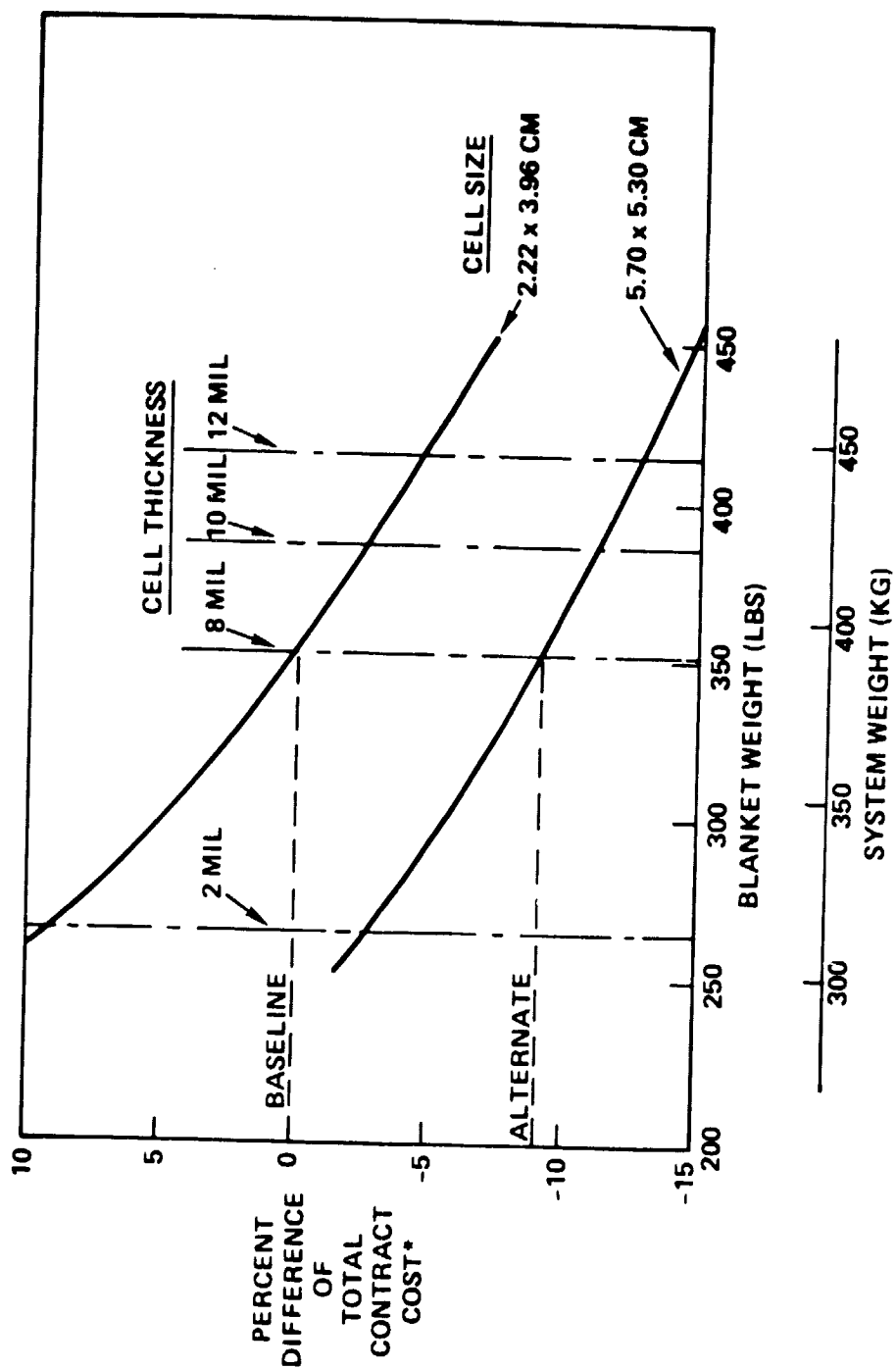
Figure 29. Cost/Weight Trade Study

and constraints. Since there were certain inherent features that must be incorporated, in order to achieve a workable design, a specific set of goals was formulated for the flexible, foldup solar array. These goals are as follows:

- o Provide solar cell panel enhanced stiffness during deployment and restowing operation.

- o Provide a positive force on the panels during the initial motion of the restowing sequence.

- o Provide adequate solar cell protection in the stowed condition.

- o Minimize solar cell laydown time during the manufacturing phase.

- o Minimize torque and enhance fatigue resistance of harness fold points.

The basic design approach to the PEP solar array considered large, rigid frames with stretched membrane panels, a roll-up design with STEM deployment devices, and a flatpack, fold-out design. The latter was selected as the most feasible in light of the size of the array, the deployment techniques to be used, and the packaging constraints. To meet the weight requirements the substrates are made of thin sheet of Kapton polymer film material with the solar cells bonded to it. Since it acts essentially like a membrane, it is maintained under a constant tension load in the deployed condition in order to provide adequate stiffness. However, during the restowing operation, the tension load is removed and the panel must then have a built-in stiffness in order to properly control it. The panels have an aspect ratio of about 10 to 1, hence the stiffness in-the-length direction needs to be considerably greater than in-the-width direction. This panel stiffness goal was achieved by a combination of built-in ribs and hinge stiffeners. A discussion of the features will be presented in the next section. The goals of positive folding and solar cell protection were also met by design features of the hinges and the ribbed substrate concept.

The design goal associated with the minimum solar cell laydown time is to reduce costs and to ensure high reliability. This is achieved by making maximum use of TRW's highly automated solar cell assembly line, and

was best accomplished by preassembly of the substrate blanket and solar cell strings in separate production lines until final assembly of the blanket is accomplished. The possibility of doing this is enhanced if the solar cell interconnects are independent of the substrate and if there are no critical alignment requirements between the solar cell strings and the substrates. The choices of the discrete interconnectors and the ribbed substrates achieve this goal with the advantages of reduced risks and minimum costs.

The final item associated with the harness folding characteristics is approached with the idea of a single layer of stranded wires and pre-folded hinge points. Component testing of this concept will be required to assess feasibility. A discussion of the baseline design in more detail is presented in the next section.

3.3.2 Baseline Blanket Design

The PEP solar array blanket includes the solar cells and cover glasses, interconnects, substrates, hinges, harness, terminator strips and connector ribbons. The design trades leading to the selection of the baseline solar cells, cover glasses, interconnects and the harness electrical features were covered in Section 3.2. The mechanical aspects of the design are discussed in this section.

Figure 10 shows the complete wing assembly and the dimensions of a single solar cell panel. The design trades leading to the sizing of the panel and other principal features are summarized in Figure 30. The panel size is controlled primarily by the volume constraints. Since it is desirable to make the panel as large as possible in order to reduce the number of panels, the actual size is determined first by the space available for the container and then secondly by the construction details of the container. To a limited extent, the panel/hinge design features and the solar cell string arrangement (panel voltage) also must be accommodated. From the volume constraints presented in Figure 7, the net panel dimensions as shown in Figure 10 were selected as the PEP solar array baseline design.

TRADE ITEM	OPTIONS	SELECTION CRITERIA	SELECTED DESIGN
PANEL SIZE	VARIABLE	• PEP VOLUME CONSTRAINTS • CONTAINER DESIGN FEATURES • PANEL DESIGN FEATURES • STRING ARRANGEMENT	150 IN. x 14 IN.
PANEL STIFFENER ARRANGEMENT	• PERIMETER STIFFENERS • BONDED DIST RIBS • INTEGRAL RIB WITH FLAT PLY • DOUBLE RIB-NESTED • WAFFLE PATTERN	• STIFFNESS LEVEL REQUIRED • ATTACHMENT STRENGTHS • MANUFACTURING PROCESSES • SOLAR CELL PACKING EFFICIENCY • CONTAINER HEIGHT • WEIGHT	DOUBLE RIB-NESTED
HINGES	• PIANO • STIFFENED • PRESTRESSED/STIFFENER	• FLEXIBILITY • STRENGTH CAPABILITY • PANEL STIFFNESS DURING REFOLDING • FORCES TO AID REFOLDING	PRESTRESSED/STIFFENER

Figure 30. Solar Panel Design Trades

3.3.2.1 Substrate Design

A variety of panel stiffener arrangements were considered, including perimeter stiffeners, bonded distributed ribs, integral rib with flat backside, a waffle stiffener pattern and a double rib-nested arrangement. The factors considered in making the selection were the magnitude of the stiffness obtainable, the impact on stack height which affects container height, the effect on solar cell packing efficiency, the attachment strength, particularly in shear and peel, the weight, and manufacturing processes. The concept that appeared to meet most of the criteria was a combination of double rib-nested design which has the rib formed directly into the substrate material, and stiffeners in the hinge design. The substrate ribs provide primarily the stiffness along the width dimension and the hinge stiffeners are oriented along the panel length dimension. The combination of stiffness is designed primarily for the panel during the refolding operation when it would be under partial compression.

The substrate concept selected for the baseline design is composed of two plies of one mil Kapton bonded with a nitrile film adhesive (Freylock F186). The Kapton plies have a pattern of integral formed ribs in each ply. The ribs on the solar cell (upper) ply run the length of the panel (137.6 inches), parallel to the solar cell string direction. The ribs on the back side ply run the panel width dimension and are spaced at the center of alternate solar cells. This ply also has space at either end to accommodate the harness runs (approximately 5.6 inches each) and includes a ground handling loop (0.5 inches) at each end. The rib height and spacing is determined by solar cell geometry, and by the stiffness and cell cushioning requirements. The ribs on adjacent panels are similar but slightly offset such that there is cell-to-rib contact in the stowed condition when two panels have their solar cell sides facing each other, and with the ribs centered under the solar cells when two panels are back to back.

This selective orientation of the ribs accomplishes several important objectives. It cushions every solar cell between ribs on the front and back sides when in the stowed configuration. It minimizes the stack height of the stowed blanket because of the nested-rib arrangement between adjacent panels. It provides area contact between cell and rib, or substrate and rib

-61-

tc reduce the bearing stresses. It permits automated solar cell series processing because the interconnects do not penetrate the Kapton and hence do not require tight alignment between cells and substrates. And finally because the ribs are an integral part of the Kapton plies, it provides stiffening and cell cushioning with a minimum impact on weight.

3.3.2.2 Hinge Design

The hinges are used to link the panels together to make up the blanket. They must be flexible enough to permit easy deployment and refolding operation and should have an inherent property that will ensure refolding in the proper direction. Three design concepts were considered. The piano hinge is the simplest and lightest, and consists of a small wire threaded through loops on adjacent panels. The stiffened hinge is a variation of the piano hinge but with increased out-of-plane bending stiffness by either add-on stiffeners or thicker wire. The prestressed/stiffener hinge concept is a bonded assembly that provides a positive force during refolding and also incorporates significant stiffness.

The selected baseline hinge design consists of a rigid non-metallic spacer that is bonded between two plies of 3-mil Kapton. An inner strip of 1-mil Kapton is bonded to the two strips of 3-mil Kapton and the entire assembly is bonded to the adjacent solar cell panels with lap joints. The assembly is formed with the two strips of 3-mil Kapton in a flat orientation similar to the folded blanket condition. When the blanket is deployed, the 3-mil Kapton strips rotate through a 90 degree angle, storing a certain amount of strain energy. The inner 1-mil ply also opens up to a flat condition to take tension load across the hinge line, but because of the thinner gage it stores less train energy. When the tension preload is relaxed during the restowing sequence, the strain energy will always i..tiate refolding of the panels in the proper direction. The urethane spacer width and thickness is controlled to provide significant stiffness along the length dimension of the panel. Alternate hinges also contain reinforced inserts to accommodate the guide wire.

-62-

The hinge design therefore serves several important functions. It provides an inherent spring force for refolding the panels. It provides a significant contribution of stiffness to the panel in the long dimension for both the deployed and restowing conditions. The hinge has good tension load capability, and because it is located at the edge of the panel in the folded condition it also serves to cushion the blanket and harness in the container.

3.3.2.3 Harness Mechanical Design

The power harness carries the solar electrical current from the panel collectors to the base of the array where it terminates at connector boxes in the blanket housing. As discussed in Section 3.2.8, several concepts were considered from an electrical performance viewpoint and the baseline concept selected was copper-clad aluminum, stranded wires, These wires would vary in gage depending on the length of the run, and would be separated into two harness groups, mounted on opposite edges of the panels to provide weight and magnetic torque balances. The principal design concerns of the harness from a mechanical viewpoint are flexibility, stowed stack height, and fatigue life. Specific features were incorporated into the design to accommodate the concerns.

The baseline harness design for PEP is illustrated in Figure 31. It consists of a single flat layer of round stranded wires encapsulated in two plies of 1-mil Kapton. The upper ply is formed over the individual or paired conductors to provide electrical insulation and spacing. The harness subassemblies are bonded to the individual solar cell panels in the harness run areas that were allocated. The harness hinge configuration consists of a prefolded design with the 180 degree fold at the tip. The tip is set with epoxy to prevent flexing at the sharp curve point. The flexing is then permitted at two points on either side of the tip fold with a bend radius about five times the wire diameter. The angle of rotation at each of these points is only 90 degrees.

The selected approach yields several advantages in that the flexibility is enhanced by using a single layer of wires and by requiring flexing at a larger radius at two locations for each hinge point rather than a single,
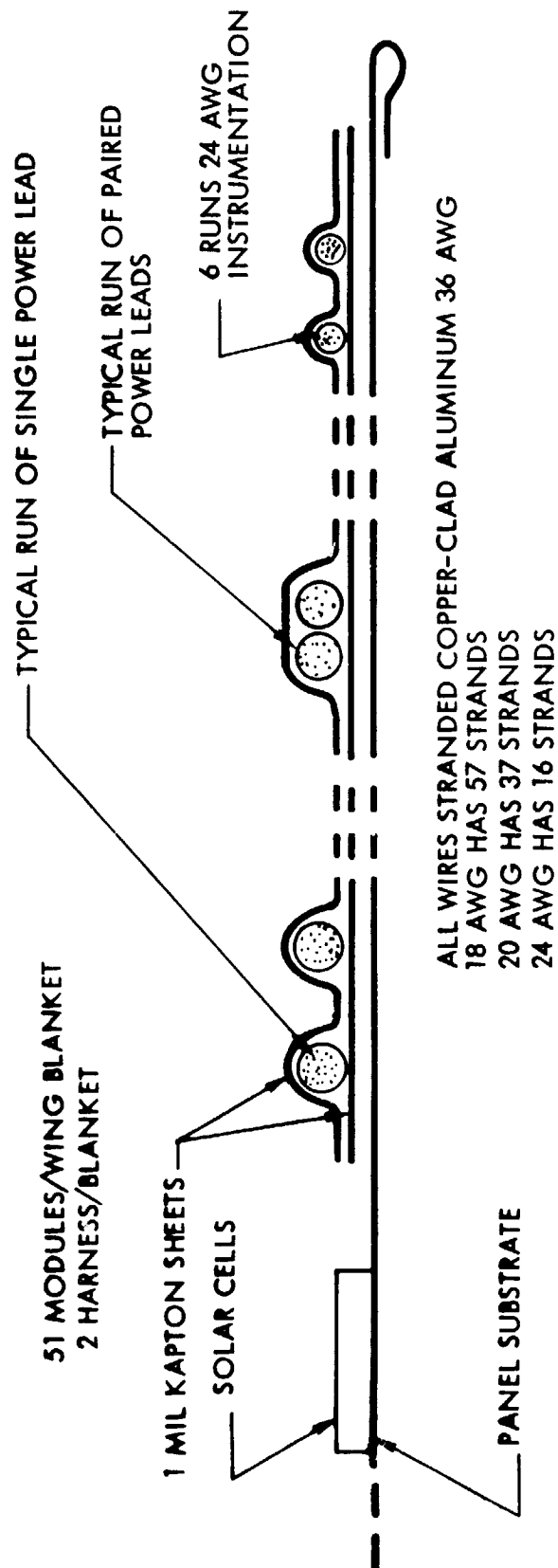
-63-

Figure 31. Harness Design Features

TYPICAL RUN OF SINGLE POWER LEAD

TYPICAL RUN OF PAIRED POWER LEADS

6 RUNS 24 AWG INSTRUMENTATION

ALL WIRES STRANDED COPPER-CLAD ALUMINUM 36 AWG
18 AWG HAS 57 STRANDS
20 AWG HAS 37 STRANDS
24 AWG HAS 16 STRANDS

51 MODULES/WING BLANKET
2 HARNESS/BLANKET

1 MIL KAPTON SHEETS
SOLAR CELLS

PANEL SUBSTRATE

-64-

sharp bend point. For the same reasons, the fatigue life is also increased because the strain levels at the bend points should be much reduced with 90 degree bend angles rather than 180 degree angles. The single flat layer with Kapton covers should also result in a stack height at two adjacent panels that is less than the stack height of the two nested-rib solar cell panels. This approach simplifies the container design since special provisions are not required in the container to accommodate the folded harnesses.

3.3.3 Alternate Blanket Design

The baseline blanket design described in the previous section is based on the use of 2.22 x 3.96 cm solar cells. The cell dimensions depart slightly from the more standard 2 x 4 cm cell size in order to maximize the packaging efficiency and to satisfy the array voltage requirement. One alternative investigated was the use of large cells because of the potential significant cost saving that could be realized, as discussed in Reference 1. Although this is not a solar cell design that is in current production, it is recognized that NASA is planning to assess and possibly assist in its development. In view of this potential cost-saving development, an alternate blanket design was formulated based on the large solar cell usage.

The baseline panel design was reassessed considering initially a nominal 5 x 5 cm cell. To maintain as efficient usage of solar panel area as possible, and to meet the system voltage requirement, a solar cell dimension of 5.70 x 5.30 cm was selected, (Figure 32). This results in a panel arrangement with 60 solar cells in series and 6 strings of cells per panel. This produces approximately 25 volts per panel and necessitates 5 panels in series in order to reach the required voltage range of 100 to 125 volts.

The principal impact on the baseline design is to require a slight change in the rib spacing on each panel and to modify the size and number of wire conductors in the harness. The overall panel dimensions do not change. The rib spacing on the solar cell side increases to accommodate the 2.087 inch dimension as shown in Figure 32, resulting in a reduction of the number of ribs. The rib spacing on the back side also increases slightly to provide two ribs of cushioning on each cell with one rib on the panel itself and the other rib from the adjacent panel. The hinge design
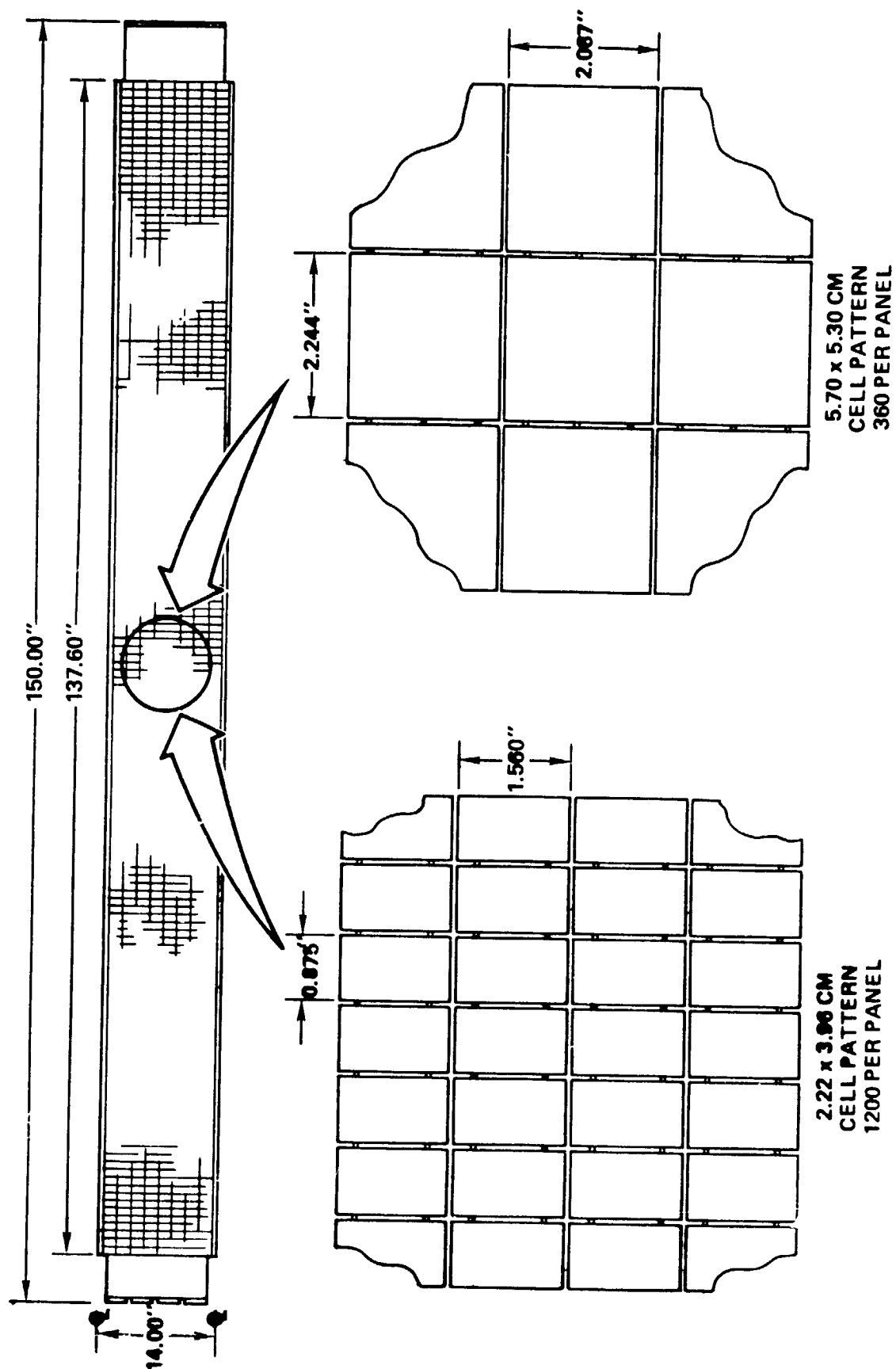
-65-

Figure 32. Alternate Cell Panel Design

5.70 x 5.30 CM
CELL PATTERN
360 PER PANEL

2.067"

2.244"

150.00"

137.60"

14.00"

2.22 x 3.96 CM
CELL PATTERN
1200 PER PANEL

1.560"

0.875"

is not changed nor are any elements in the container, tensioning and guide wire systems. However, because of the increased packing efficiency on each panel, two less panels per wing are required compared to the baseline configuration. A summary of the wing details for the baseline and alternate designs are presented in Figure 33. The compatibility of the large solar cell and the ribbed Kapton substrate was demonstrated for the temperature environment by thermal cycling a small test panel over the -80°C to +60°C range for 3275 cycles. A description of the test set-up and discussion of the results are presented in Appendix A.

3.3.4 Blanket Housing Design

The blanket housing supports and protects the solar cell panels during the launch and reentry phases of the mission. The principal elements of the housing assembly are the container, lid, preload and latching mechanism, blanket tensioning mechanisms and the guide wire system.

3.3.4.1 Container and Lid

Trade studies were undertaken to select a container-lid design and the concepts considered are summarized in Figure 34. One concept has the lid attached to the mast tip and travels with the upper end of the blanket during the deployment sequence. It acts as a rigid spreader bar in the deployed mode and as the blanket compression device in the restowing operation. The lid latches and locking mechanisms are designed into the linkages between the mast tip and lid, and the motors on the mast canister are used to latch/unlatch the lid and compress the blanket in the container.

The other concepts consider hinging the lid to the container and using separate motors to latch/unlatch the lid and compress the blanket. A single full lid concept hinges the lid on the container side opposite the mast. The other two concepts used split lids with a clam shell configuration (longitudinal split) in one and a mast side hinge in the other with the lid split in the width direction. Advantages and disadvantages of each are summarized in Figure 34.

PARAMETERS	WING CONFIGURATION	
	2.22 x 3.96 CM SOLAR CELL	5.70 x 5.30 CM SOLAR CELL
PANEL WIDTH – IN. ($\mathcal{C}$ TO $\mathcal{C}$)	14.00	14.00
PANEL LENGTH – IN.	150.00	150.00
NO. OF PANELS	102	100
NO. OF LEADERS	2	2
BLANKET LENGTH – IN.	1456.00	1428.00
CELL THICKNESS – MILS	8	8
COVER THICKNESS – MILS	6	6
NO. OF CELL/PANEL	1200	360
TOTAL NO. OF CELLS (10^3)	122.4	36.0
WEIGHT (LBS)	355	357

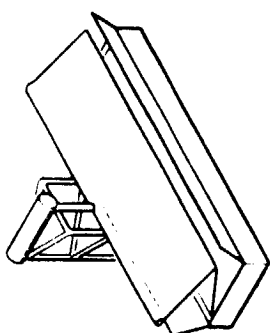Figure 33.   Wing Design Comparison – Baseline and Alternate
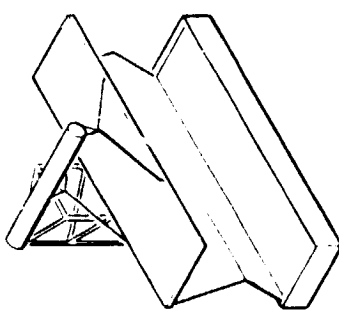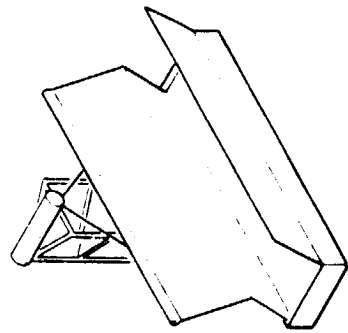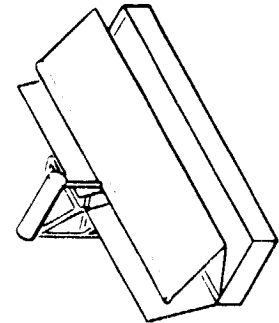
MAST ATTACHED	COVER HINGED TO CONTAINER		
	FULL COVER		HALF COVERS
	HINGE AWAY FROM MAST	HINGE ADJACENT TO MAST	
ADVANTAGES	**ADVANTAGES**	**ADVANTAGES**	**ADVANTAGES**
PROTOTYPE DEMONSTRATED. NO DRIVE MOTORS REQUIRED.	MINIMUM WEIGHT ON END OF MAST. SIMPLER COVER PRELOAD AND LATCH WITH GREATER DESIGN FLEXIBILITY. DEPLOYMENT BRAKE PROVIDES FOR REGULATED DEPLOYMENT OF PANELS.	MINIMUM WEIGHT ON END OF MAST. SIMPLER COVER PRELOAD AND LATCH WITH GREATER DESIGN FLEXIBILITY. DEPLOYMENT BRAKE PROVIDES FOR REGULATED DEPLOYMENT OF PANELS.	MINIMUM WEIGHT ON END OF MAST. SIMPLER COVER PRELOAD AND LATCH WITH GREATER DESIGN FLEXIBILITY. DEPLOYMENT BRAKE PROVIDES FOR REGULATED DEPLOYMENT OF PANELS.
DISADVANTAGES	**DISADVANTAGES**	**DISADVANTAGES**	**DISADVANTAGES**
COVER & LOCKING LEVERS ADD WEIGHT TO END OF MAST AND LOWER BENDING NAT'L FREQUENCY. LOCKING MECHANISM COMPLEX, AND DEPENDS ON MAST THRUST CAPABILITY. SERIOUS IMPACT IF DESIGN LOAD CAPABILITY INSUFFICIENT.	DOOR MUST BE RETURNED TO CLOSED POSITION TO AVOID SHIELDING ARRAY. TWO DRIVE MOTORS REQUIRED.	DOOR MUST BE SPLIT TO ACCOMODATE MAST TO ARRAY MEMBER. TWO DRIVE MOTORS REQUIRED. FOUR LATCHS REQUIRED.	DOOR MUST BE SPLIT TO ACCOMODATE MAST TO ARRAY MEMBER. DIFFICULT TO APPLY DESIRED PRELOAD PRESSURE.

Figure 34. Container/Lid Trade Study

The container/lid concept selected for the baseline design is shown in Figure 35. It has the lid hinged on the opposite side of the container from the mast. The lid and container base are honeycomb construction and the four walls are thin sheet material with fittings at four locations for the hinges and latches. The preliminary selection is to use aluminum construction to minimize costs and to simplify construction processes; however, a composite structure has also been formulated and will be selected if weight becomes a problem. Internal padding of the container is not planned.

3.3.4.2 Preload and Latching Mechanism

The container lid is opened and closed by two stepper motors that are attached to the side of the container. The motor shafts are coupled through gears to linkages that latch/unlatch the lid and also preload the blanket in the container. There are slots in the hinges to permit lid translation and rotation since about one inch of vertical translation is required to preload the blanket sufficiently to prevent lateral motion during launch and re-entry flight conditions.

The lid latch and preload mechanism is presented in Figure 36. A rigid link passes through a channel in the lid to a cam arm on the opposite side of the container. During the unlatching sequence the initial rotation of the latch shaft permits vertical translation of the lid. A pin in the cam slot on the latch arm prevents the latch from rotating until near the end of the vertical motion. At this time the latch will disengage the latch pin and the lid and latch arm will rotate through an angle greater than 90° to permit blanket deployment. Torque springs in the end of the motor shaft will hold the lid in the open position.

3.3.4.3 Blanket Tensioning Mechanism

The PEP solar array blanket is extremely flexible and acts like a membrane. To introduce stiffness in the longitudinal direction and to prevent blanket-to-mast contact, a uniform tension load is applied in the fully-deployed condition. The tension load is applied by the canister motors through the mast. The blanket tensioning mechanism reacts against the mast loading to maintain the blanket under a relatively constant load for both thermal and acceleration environments. Both in-plane and out-of-plane distortions of the blanket must be accommodated. The concepts shown
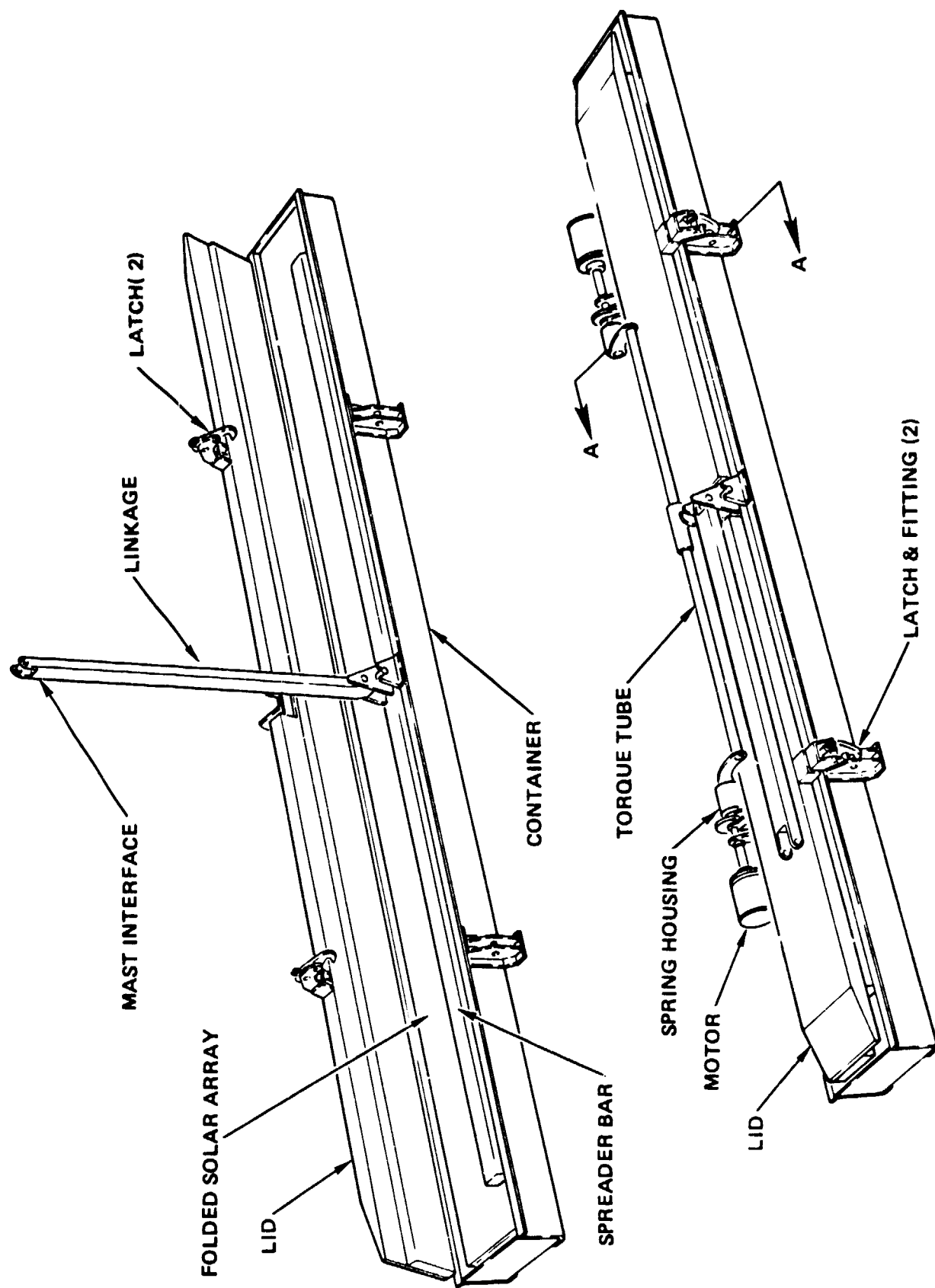
-70-

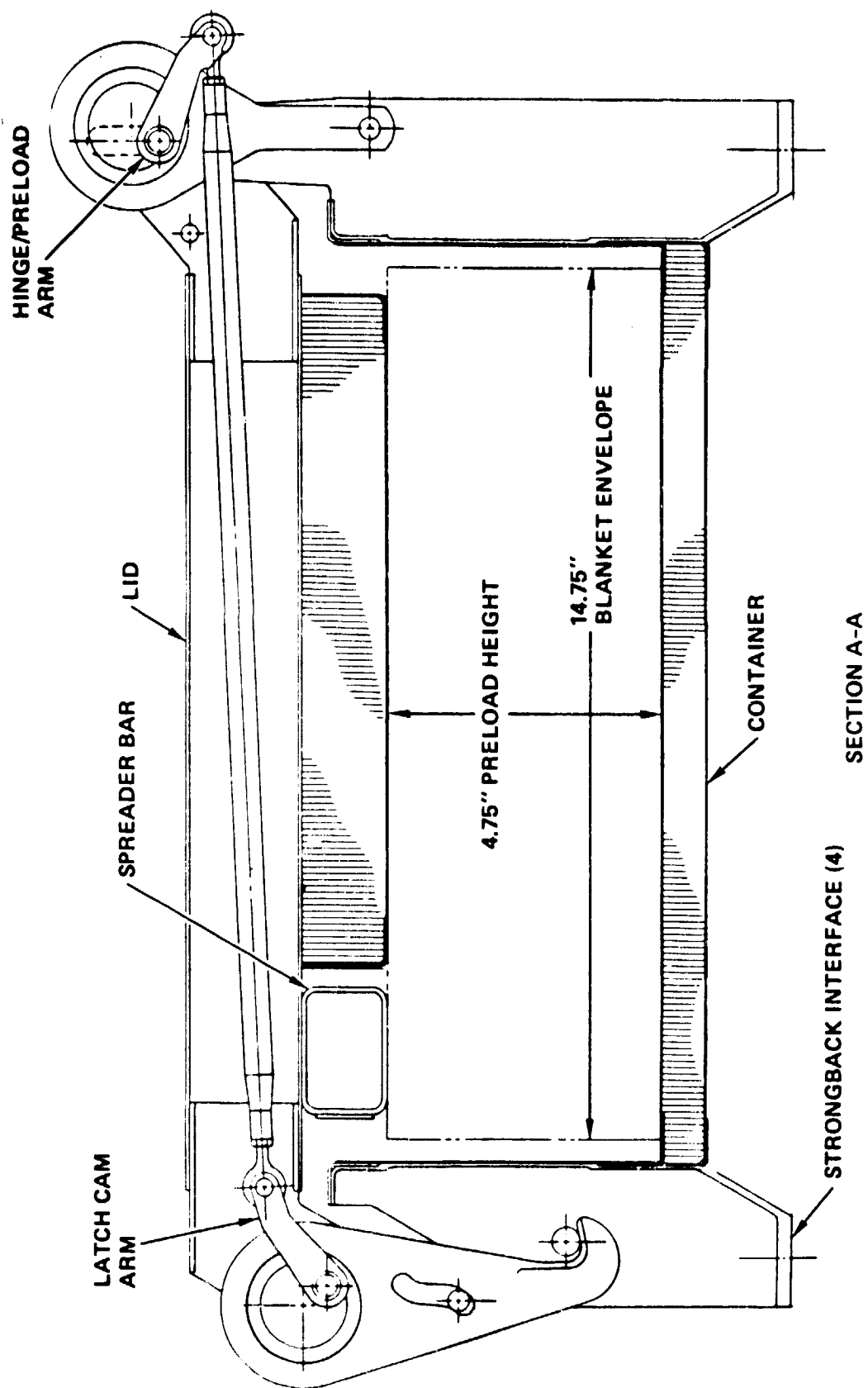Figure 35. Blanket Housing Baseline Design

LATCH(2)

LINKAGE

MAST INTERFACE

FOLDED SOLAR ARRAY

LID

CONTAINER

SPREADER BAR

A

A

TORQUE TUBE

LATCH & FITTING (2)

SPRING HOUSING

MOTOR

LID

-71-

HINGE/PRELOAD ARM

LID

SPREADER BAR

LATCH CAM ARM

4.75" PRELOAD HEIGHT

14.75" BLANKET ENVELOPE

CONTAINER

STRONGBACK INTERFACE (4)

SECTION A-A

Figure 36. Lid Latch and Preload Mechanism

in Figure 37 were considered and the multiple negator spring concept was selected. The principal advantages are to simplify the container design and blanket stowing condition, and to minimize the effect of single point failures.

The baseline design uses ten individual negator springs distributed over the length of the panel with a nominal two pounds of force in each spring. The length is sized to permit the base of the leader to extend above the open container lid and to accommodate all thermal and acceleration displacements that will occur in the deployed blanket. The flat negator springs pass through slots in the honeycomb floor of the container to take up reels mounted on the external side of the floor as illustrated in Figure 38.

3.3.4.4 Guide Wire System

The blanket guide wire system consists of two small diameter wires that are under a nominal constant 2-pound tension load during the deployment and retraction operation of the blanket. The wires, located at about one-third panel points, pass through holes in every other panel hinge (every hinge on shade side of blanket), to take up reels on the lower, outside surface of the container. Since the reels are relatively large, they are mounted flush to the container, requiring guide pulleys to rotate the wire through 90 degrees before reaching the reels. The negator springs are attached to the take-up reel shaft to impose a constant torque and hence a constant force on the wires. A sketch of the design features is presented in Figure 38.

3.3.5 Spreader Bar and Linkage

The upper end of the blanket is attached to the deployment mast through a spreader bar and linkage. The spreader bar provides a small, rigid member running the width of the blanket to provide stiffness in that direction, and to make the tension system effective during blanket in-plane motion. The baseline design concept for the spreader bar is a rectangular graphite tube. It attaches to the upper leader by bonding and/or bolts. It will have a pin on the fitting where the linkage attaches to engage a V-shaped
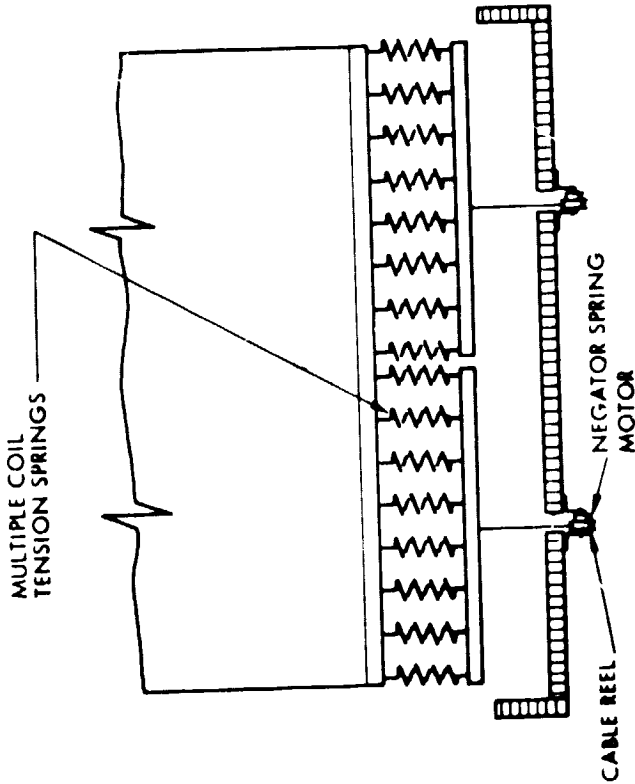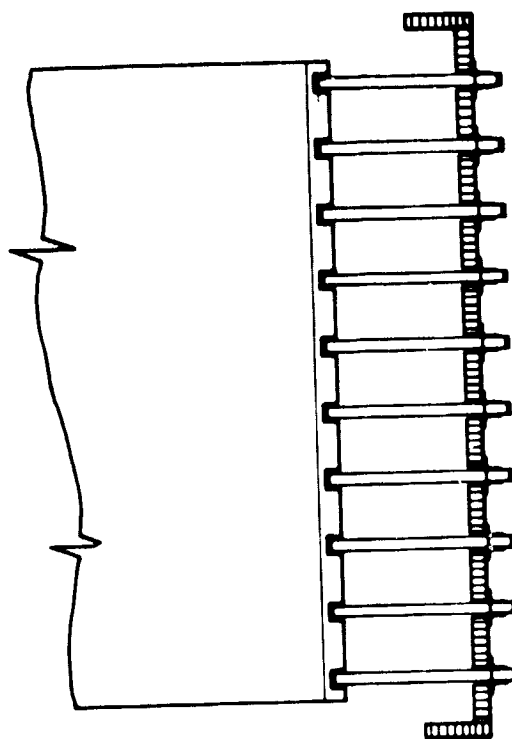
-73-

Figure 37. Blanket Tensioning System Concepts

BEAM + COIL TENSION SPRINGS

MULTIPLE COIL TENSION SPRINGS

NEGATOR SPRING MOTOR

CABLE REEL

ADVANTAGES	DISADVANTAGES
SINGLE TENSION SP... ...INIMUM FAILURE WOULD HA... EFFECT.	BAR & COIL SPRINGS THICKNESS INTERFERES WITH SMOOTH PACKING OF ARRAY PANELS. NEGATOR FAILURE COULD HAVE MAJOR ADVERSE EFFECT.

MULTIPLE NEGATOR TENSION SPRINGS

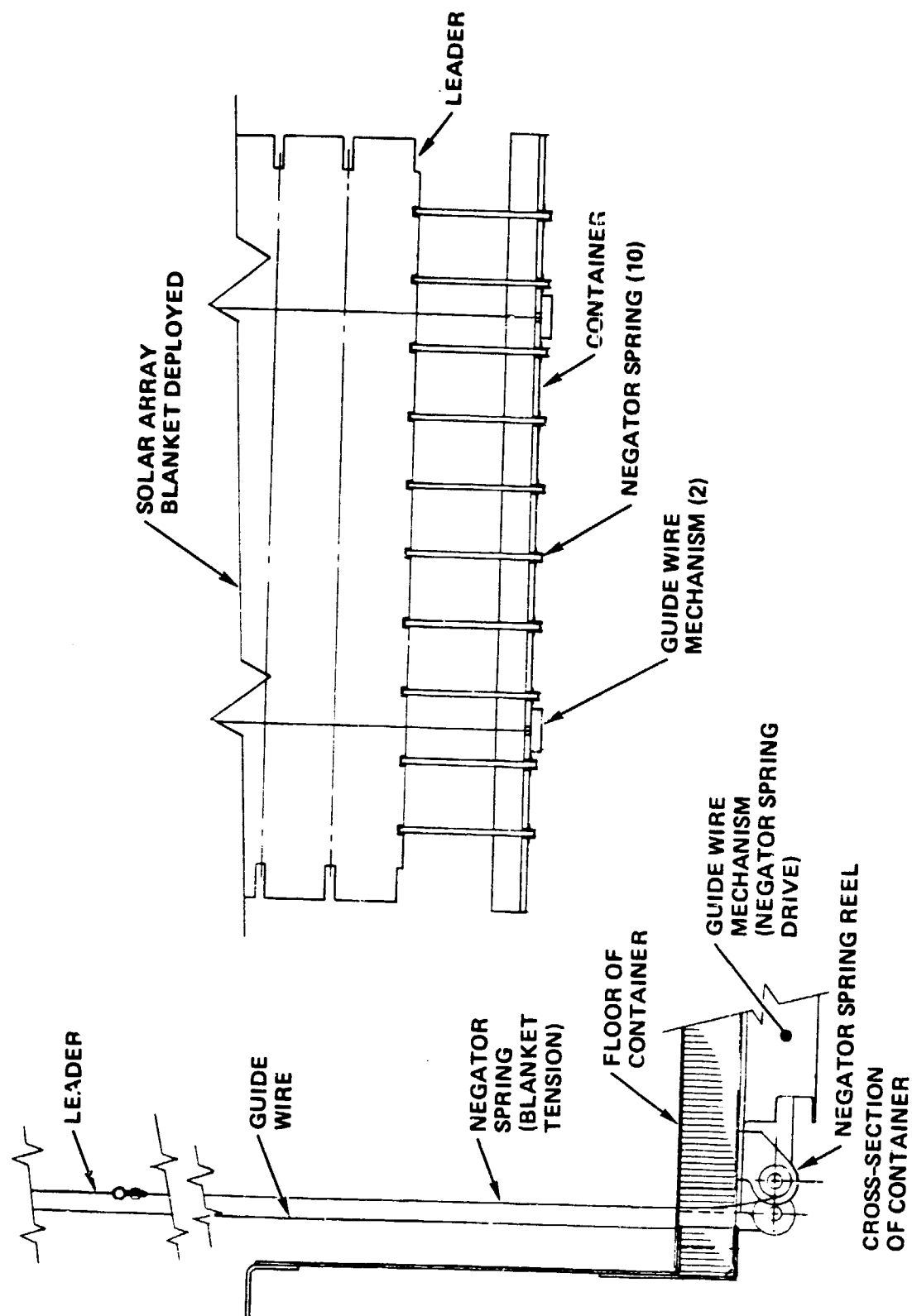| ADVANTAGES	DISADVANTAGES
NEGATOR AND MECHANISM RE-MOVED FROM PANEL STOWAGE AREA PERMITTING SMOOTH PACKING OF PANELS. SINGLE NEGATOR FAILURE WOULD HAVE A MINIMUM EFFECT.	FRICTION EFFECTS ARE GREATER.

Figure 38. Blanket Tensioning and Guide Wire Mechanism

fitting on the container. The pin will engage the V-fitting during the restowing operation to ensure proper positioning of the spreader bar in the container.

The linkage connects the mast tip fitting to the center of the spreader bar. For the rotating canister configuration, the linkage must be hinged at the joint with the spreader bar. The length is detemined by the distance between the stowed mast tip and the center of the spreader bar. A composite rectangular tube construction, as shown in Figure 35, is planned.

3.4 Weight Summary

A summary of the PEP solar array wing weight for the baseline design is presented in Figure 39. A total of 438 pounds is estimated if an aluminum container is used, versus a total of 417 pounds if a graphite container is used. The wing blanket is about 80 percent of that total. The solar cell stack weight is approximately 80 percent of the blanket weight, hence any significant weight savings, if required, would have to come from these elements. The cell stack and substrate weight items are based on extrapolated data taken from measurements of sample test panels, hence uncertainties regarding adhesive thickness and weight have been considerably reduced. The weight data is also based on an 8-mil thickness for the solar cell and a 6-mil thickness for the microsheet cover glass. Slightly thinner cells and covers and the substitution of fused silica in lieu of microsheet for the cover glass could provide substantial weight saving at higher costs.

3.5 Loads and Frequency Assessment

3.5.1 Design Loads

A preliminary assessment of the loads environment `s made for each component of the PEP design. The loads conditions and  namic environments `s specified in Reference 2 were used to make the assessment. A summary of the critical condition for each major component of the solar array is presented in Figure 40. The container primarily supports the blanket during launch and reentry, hence the critical conditions are the accelerations dur` lift-off transients and the high steady state loads

-76-

●WING BLANKET ASSEMBLY 355

● CELL STACK (CELLS, COVER SLIDES, INTERCONNECTS, ETC) 279

● SUBSTRATES 39

● HINGES 8

● TERMINAL STRIPS 1

● HARNESS 26

● TENSION AND GUIDE WIRE SYSTEM 5

● SPREADER BAR AND LINKAGE (GRAPHITE) 5

	ALUMINUM	GRAPHITE
●WING CONTAINER ASSEMBLY	73	52
● BASIC BOX STRUCTURE	47	31
● DEPLOYMENT, FITTINGS, ETC	26	21
TOTAL WEIGHT PER WING	438 LB	417 LB

Figure 39. PEP Solar Array Weight Summary

ITEM	CRITICAL CONDITION	COMMENT
• CONTAINER AND LID	LIFTOFF AND LANDING LOADS, BLANKET PRELOAD (STOWED)	PRELOAD DEPENDENT ON FLIGHT LOAD FACTORS AND FRICTION COEFFICIENTS. TEST DATA REQUIRED
• BLANKET ELEMENTS		
• SOLAR CELLS	VIBRATION AND FLIGHT LOADS IN STOWED CONDITION	CUSHIONED BY SUBSTRATE RIBS. DEPENDENT ON STOWED PRELOAD
• INTERCONNECTS AND SOLDER JOINTS	TEMPERATURE EXTREMES AND THERMAL CYCLES	
• SUBSTRATE AND HINGES	PRELOAD (DEPLOYED) IN COM-BINATION WITH PLUME PRES-SURES AND ORBITAL ACCELERATIONS	COMPLEX INTERACTION OF BLANKET TENSION, MAST STIFFNESS, PLUME LOADS, VEHICLE DYNAMICS AND ALLOWABLE DEFLECTIONS
• SPREADER BAR	BLANKET PRELOAD	

Figure 40. Loads Assessment

during reentry. These loads are highly dependent on the Orbiter cargo bay environments and the dynamic response characteristics of the PEP array deployment assemblies. Since Orbiter has not yet flown and the dynamic characteristics of the deployment assembly are preliminary, it is anticipated that several loads iterations will be required. The container lid is designed primarily for the blanket preload in the stowed condition. This preload, however, is partly dependent on the friction loads between the Kapton ribs and the solar cells. Preliminary loads have been determined and updates will be made after the component testing data has been evaluated.

The critical solar cell conditions are the vibration and flight loads in the stowed condition during boost, re-entry flight and landing. The protection for the cells comes from the ribs and blanket preload provided by the lid. Component testing will determine the magnitude of preload required. The interconnects and solder joints are usually critical for the thermal environments. The PEP baseline designs are identical to flight-proven configurations and because the PEP environment is more benign, this is not expected to be a critical problem area. The substrates and hinges are designed primarily for the tension load in the deployed configuration in combination with plume pressures and orbital accelerations. Current evaluations show a relatively low stress condition, however the actual loads are determined from a complex dynamic interaction of solar array, plume forces and Orbiter motions. Extensive analyses based on coupled models of the array, gimbals, RMS and Orbiter will be required. The spreader bar design condition is due to the tension load in the blanket and current sizing is based on a nominal twenty-pound load. Future trade studies on blanket/vehicle dynamics may revise this tension preload value, however changes in the spreader bar design should be minimal.

3.5.2 Frequency Assessment

Several dynamic models of the PEP solar array have been developed to determine the dynamic characteristics of the cantilevered mast/blanket combination and for use with the System Study Contractor's dynamic model of the core structure and RMS. A three-view picture of the cantilevered

model is presented in Figure 41. The mast and canister are represented
by a series of beam elements and are offset from the plane of the blanket
by 18.5 inches. The stiffness and mass characteristics are as follows:

$$L \quad = \quad 1500 \text{ inch}$$
$$D \quad = \quad 19.0 \text{ inch}$$
$$EI \quad = \quad 64 \times 10^6 \text{ lb-in}^2$$
$$GJ \quad = \quad 83 \times 10^6 \text{ lb-in}^2$$
$$Wt/L \quad = \quad 0.0576 \text{ lb/in}$$

The blanket, hinges, tensioning system, spreader bar and linkages are repre-
sented by a combination of membrane and beam elements. Since the membrane
elements out of plane stiffness are dependent on the tension preload, a
nominal value of 20 pounds was used in one version of the model. It should
also be noted that the negator springs carry a constant load independent of
the displacement, hence in the blanket longitudinal direction these items
were modeled with a zero spring rate. The blanket parameters are:

$$L \qquad \qquad = \quad 1500 \text{ inch (blanket panels, leaders, linkage)}$$
$$W \qquad \qquad = \quad 137.6 \text{ inch (effective width)}$$
$$Wt/A \qquad \quad = \quad 0.00171 \text{ lb/in}^2$$
$$\text{Tip Wt} \qquad \quad = \quad 15.0 \text{ lbs}$$
$$\text{Blanket tension} \quad = \quad 20 \text{ lbs}$$

A summary of the dynamic characteristics of the cantilevered model is
presented in Table 4. Plots of the first five mode shapes are presented in
Figures 42 through 56. Each mode shape is plotted with three different views
to provide a better understanding of the model characteristic. It is evident
that the first mode is out-of-plane bending of the mast and blanket. The
second mode is pure in-plane bending which is controlled entirely by the mast
stiffness. Mode 3 is the second out-of-plane bending mode and Mode 4 is a
pure torsion (i.e., twist) mode about the blanket's longitudinal axis. The
higher modes involve coupled motion of blanket and mast.
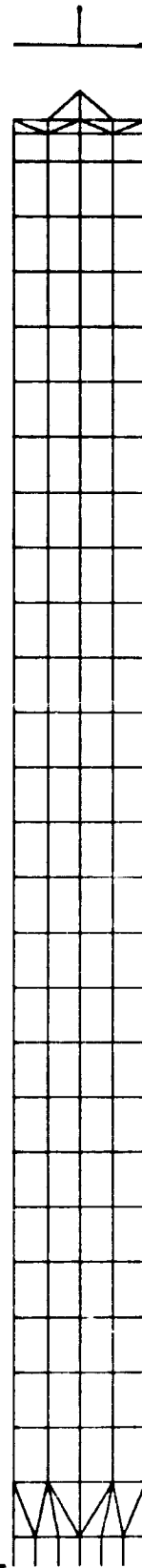
-80-

Figure 41
PEP SOLAR ARRAY DYNAMIC MODEL, 11/2/79

PLAN VIEW (Z-VIEW)

SIDE VIEW (Y-VIEW)

END VIEW
(X-VIEW)

X = 0

Y = 0

I = INFEG
M = PEPMOD

PJV4 3.3
11/21/79.
09.52.40.

(TRWSAP)

Table 4
PEP SOLAR ARRAY DYNAMIC MODEL
DYNAMIC CHARACTERISTICS

MODAL DESCRIPTION	FREQUENCY Hz	PARTICIPATION FACTORS		
		X	Y	Z
1st Blanket/mast (out-of-plane) bending	.0493	-.016	0	-.969
1st Mast bending (in-plane), blanket rigid, mast and blanket in-phase	.0691	0	.925	0
2nd Blanket (out-of-plane) bending	.0966	-.025	0	.009
1st Blanket torsion	.1004	0	.001	0
3rd Blanket (out-of-plane) bending	.1490	.023	0	.273
2nd Blanket torsion	.2006	0	0	0
4th Blanket (out-of-plane) bending	.2098	.018	0	-.068
1st Mast bending (in-plane), blanket rigid, mast and blanket out-of-phase	.2772	0	-.458	0
5th Blanket (out-of-plane) bending	.2780	.014	0	.131
3rd Blanket torsion	.3008	0	-.002	0

Modes normalized to a generalized mass of 1.0.

Figure 42.

PEP SOLAR ARRAY DYNAMIC MODEL, 11/2/79
PEP SOLAR ARRAY   X-VIEW
FREQUENCY   .049 HZ (11/20/79.   11.13.44.)

MODE NUMBER   1

I = INFEG
M = PEPMOD
MX = PEPMOD8

PJV4 4.4
11/21/79.
09.52.40.

SCALE = 5.75E+1

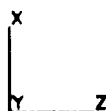(TRWSAP)

-83-

PJV4 5.5
11/21/79.
09.52.40.

PEP SOLAR ARRAY DYNAMIC MODEL, 11/2/79
PEP SOLAR ARRAY   Y-VIEW
MODE NUMBER   I   FREQUENCY   .049 HZ (11/20/79.   11.13.44.)
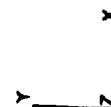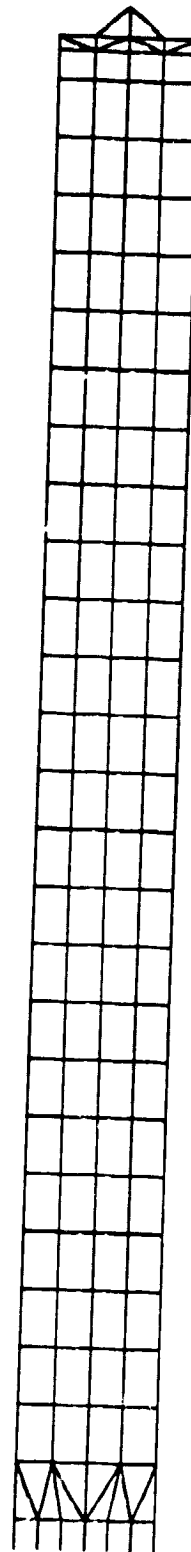
I = INFEG
M = PEPMOD
MX = PEPMOD8

Figure 43.

(TRWSAP)

SCALE = 5.75E+1

Figure 44.

PEP SOLAR ARRAY DYNAMIC MODEL, 11/2/79
PEP SOLAR ARRAY   Z-VIEW
MODE NUMBER   1   FREQUENCY   .049 HZ (11/20/79.   11.13.44.)

I = INTEG
M = PEPMOD
MX = PEPMODS

SCALE = 5.75E+1

(TRWSAP)

Y
Z   X

Figure 45.

PEP SOLAR ARRAY DYNAMIC MODEL 11/2/79
PEP SOLAR ARRAY   X-VIEW
MODE NUMBER   2   FREQUENCY   .069 HZ (11/20/79.   11.13.44.)

I = INFEO
M = PEPM00
MX = PEPM006

PJM4 7.7
11/21/79.
09.52.40.

SCALE = 4.71E+1

(TRWSAP)

-86-

PJW 8.8
11/21/79.
09.52.40.

PEP SOLAR ARRAY DYNAMIC MODEL, 11/2/79
PEP SOLAR ARRAY   Y-VIEW
MODE NUMBER   2   FREQUENCY   .069 HZ (11/20/79.   11.13.44.)

I = INFEG
M = PEPMOD
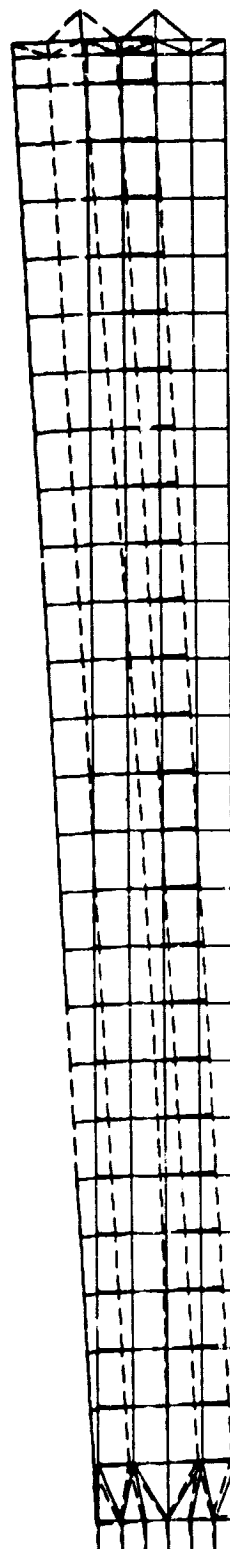MX = PEPMODB

Figure 46.

(TRWSAP)

SCALE = 4.71E+1

Figure 47.

PEP SOLAR ARRAY DYNAMIC MODEL, 11/2/79
PEP SOLAR ARRAY   Z-VIEW
MODE NUMBER   2   FREQUENCY   .069 HZ (11/20/79.   11.13.44.)

I = INFE9
M = PEPMOD
MX = PEPMODB

PJVE 9.9
11/21/79.
09.52.40.

SCALE = 4.71E+1

(TRNSAP)

-88-
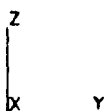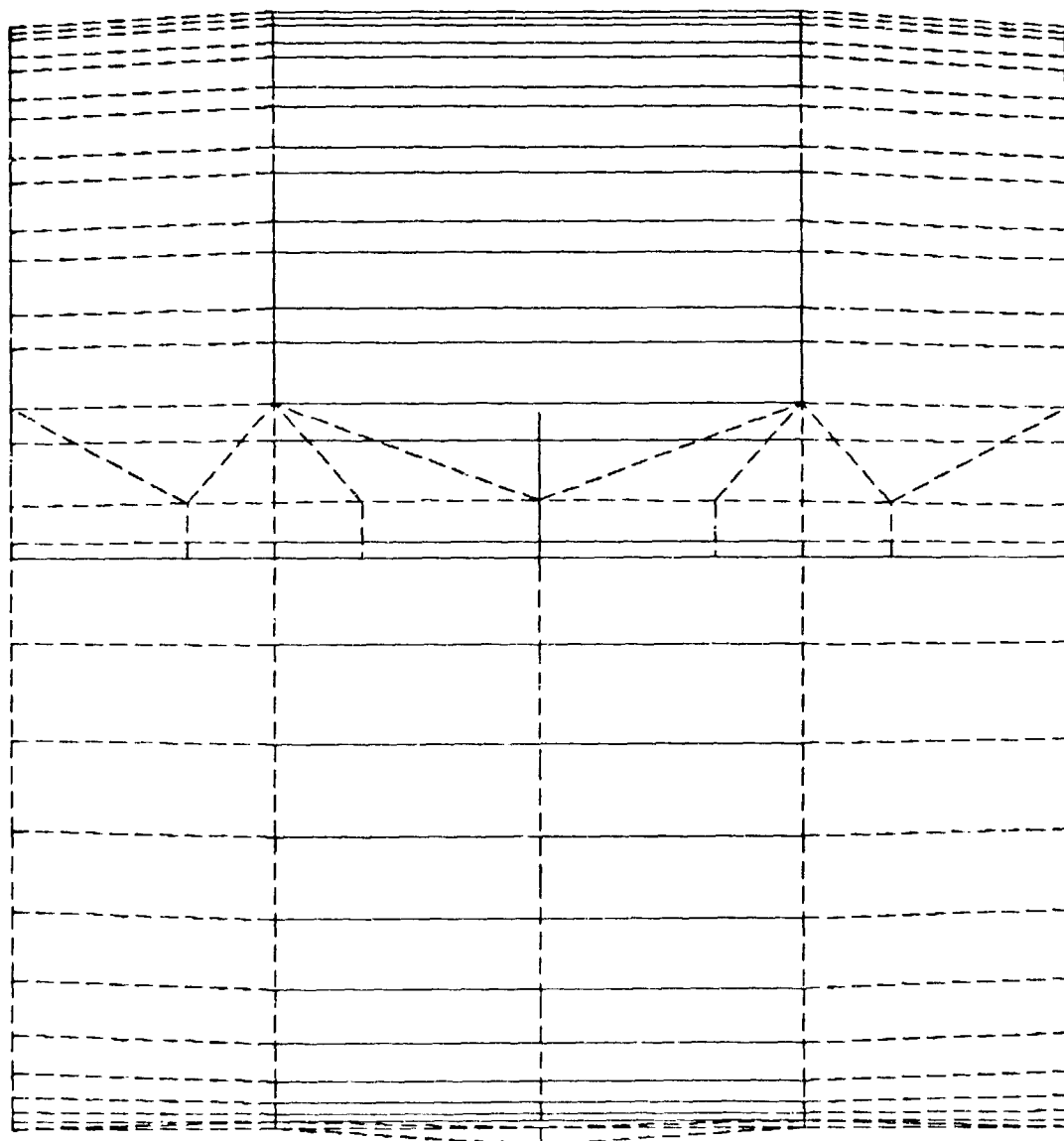
PJV4 10.10
11/21/79.
09.52.40.

PEP SOLAR ARRAY DYNAMIC MODEL, 11/2/79
PEP SOLAR ARRAY   X-VIEW
MODE NUMBER   3   FREQUENCY   .097 HZ (11/20/79.   11.13.44.)

I = INFEG
M = PEPMOD
MX = PEPMOD8

Figure 48.

Z

X____Y

(TRWSAP)

SCALE = 5.32E+1

PEP SOLAR ARRAY DYNAMIC MODEL, 11/2/79   I = INFEG
PEP SOLAR ARRAY   Y-VIEW   M = PEPMOD
MODE NUMBER   3   FREQUENCY   .097 HZ (11/20/79.   11.13.44.)   MX = PEPMOD8

Figure 49.

(TRWSAP)   SCALE = 5.32E+1

Figure 49.

Figure 50.

PJV4 13.13
11/21/79.
09.52.40.

PEP SOLAR ARRAY DYNAMIC MODEL, 11/2/79
PEP SOLAR ARRAY   X-VIEW
MODE NUMBER   4   FREQUENCY   .100 HZ (11/20/79.   11.13.44.)

I = INFEG
M = PEPMOD
MX = PEPMOD8

Figure 51.

Z

X   Y

(TRWSAP)

SCALE = 3.35E+1

PJW 14.14
11/21/79.
09.52.40.

PEP SOLAR ARRAY DYNAMIC MODEL, 11/2/79
PEP SOLAR ARRAY   Y-VIEW
MODE NUMBER   4   FREQUENCY   .100 HZ (11/20/79.   11.13.44.)

I = INFEG
M = PEPMOD
MX = PEPMOD8
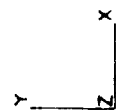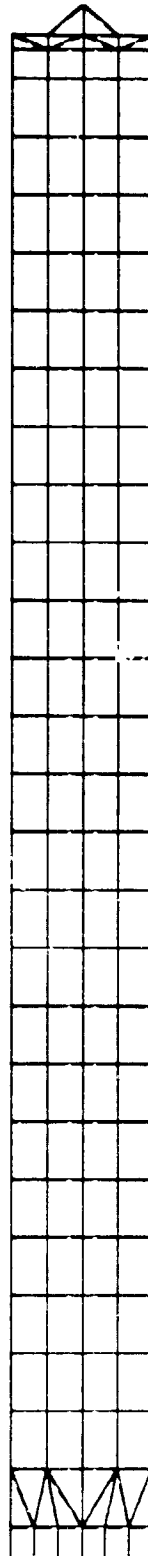
Figure 52.

X

Y   Z

(TRWSAP)
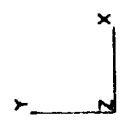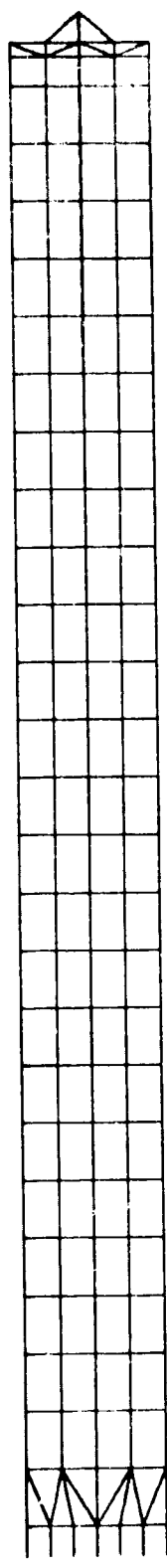
SCALE = 3.35E+1

Figure 53.
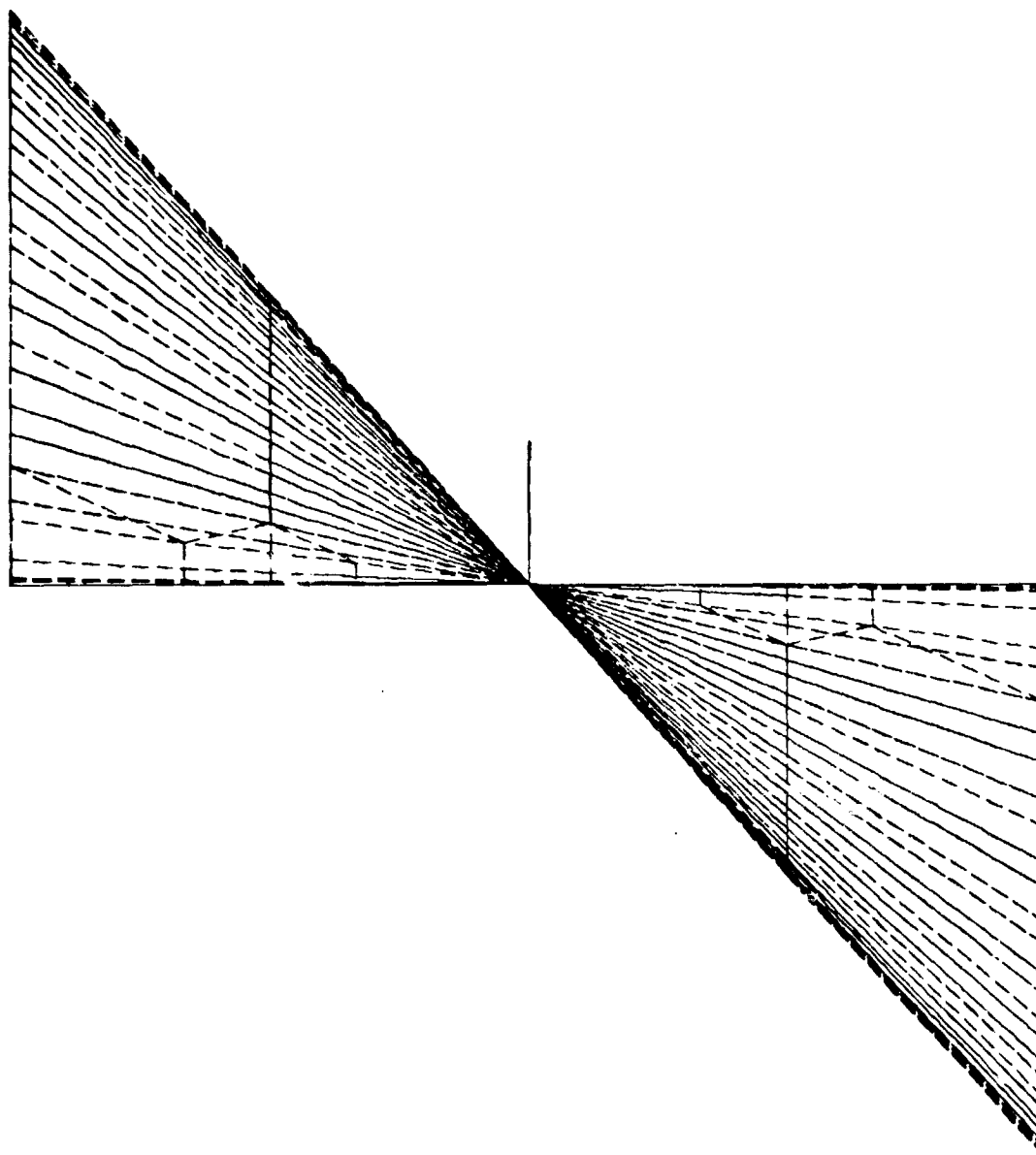
PJV4 16.16
11/21/79.
09.52.40.

PEP SOLAR ARRAY DYNAMIC MODEL, 11/2/79
PEP SOLAR ARRAY   X-VIEW
MODE NUMBER   5   FREQUENCY   .149 HZ (11/20/79.   11.13.44.)

I = INFEG
M = PEPMOD
MX = PEPMOD8

Figure 54.
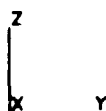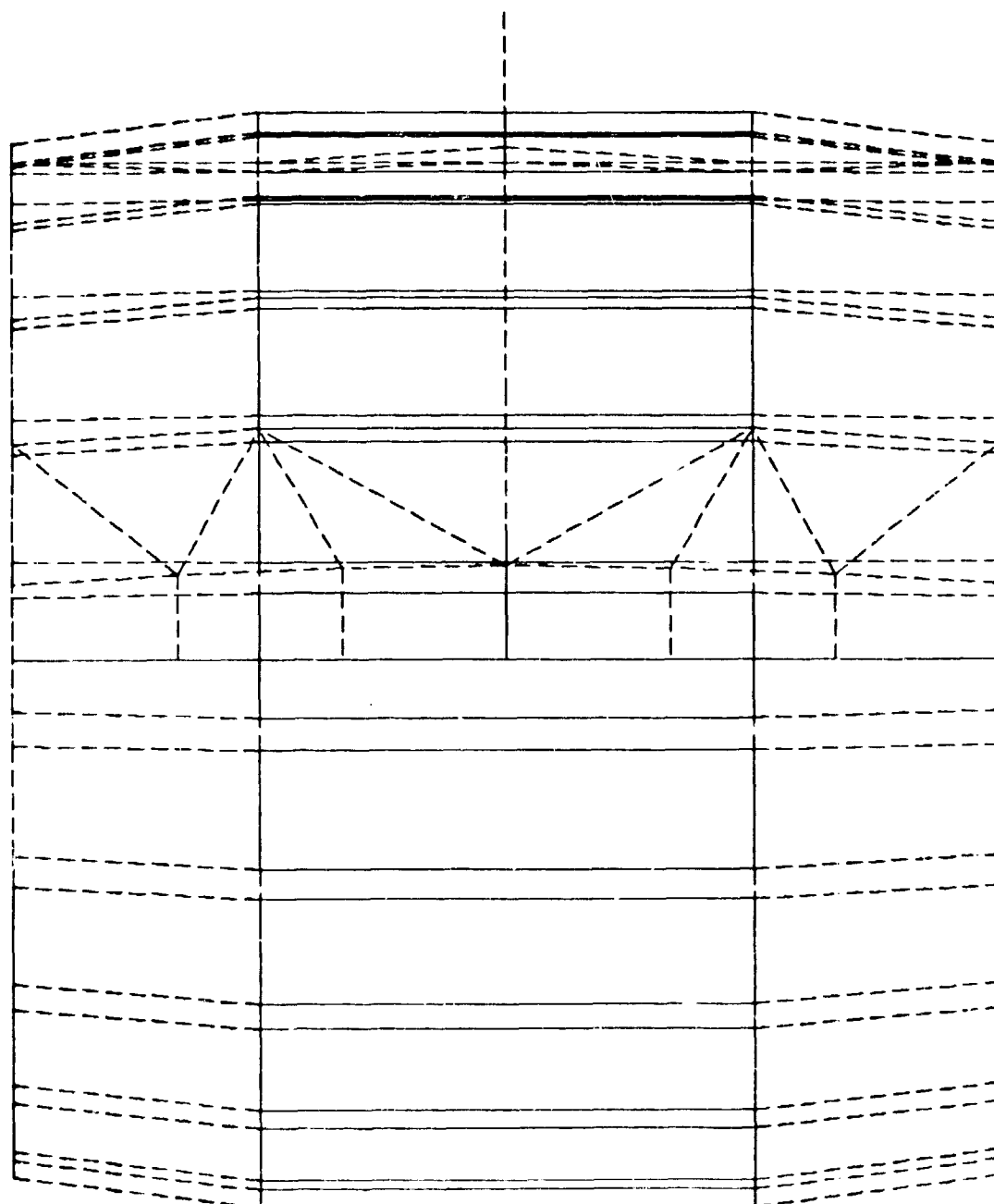
(TRWSAP)

SCALE = 5.35E+1

PEP SOLAR ARRAY DYNAMIC MODEL, 11/2/79
PEP SOLAR ARRAY   Y-VIEW
MODE NUMBER   5   FREQUENCY   .149 HZ (11/20/79.   11.13.44.)

I = INFEG
M = PEPMOD
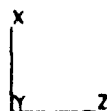MX = PEPMOD8

Figure 55.

X

Y   Z

(TRWSAP)

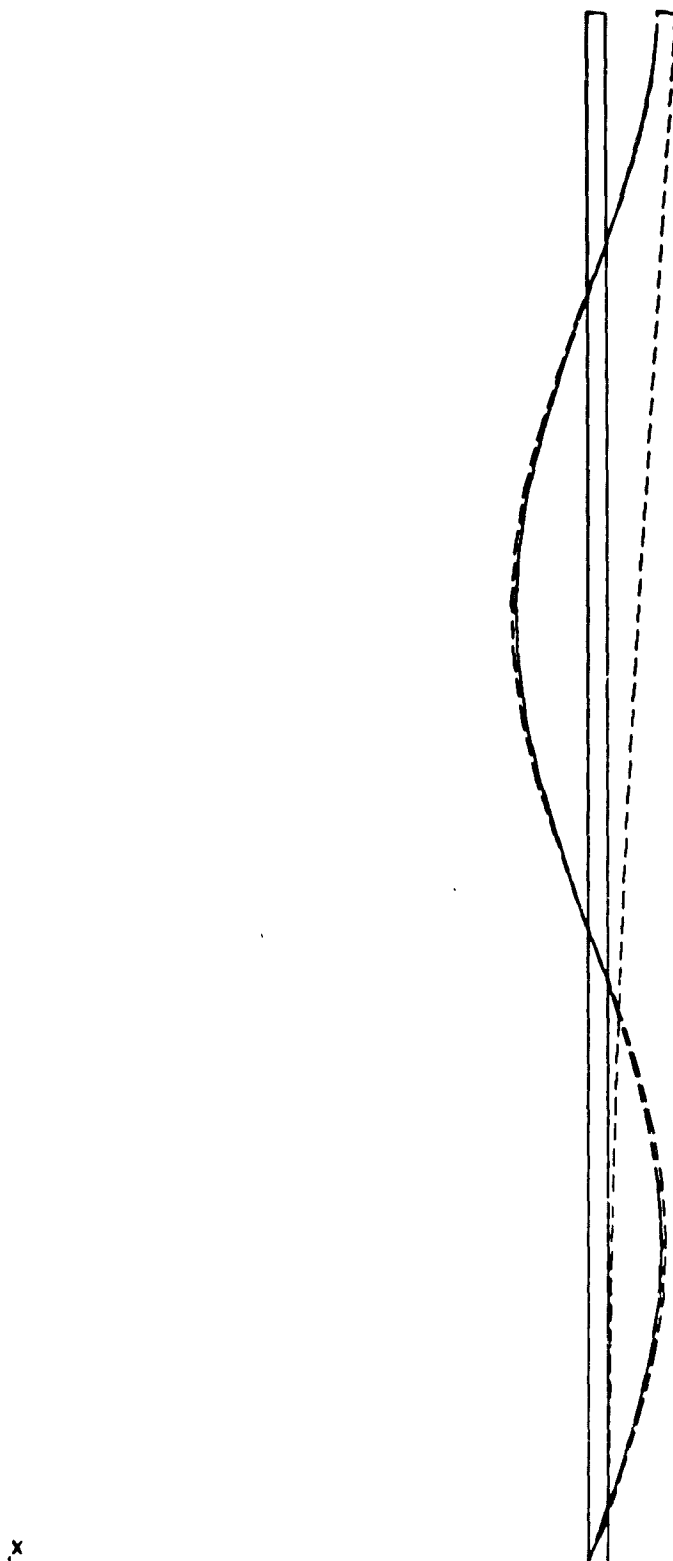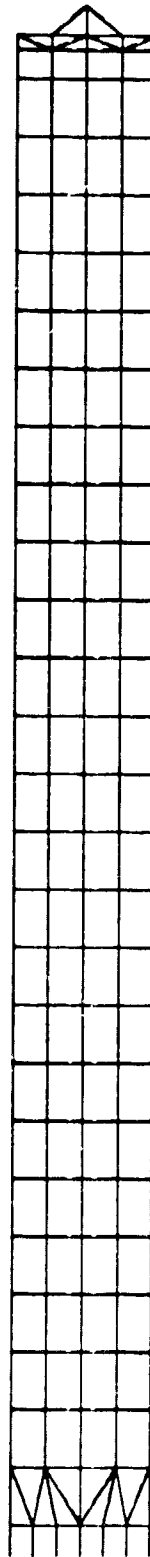SCALE = 5.35E+1

Figure 56.

PEP SOLAR ARRAY DYNAMIC MODEL 11/2/79
PEP SOLAR ARRAY Z-VIEW
FREQUENCY .149 HZ (11/20/79. 11.13.44.)

MODE NUMBER 5

PJV4 18.18
11/21/79.
09.52.40.

I = INFEQ
M = PEPMOD
MX = PEPMODB

SCALE = 5.35E+.

(TRKSQD)

-97-

There are certain parametric studies of the solar array dynamic characteristics that can be made, however the primary requirement is to perform the coupled system response analyses. These analyses would determine the need for an isolation system for the array wings, the adequacy of the mast strength and stiffness, and the relative deflections between mast and blanket. Once the baseline design has been analyzed then the need and direction for any solar array changes can then be formulated.

3.6 Thermal Analyses Summary

The thermal analysis/design tasks include the following: array configuration-thermal tradeoffs, nominal orbit-cell transient temperature prediction, cell hot spot/open circuit thermal analysis and distortion thermal analysis.

3.6.1 Array Configuration-Thermal Tradeoffs

A tradeoff involving cell solar absorptance and substrate Kapton thickness has been completed. The array heating (solar, earth albedo and earth infrared) was taken at the subsolar point for the nominal 220 nautical mile earth orbit altitude (Beta = 50°). The solar absorptance was varied between 0.7 and 1.0 for total thicknesses of 1, 2 and 4 mil Kapton. The corresponding solar absorptance (α) and infrared hemispherical emittance (ϵ) for Kapton was:

Total Kapton Thickness (mil)	α	ϵ
1	.36	.5
2	.44	.78
4	.53	.8

The emittance of the glassed cell was 0.81.

The results of the tradeoff are presented in Figure 57, which contains plots of cell temperature versus solar absorptance for total substrate thicknesses of 1, 2 and 4 mil. Temperature-wise, there is no difference between 2 and 4 mil. With the obvious selection of the 2-mil thickness, the baseline operating temperature is 58°C and non-operating temperature is 69°C (α = .75) as shown in Figure 17.
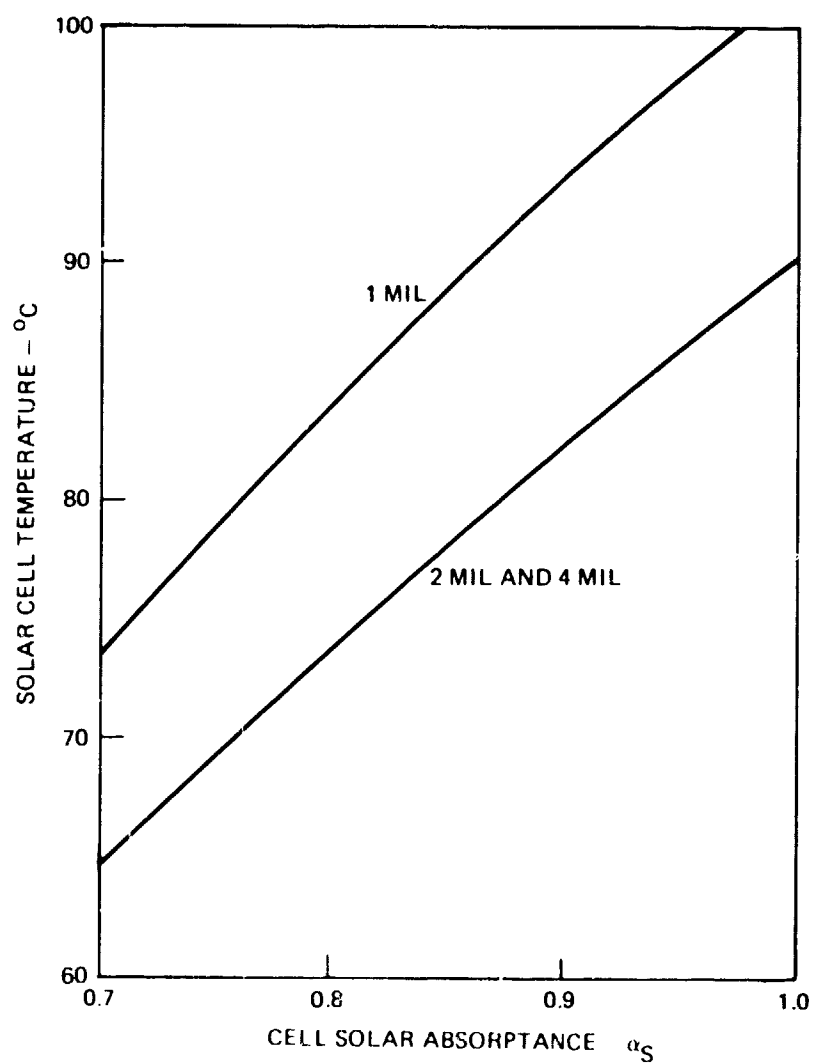
Figure 57. Solar Cell Temperature versus Solar Absorptance and Substrate Thickness

3.6.2 Cell Hot Spot/Open Circuit - Thermal Analysis

A cell hot spot/open circuit thermal analysis was completed and the results are summarized in Figure 58. The thermal properties and orbital heating are the same as those defined above for the two plies of 1-mil Kapton configuration. Hot spot cell heating was varied from 0 to 15 watts per cell for the nominal solar cell and expressed for convenience in units of equivalent solar constants.

3.6.3 Nominal Orbit - Cell Transient Temperature Prediction

A transient thermal analysis of the selected array configuration was performed and solar cell temperature levels in the nominal orbit (Beta = 50° - 220 nmi altitude) were determined. Results are presented in Figure 59. The operating array thermophysical properties were as previously defined. The transient orbital heating was determined utilizing TRW's version of the computer program FLUXORB. The heating rates were then input to the TRW Thermal Analyzer Program (TAP) to obtain the solar cell temperature levels. As may be observed in Figure 59, the cell temperature varies from a maximum of 57°C at the subsolar point to a minimum of -87°C at the end of the eclipse.

3.6.4 Distortion - Thermal Analysis

A first order thermal analysis of the PEP solar array including ribs, hinges and harness was completed in order to perform an initial evaluation of array distortion. Typically, the analysis was done steady state at the subsolar point and the thermophysical properties utilized were the same as described above.

Cell and rib temperature levels and gradient calculations were performed for the cell and cell side ribs, and for the substrate side rib. The rib solar transmittance was measured by TRW's Thermophysics Laboratory and found to be 0.6ᶠ. The calculations show the temperature gradient for the bulk of the array (cover, cell, etc.) is very small (2°F) and that for the relatively small rib area is large, averaging 180°F on the cell side and 250°F on the substrate side.
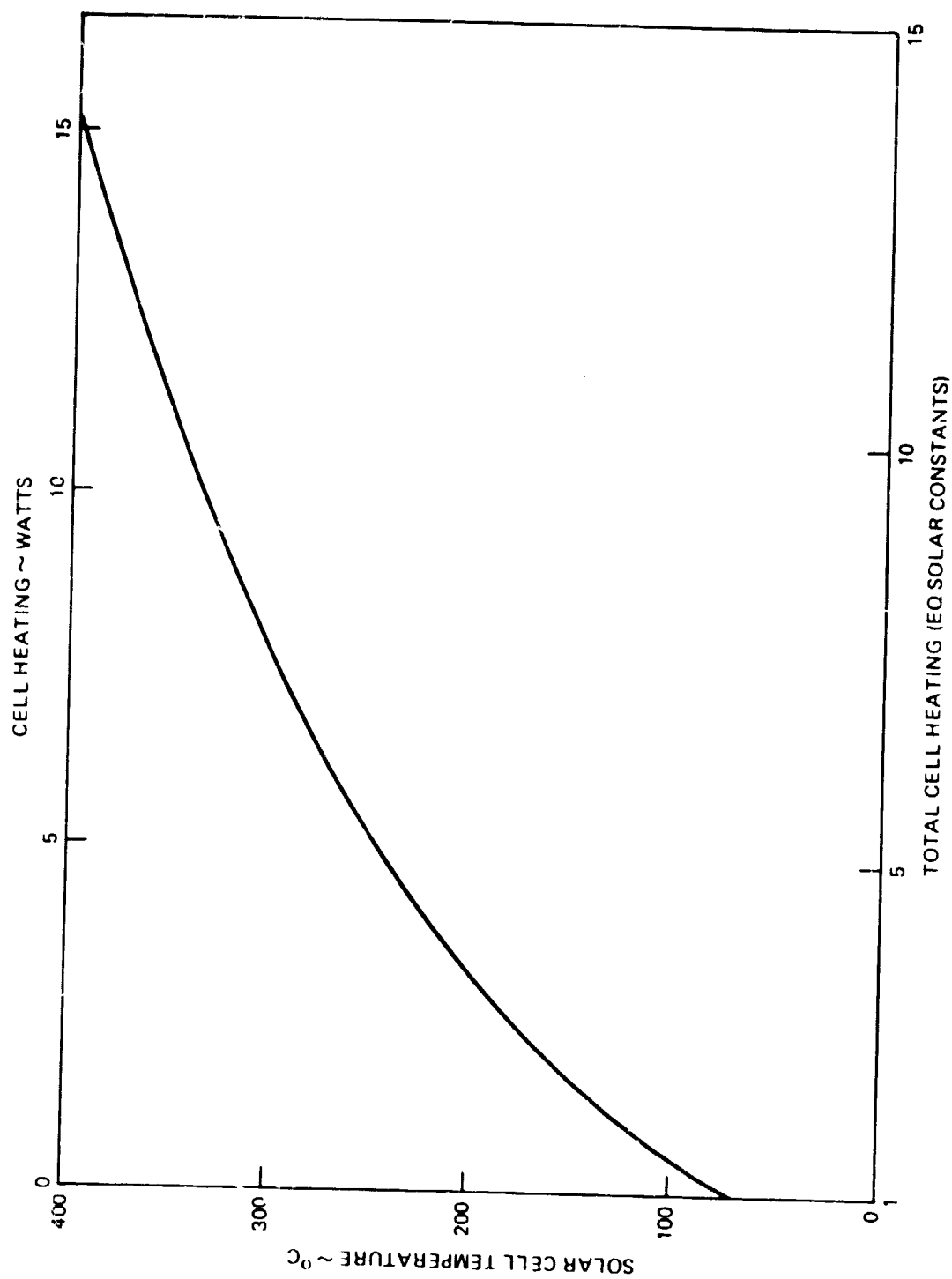
-100-

Figure 58. Solar Cell Hot Spot Temperature versus Cell Heating
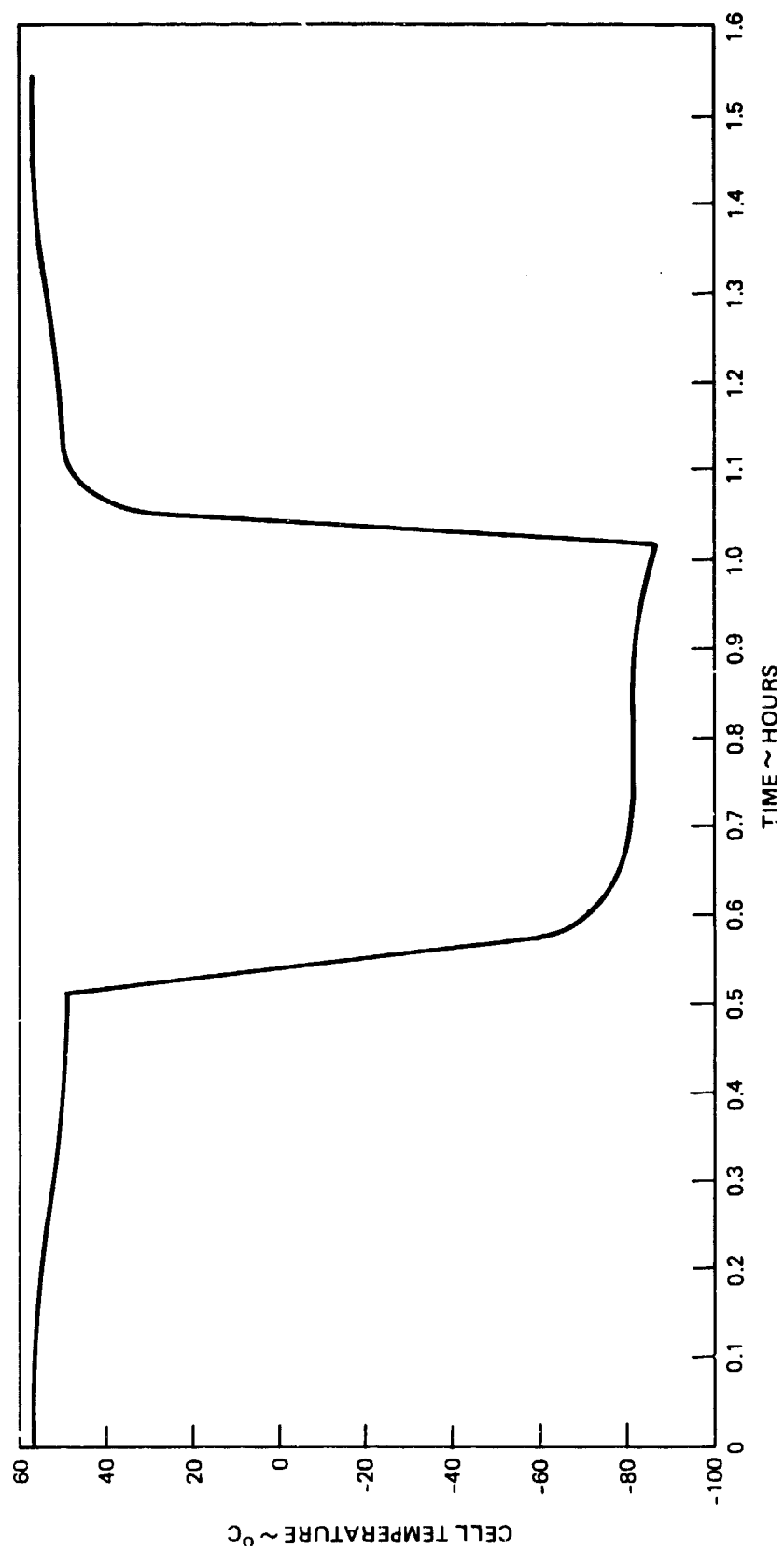
Figure 59. Solar Cell Orbital Temperature Profile

The hinge temperature data was also determined for an extreme orbital condition. The solar absorptance and infrared hemispherical emittance of the spacer was considered to be 0.8 and 0.9, respectively. Hinge gradients were found to be relatively large; i.e., 270°F for the cell side hinge and 245° F for the substrate side hinge.

The final definition of line losses and the harness design details were not available prior to completion of the thermal analysis. Therefore the analysis was done parametrically (wire size and line loss) for utilization in the harness definition and the results are presented in Figure 60. Actual power lead losses ranged from 190 milliwatts/ft for inner panels to 45 milliwatts/ft for outer panels. The temperature gradient across the harness is estimated to be negligible for 3% line losses.

4.0 DESIGN SUMMARY

4.1 Baseline Configuration

The baseline configuration for TRW's concept of the PEP solar array wing is presented in Figure 61. The design is a flexible, lightweight, foldout array consisting of 102 solar cell panels per wing. The overall wing length is 37.0 meters (1456 inches) and 3.81 meters (150 inches) wide. Each panel consists of 1200 solar cells mounted on a substrate of two plies of one mil Kapton. Rib stiffeners are formed into each ply to provide solar cell protection in the stowed condition and panel stiffening in the deployed configuration.

The silicon solar cells are 2.22 x 3.96 cm in size, 8 mils thick with a power conversion efficiency of 14% at 28°C. Each cell is covered with a microsheet cover glass of 6 mils. Conventional shaped Invar interconnects are soldered to the cells to provide 8 strings of 150 cells for each panel. Pair of adjacent panels are wired in series to produce approximately 122 volts and a total power output of 16.4 kilowatts per wing.

The baseline solar array is deployed from an aluminum honeycomb container by a mast/canister device. The container lid is opened and closed by redundant stepper motors which also compress the blanket in the stowed position and
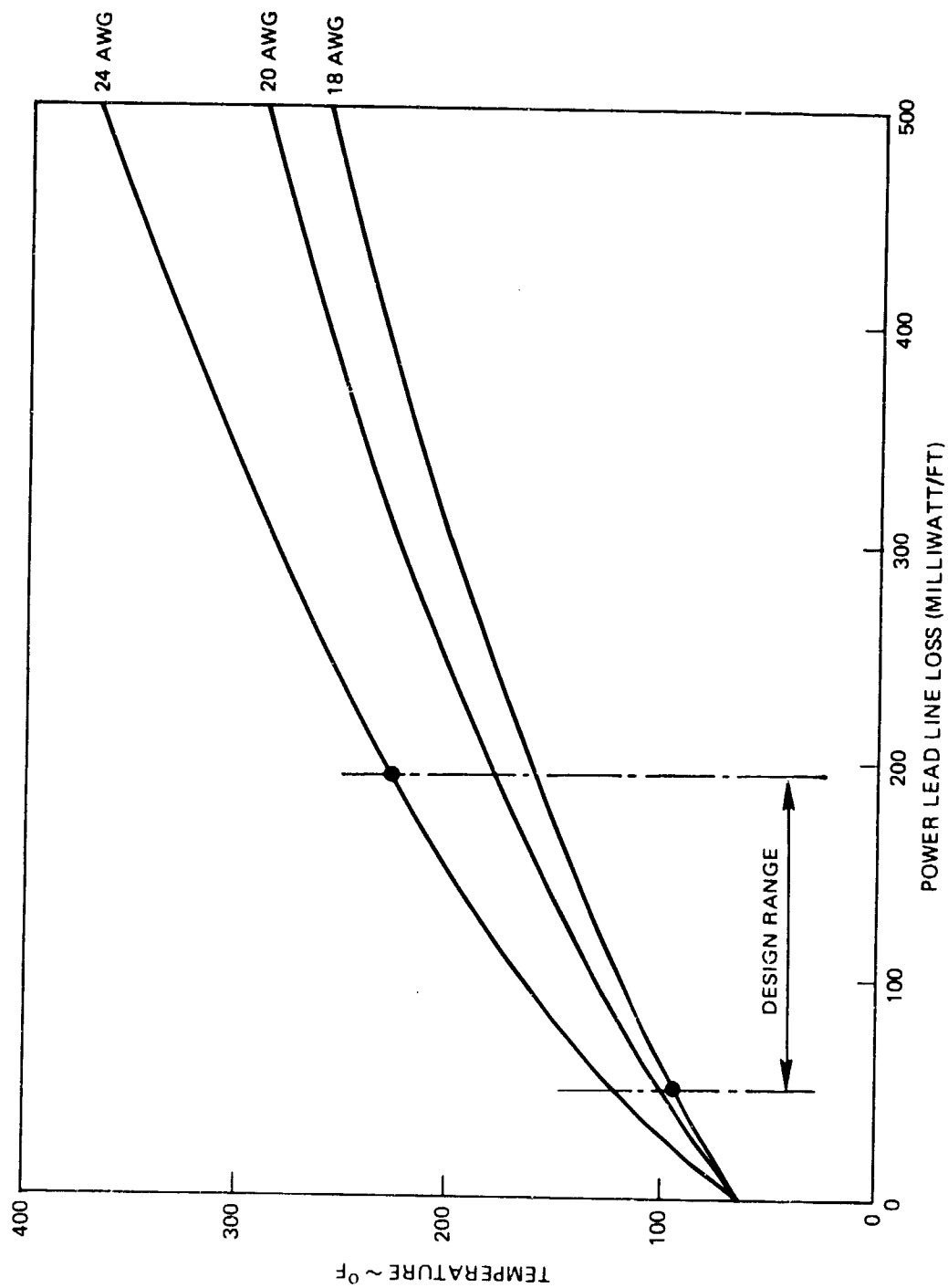
Figure 60. Harness Temperature versus Power Lead Line Loss

DESIGN FEATURES

- SOLAR CELLS — 2.22 x 3.96 CM
  8 MIL THICK
  14% EFFICIENCY
  CONVENTIONAL SOLDERED
  INTERCONNECTS

- COVER GLASS — 6 MIL MICROSHEET

- SUBSTRATE — 2 PLIES OF ONE MIL
  KAPTON WITH INTEGRAL
  RIB STIFFENERS

- PANEL SIZE — 0.36 x 3.81 M

- WING SIZE — 102 PANELS
  3.81 x 37.0 M
  140.9 M² AREA

- POWER OUTPUT (BOL) — 16.4 KW
  (PER WING)

GUIDE WIRE

PANEL HINGE

EXTENSION/
RETRACTION*
MAST

ARRAY
CONTAINER

LINKAGES

SPREADER
BAR

ARRAY
HARNESS

MAST*
CANISTER

CORE
STRUCTURE*

*SYSTEM CONTRACTOR ELEMENTS

Figure 61. PEP Solar Array Design – Baseline Concept

-105-

activate the latches which seal the lid closed. Other essential elements of the baseline design include a 10 spring tensioning mechanism to maintain the blanket under a constant load when deployed, and a guide wire system to provide blanket displacement control during the deployment and restowing operations.

The TRW baseline solar array design meets all of the requirements. The concept is low risk to the extent that the solar cell type, solar cell size and the interconnector designs are selected from existing, flight proven, conventional designs and uses manufacturing processes currently in operation by solar cell suppliers. The substrate designs are new and unique, however test samples have been built and thermal cycling tests have been performed to demonstrate the compatibility of substrate and solar cells in a thermal environment.

4.2 Alternate Design

A variety of design concepts have been evaluated for various elements of the PEP solar array. The principal alternate design, that has the potential for significant cost savings, is the use of large solar cells. An assessment of the solar array configuration using the large 5.3 x 5.7 cm cells shows only minor impacts on the panel design. The use of this cell size improves the package efficiency per panel to the extent that two less panels per wing are required compared to the baseline design to meet the wing power output requirement. Because of the fewer number of cells in series the voltage per panel is less, necessitating that 5 panels be connected in series to meet the array voltage requirement.

Another possible design alternative is the use of a composite material container in lieu of the aluminum design. There is a cost penalty associated with the weight saving and the final selection of container material is dependent on whether weight or cost is the primary driver. Another study to be performed is cost-weight trades associated with solar cell and cover glass thickness. Reducing the thickness of these items below the baseline design could have an impact on other elements such as the substrate and container and further study would be required before this alternative is considered viable.

References

1. TRW Report 35515-6002-RU-00, "PEP Solar Array Definition Study, Final Programmatic Report," 30 October 1979

2. MDAC Briefing Charts MDC G7890, "Power Extension Package, Final Review", 14 August 1979

3. MDAC Report MDC G7870, "Power Extension Package, System Definition Extension, Orbital Service Module System Analysis Study", August 1979 Volumes 1-12.

4. MDAC Letter A3-900-CJD-L-71, "PEP Solar Array Study, Revised Coordination Plan," 25 May 1979

APPENDIX A

RESULTS OF THERMAL CYCLING TEST

ON PEP SOLAR CELL PANEL

APPENDIX A

THERMAL CYCLING TEST ON PEP SOLAR CELL PANEL

A-1 INTRODUCTION

This Appendix presents data on a thermal cycling test that was performed on a small solar cell panel using 5 x 5 cm solar cells and the TRW type flexible ribbed substrate. The test was performed in accordance with the general requirements as defined in the NASA/JSC Statement of Work. Included here are details on the solar cells and cover glass, the fabrication processes of the test panel, and results of the thermal cycling test.

The primary purpose of the test was to demonstrate the compatibility of the large 5 x 5 cm solar cells and the TRW flexible substrate design in a typical operational environment. Thirty-six of the 50 x 50 x 0.25 mm BSR cells were bonded to the two-ply, ribbed Kapton substrate. The panel was mounted in a temperature-controlled test chamber and subjected to thermal cycling between -80°C and +60°C. The power output from individual 6-cell strings was periodically measured to determine any changes in performance caused by the cycling process. A total of 3275 thermal cycles were achieved in the time period allocated to the test. Some solar cell cover glass cracks were observed, but electrical performance did not degrade as a result of the environmental exposure.

A-2 TEST PANEL DESCRIPTION

Two test panels were fabricated using ribbed Kapton substrates. Each substrate consists of two plies of 0.001 inch thick Kapton sheets with integral formed ribs on both front and back plies. The ribs on the back side run 90° with respect to the ribs on the front side. The two plies are bonded together using a nitrile film adhesive. The solar cell strings are between the front ribs. Each panel holds six solar cell strings, consisting of six glassed 5 x 5 cm cells per string, all interconnected with three

U-shaped Tracking and Data Relay Satellite System (TDRSS) type interconnectors per cell. The following is the material list:

Solar Cell, (5x5 cm):	1.969 x 1.969 x 0.012 in. Solder covered
Interconnector (TDRSS):	Invar, 0.001 in. thick, Ag-plated
Cover Glass:	Microsheet, 1.980 x 1.980 x 0.006 in.
Adhesive, (cover-to-cell):	DC 93-500
Termination Bars, (Pos.&Neg.):	0.0065 in. thick x 0.2 in. wide(TDRSS)
Adhesive, (cell-to-substrate):	RTV-118
Substrate:	Kapton, 14.25 x 14.25 x 0.0045 in.

A-3 TEST PANEL ASSEMBLY

The sequence of assembly was as follows:

1. Reflow-soldering of three interconnectors/cell to front cell contact.

2. Application of cover glass.

3. Preliminary performance test (low light intensity).

4. Stringing of six series connected cells (reflow-soldering of interconnector to rear cell side).

5. Reflow-soldering of positive and negative termination bars.

6. Bonding of six-cell strings to Kapton substrate.

7. Panel inspection and performance test with pulsed solar simulator.

Simple assembly fixtures were fabricated in order to accommodate the large 5 x 5 cm cells in the various assembly operations:

a. Soldering fixture - for the positioning of interconnectors above the front cell contact during reflow soldering.

b. Glassing fixture - for proper cover glass alignment with respect to the solar cell during the bonding operation.

c. Cell string assembly fixture - for cell-to-cell alignment and spacing during rear contact reflow soldering.

Existing assembly and test equipment was used throughout.

All soldering operations went without difficulty, however, the cover-to-cell and cell-to-substrate bonding operations posed some problems that require further study and development. The main reason for these bonding problems encountered in comparison to the 2 x 4 cm cells now processed without difficulty is the increase in cell size and the cell shape. For example, a 2 x 2 cm cell is glassed and bonded with a single adhesive dot. A 2 x 4 cm cell is glassed with two adhesive dots. When glassing the 5 x 5 cm cell, several experiments were conducted using a) one large adhesive dot which was found to be impractical because the adhesive does not flow into the cell edges in time, b) four adhesive dots equally spaced, produced one large bubble in the center of the cell, c) six adhesive dots, two in the center of the cell and four dots in each cell corner. This was an improvement but still produces periodic bubbles and voids in the cell corners. d) The final method of adhesive application was accomplished by dispensing one dot of adhesive (170 mg of DC 93-500) onto the center of the cell and then manually raking some portion of that adhesive into the four cell corners. This method was further improved by placing a weight, slightly smaller than the cell stack, on top of the cover glass in order to speed up the adhesive spreading between cell and cover glass. This weight was removed when the adhesive had almost reached the cell edges. The adhesive bond line thickness ranged from 0.001 to 0.003 inch.

Similar problems were encountered as the six-cell module strings were bonded to the Kapton substrate. The adhesive dot pattern used here consisted of six dots, two dots in the center of the cell and four dots in each corner. As stated earlier, the bonding methods do require further development. The modules were assembled by one operator, who is experienced with the assembly of conventional solar cell assemblies where cell thicknesses of 0.003, 0.008 inch and thicker have been involved. All assembly steps were submitted to the operator in writing prior to assembly. The resulting usable device yield for the cells processed was about 90%.

```
Cell used (two test panels)        72
Glassed cells broken                9
```

The front and rear view of one of the completed modules is shown in Figures 2 and 3.

A-4 INSPECTION AND TEST

A visual inspection was performed on both panels after assembly. The performance measurements of the two modules were obtained with the Large Area Pulsed Solar Simulator, (LAPSS) at one sun, AMO intensity, 28°C. The results are shown in Tables 1 and 2. The cells were not matched by performance prior to cell string assembly.

A-5 COMPONENT WEIGHT/THICKNESS

Prior to and after cell stack assembly, the individual component weight of 20 units were measured and recorded, along w,th the cell, cover and cell stack thickness. The cell thickness specified in the Purchase Order was 0.008 ± 0.002 inch. However, the actual cell thickness measurement revealed an average thickness of 0.012 inch, representing the thinnest cells of that size available at this time.

The component weight and thickness is summarized in Table 3. The final cover glass-to-cell adhesive weight was 151 mg based on the average results presented.

A-6 TEST SETUP

The apparatus used in this test consisted of an aluminum frame, air cycling chamber, strip chart recorder, automatic temperature control equipment, and the large Area Pulsed Solar Simulator (LAPSS). The test panel was mounted on the frame using springs as shown in Figure 1. Thermocouple and instrumentation wires were connected and the test panel was then placed in the air chamber as shown in Figure 1. The air chamber was cooled with LN_2 until a temperature of -80°C was reached. The cycle was then automatically reversed using electrically-heated forced convection

of GN_2 until a temperature o- +60°C was reached with the cycle time being set for approximately 17 minutes. Once a week (approximately every 500 cycles) the instrumentation wires were disconnected and the test panel removed from the chamber and visually inspected for defects. The test panel was then illuminated with the LAPSS and the test sequence was repeated. The appearance of the panel did not change as a result of the test.

A-7 TEST PROCEDURE

1. Each of the six strings of the 36-cell panel was given a 10-point I-V curve on the Large Area Pulsed Solar Simulator and then mounted in the air cycli g chamber and subjected to 500 temperature cycles per week betweer -80°C and +60°C.

2. The panel was removed from the chamber and illuminated after 100, 400, 1600, 2200, 2855, and 3275 cycles, and data was recorded.

3. The recorded data from the LAPSS was averaged for the six strings on the test panel in terms of power, voltage, and current. Results are summarized in Table 4. Plots of these parameters as a function of thermal cycles are presented in Figures 4 through 6.

4. The panel was thoroughly inspected each time and any damage was recorded on a standard form. Copies of these inspection records are presented in Figures 7 through 11.

A-8 DISCUSSION OF TEST DATA

After 1600 cycles of thermal cycling and after the power output measurements, the standard reference cell was accidentally dropped and broken. This required a new standard cell to be used for subsequent illumination tests. The maximum power data after 2200 cycles is lower by about 90 milliwatts from the previous tests and is attributed to a calibration difference in the new cell.

A-5

Upon being visually inspected after each cycling test, cracked cover
glasses were noted after 100. 400 and 1600 thermal cycles. No additional
defects occurred through the completion of the test.

CONCLUSIONS

1. A sudden decrease of 3% in current at 2200 cycles was observed and
    has been attributed to the change in standard cell. All data taken
    with the old and the new standard cells were within $\pm$ 0.5% of the
    initial measurement. Therefore, it is concluded that no electrical
    degradation resulted from environmental exposure up to 3275 cycles.

2. Three solar cell cover cracks were observed in the first 1600 cycles
    but they did not affect solar panel performance.

3. For the range of temperature and number of thermal cycles tested,
    there appears to be an acceptable compatibility between the 50 x 50 x
    0.25 mm solar cells and the flexible, ribbed, Kapton substrate.

TABLE 1. Panel Current-Voltage Characteristic at 1 Sun Intensity, AM=0 ,28°C
Panel S/N 1, measured after fabrication

PANEL SERIAL/STRING # S/N-1- A
STD CELL S/N FSC-OC-212
ISC 0.2655 AMP
TEMP 22.9C
TEMP COEF 0.4283 %/DEG C

10/16/79

VOLTS	AMPS	WATTS	STD AMP
3.518	0.0005	0.0018	0.2654
3.163	0.7302	2.310	0.2658
3.092	0.7941	2.455	0.2655
3.017	0.8436	2.545	0.2652
2.910	0.8877	2.583	0.2663
2.804	0.9132	2.561	0.2652
2.552	0.9378	2.393	0.2660
2.194	0.9506	2.086	0.2662
1.799	0.9553	1.719	0.2673
0.3644	0.9592	0.3495	0.2657

PANEL SERIAL/STRING # S/N-1- B
STD CELL S/N FSC-OC-212
ISC 0.2655 AMP
TEMP 23.0C
TEMP COEF 0.4283 %/DEG C

VOLTS	AMPS	WATTS	STD AM
3.520	0.0005	0.0018	0.2669
3.165	0.7399	2.342	0.2653
3.092	0.7957	2.460	0.2654
3.019	0.8353	2.522	0.2660
2.910	0.8709	2.534	0.2655
2.803	0.8893	2.493	0.2659
2.552	0.9072	2.315	0.2661
2.193	0.9166	2.010	0.2658
1.800	0.9208	1.657	0.2658
0.3779	.9226	0.3487	0.2653

PANEL SERIAL/STRING # S/N-1- C
STD CELL S/N FSC-OC-212
ISC 0.2655 AMP
TEMP 23.0C
TEMP COEF 0.4283 %/DEG C

VOLTS	AMPS	WATTS	STD AMP
3.527	0.0004	0.0014	0.2655
3.171	0.7391	2.344	0.2659
3.101	0.7990	2.478	0.2659
3.024	0.8459	2.558	0.2652
2.918	0.8851	2.583	0.2666
2.810	0.9043	2.541	0.2655
2.559	0.9161	2.344	0.2659
2.199	0.9187	2.020	0.2661
1.803	0.9194	1.658	0.2649
0.3756	0.9207	0.3458	0.2645

PANEL SERIAL/STRING # S/N-1- D
STD CELL S/N FSC-OC-212
ISC 0.2655 AMP
TEMP 23.1C
TEMP COEF 0.4283 %/DEG C

VOLTS	AMPS	WATTS	STD AMP
3.526	0.0006	0.0021	0.2648
3.176	0.7265	2.307	0.2652
3.106	0.7912	2.457	0.2653
3.029	0.8417	2.550	0.2656
2.923	0.8843	2.585	0.2655
2.814	0.9066	2.551	0.2653
2.563	0.9186	2.354	0.2650
2.201	0.9203	2.026	0.2655
1.805	0.9213	1.663	0.2650
0.3804	0.9231	0.3511	0.2659

PANEL SERIAL/STRING # S/N-1- E
STD CELL S/N FSC-OC-212
ISC 0.2655 AMP
TEMP 23.1C
TEMP COEF 0.4283 %/DEG C

VOLTS	AMPS	WATTS	STD AMP
3.527	0.0005	0.0018	0.2652
3.173	0.7299	2.316	0.2659
3.101	0.7937	2.461	0.2646
3.028	0.8423	2.550	0.2654
2.918	0.8850	2.582	0.2661
2.811	0.9063	2.548	0.2652
2.559	0.9178	2.349	0.2665
2.199	0.9199	2.023	0.2660
1.804	0.9202	1.660	0.2653
0.3684	0.9223	0.3398	0.2657

PANEL SERIAL/STRING # S/N-1- F
STD CELL S/N FSC-OC-212
ISC 0.2655 AMP
TEMP 23.1C
TEMP COEF 0.4283 %/DEG C

VOLTS	AMPS	WATTS	STD AMP
3.527	0.0005	0.0018	0.2654
3.170	0.7358	2.332	0.2657
3.102	0.7922	2.457	0.2658
3.025	0.8428	2.549	0.2655
2.919	0.8816	2.573	0.2655
2.811	0.9013	2.534	0.2648
2.561	0.9146	2.342	0.2659
2.199	0.9178	2.018	0.2649
1.805	0.9182	1.657	0.2656
0.3589	0.9195	0.3300	0.2650

TABLE 2. Panel Current-Voltage Characteristic at 1 Sun Intensity, AM=0 ,28°
Panel S/N 2, measured after fabrication

PANEL SERIAL/STRING # S/N-2- A
STD CELL S/N FSC-OC-212
  ISC 0.2655 AMP
TEMP 23.1C
TEMP COEF 0.4283 %/DEG C

10/14/79

VOLTS	AMPS	WATTS	STD AMP
3.524	0.0006	0.0021	0.2660
3.175	0.7333	2.328	0.2648
3.105	0.7971	2.475	0.2658
3.030	0.8461	2.564	0.2660
2.921	0.8880	2.594	0.2662
2.813	0.9075	2.553	0.2656
2.563	0.9210	2.361	0.2658
2.200	0.9237	2.032	0.2663
1.805	0.9242	1.668	0.2652
0.3620	0.9263	0.3353	0.2661

PANEL SERIAL/STRING # S/N-2- B
STD CELL S/N FSC-OC-212
  ISC 0.2655 AMP
TEMP 23.1C
TEMP COEF 0.4283 %/DEG C

VOLTS	AMPS	WATTS	STD AMP
3.519	0.0005	0.0018	0.2652
3.163	0.7445	2.355	0.2659
3.093	0.8002	2.475	0.2652
3.016	0.8427	2.542	0.2666
2.911	0.8788	2.558	0.2655
2.804	0.8997	2.523	0.2656
2.552	0.9202	2.348	0.2658
2.193	0.9276	2.034	0.2649
1.800	0.9305	1.675	0.2655
0.3806	0.9313	0.3545	0.2649

PANEL SERIAL/STRING # S/N-2- C
STD CELL S/N FSC-OC-212
  ISC 0.2655 AMP
TEMP 23.1C
TEMP COEF 0.4283 %/DEG C

VOLTS	AMPS	WATTS	STD AMP
3.525	0.0004	0.0014	0.2655
3.170	0.7214	2.287	0.2666
3.101	0.7813	2.423	0.2664
3.025	0.8364	2.530	0.2662
2.918	0.8801	2.568	0.2655
2.811	0.9044	2.542	0.2662
2.561	0.9231	2.364	0.2659
2.199	0.9290	2.043	0.2661
1.805	0.9291	1.677	0.2660
0.4277	0.9317	0.3985	0.2660

PANEL SERIAL/STRING # S/N-2-D
STD CELL S/N FSC-OC-212
  ISC 0.2655 AMP
TEMP 23.1C
TEMP COEF 0.4283 %/DEG C

VOLTS	AMPS	WATTS	STD AMP
3.512	0.0005	0.0018	0.2647
3.164	0.7332	2.320	0.2654
3.093	0.7904	2.445	0.2657
3.016	0.8472	2.555	0.2651
2.910	0.8891	2.587	0.2662
2.804	0.9122	2.558	0.2653
2.552	0.9289	2.371	0.2656
2.192	0.9315	2.042	0.2658
1.799	0.9316	1.676	0.2658
0.4190	0.9339	0.3913	0.2655

PANEL SERIAL/STRING # S/N-2- E
STD CELL S/N FSC-OC-212
  ISC 0.2655 AMP
TEMP 23.0C
TEMP COEF 0.4283 %/DEG C

VOLTS	AMPS	WATTS	STD AMP
3.521	0.0004	0.0014	0.2647
3.165	0.7205	2.280	0.2651
3.093	0.7799	2.412	0.2649
3.018	0.8399	2.535	0.2643
2.913	0.8809	2.566	0.2648
2.803	0.9028	2.531	0.2657
2.554	0.9176	2.344	0.2644
2.191	0.9212	2.018	0.2648
1.798	0.9219	1.658	0.2650
0.3901	0.9223	0.3600	0.2641

PANEL SERIAL/STRING # S/N-2- F
STD CELL S/N FSC-OC-212
  ISC 0.2655 AMP
TEMP 23.1C
TEMP COEF 0.4283 %/DEG C

VOLTS	AMPS	WATTS	STD AMP
3.518	0.0004	0.0014	0.2644
3.163	0.7090	2.243	0.2639
3.094	0.7610	2.355	0.2641
3.016	0.8253	2.489	0.2651
2.911	0.8672	2.524	0.2646
2.803	0.8903	2.496	0.2654
2.553	0.9099	2.323	0.2642
2.193	0.9152	2.007	0.2652
1.800	0.9158	1.648	0.2647
0.3766	0.9178	0.3456	0.2642

TABLE 3, COMPONENT WEIGHT & THICKNESS SUMMARY

(CELL & COVERGLASS SIZE: 5×5 CM)

CELL NO.	WEIGHT (Gms)			COMPONENT THICKNESS (INCH)		
	BARE CELL	COVER GLASS	* CELL STACK	SOLAR CELL	COVER GLASS	CELL STACK
1	1.8500	0.9255	2.9523	0.011	0.006	0.019
2	1.9575	0.9185	3.0905	0.012	0.006	0.021
3	2.0100	0.8940	3.2300	0.013	0.006	0.020
4	1.8960	0.9191	2.9985	0.012	0.006	0.021
5	1.9121	0.9440	3.0385	0.012	0.006	0.019
6	1.9860	0.9545	3.1190	0.012	0.006	0.019
8	1.9288	0.9590	3.1560	0.012	0.006	0.020
11	2.0062	0.9600	3.1155	0.012	0.006	0.019
12	1.8904	1.0875	3.1510	0.012	0.007	0.020
13	1.9255	0.9400	3.0290	0.011	0.006	0.019
14	1.9846	1.1000	3.2890	0.012	0.007	0.020
16	1.9775	0.9930	3.1230	0.012	0.006	0.019
18	1.9455	0.9405	3.0490	0.012	0.006	0.019
19	1.8130	0.9200	2.9365	0.012	0.006	0.019
20	1.9600	0.9910	3.1400	0.012	0.006	0.020
AVG.	1.9362	0.9631	3.0945	0.012	0.006	0.0196

* The cell stack weight includes the weight of three interconnectors (0.044 g)

A-9

TABLE 4.

Summary of Test Results

DATE	THERMAL CYCLES	$\overline{PMP}$	PMP +2σ (watts)	PMP -2σ	$\overline{VOC}$	+2σ (volts)	-2σ	$\overline{ISC}$	+2σ (amps)	-2σ
10/16	INITIAL	2.573	2.583	2.534	3.524	3.527	3.518	.9279	.9592	.9195
10/17	0	2.566	2.580	2.521	3.515	3.519	3.508	.9275	.9589	.9185
10/18	100	2.574	2.588	2.529	3.523	3.527	3.514	.9280	.9555	.9207
10/22	400	2.589	2.603	2.550	3.530	3.535	3.518	.9298	.9562	.9231
11/5	1600	2.580	2.603	2.542	3.525	3.530	3.516	.9303	.9593	.9217
11/12	2200	2.488	2.502	2.454	3.525	3.530	3.516	.8974	.9238	.8910
11/19	2855	2.491	2.504	2.458	3.519	3.526	3.508	.8990	.9271	.8900
11/28	3275	2.484	2.496	2.453	3.516	3.520	3.505	.8981	.9219	.8905

Figure 1. Test Panel in Thermal Cycling Chamber

TRW PHOTO NO. 157293-79-7
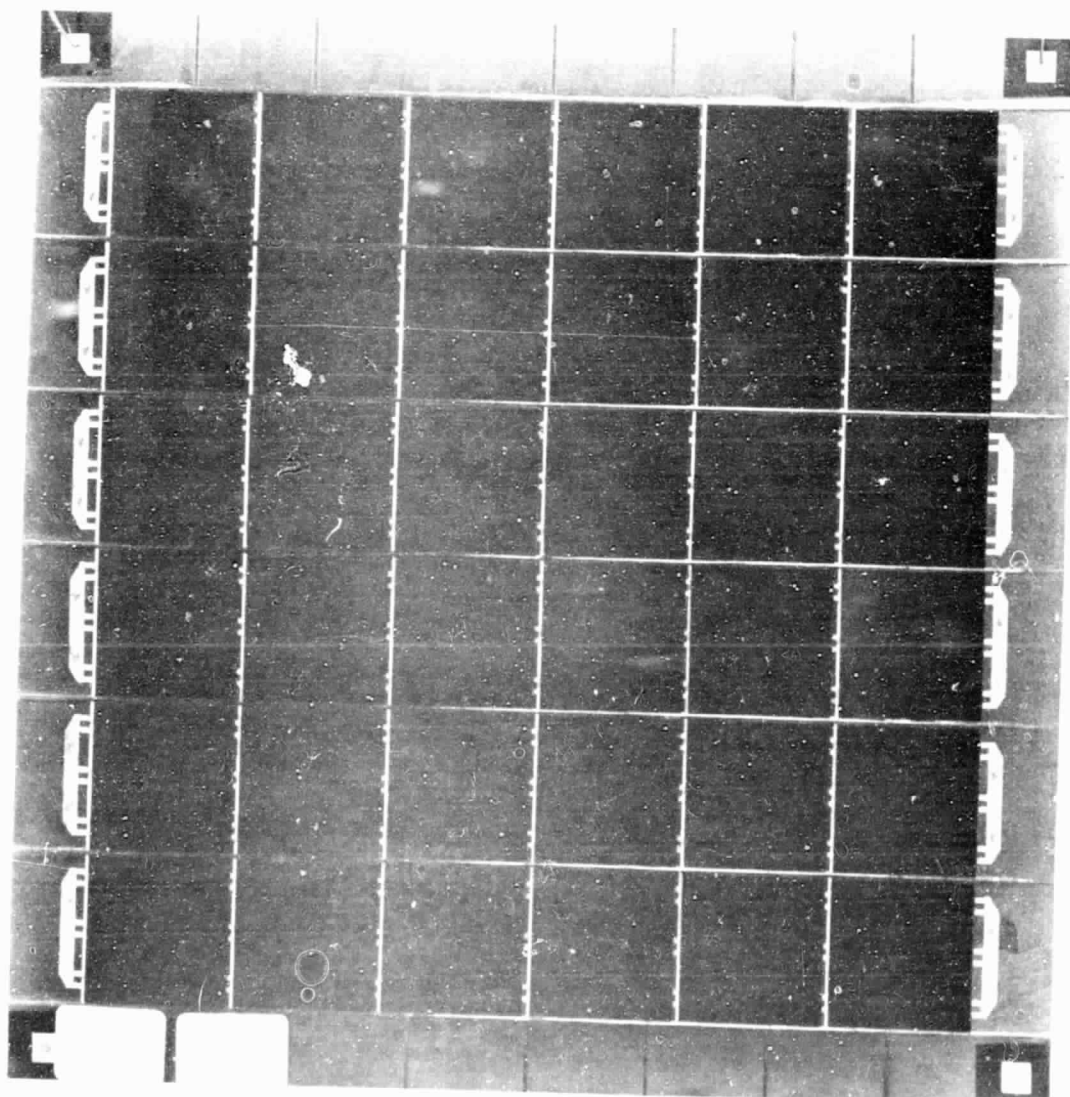
TRW PHOTO NO. 157293-79-1

Figure 2. Solar Cell Side of Test Panel
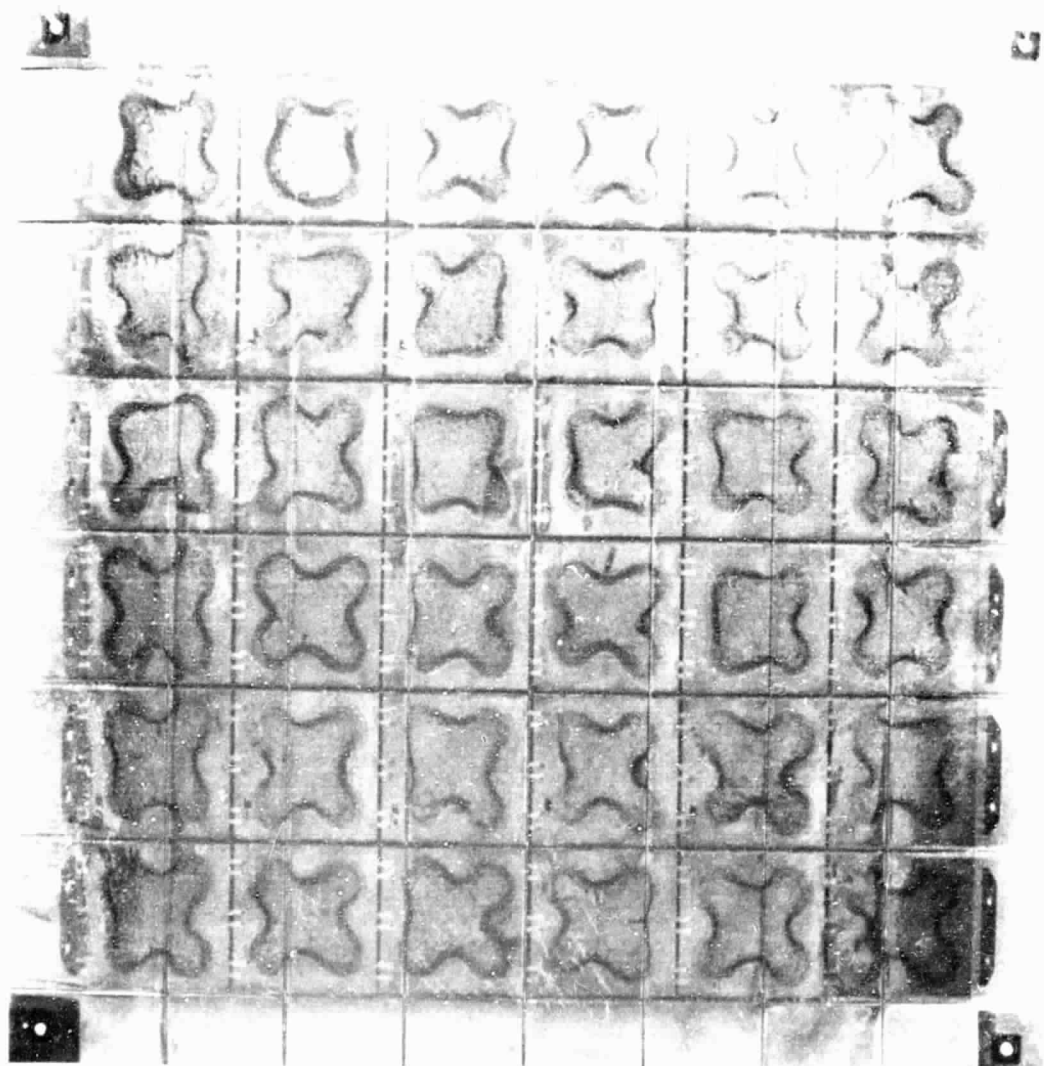
TRW PHOTO NO 157293-79-4

Figure 3   Back Side of Test Panel
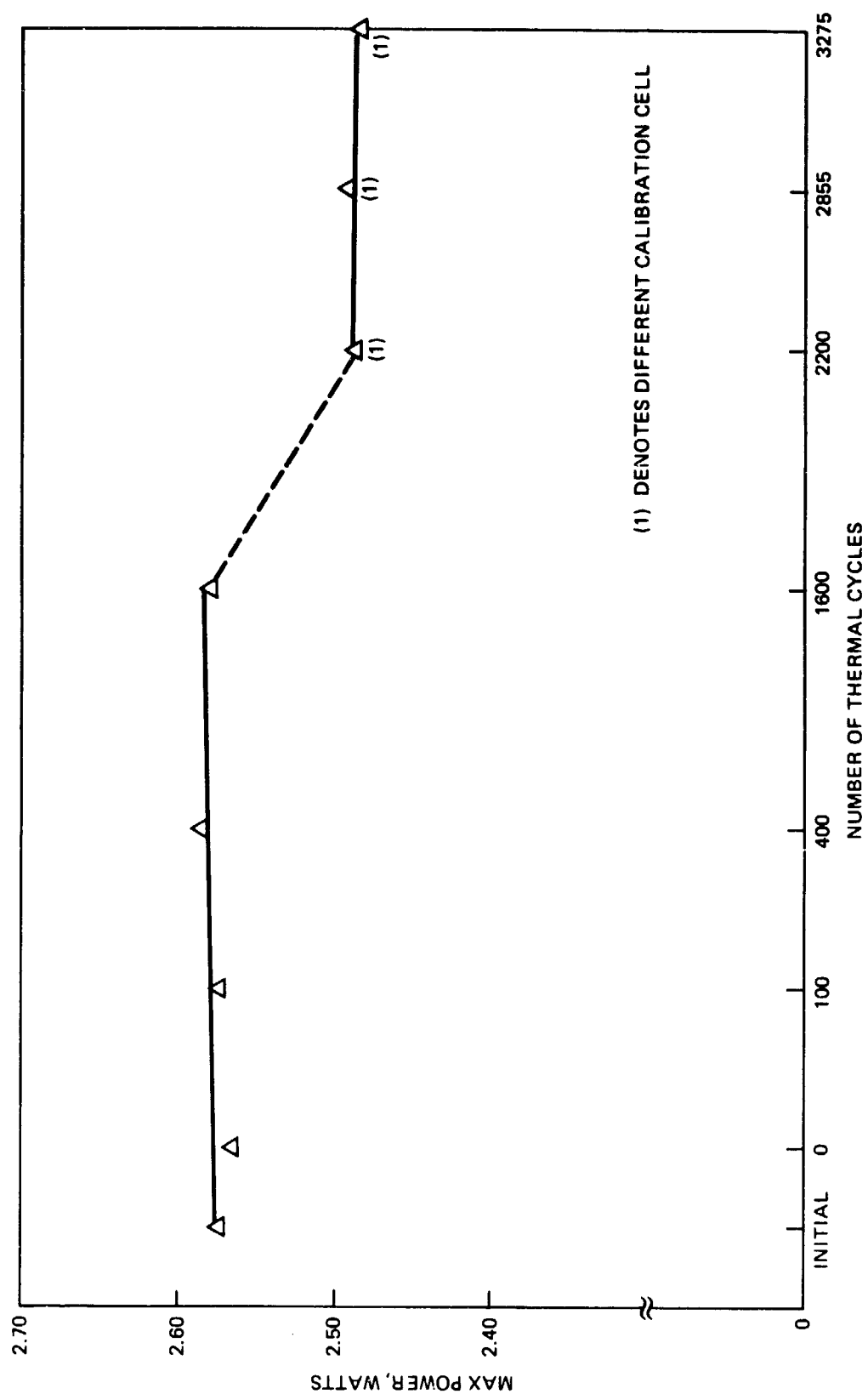
Figure 4. Power Output versus Number of Thermal Cycles

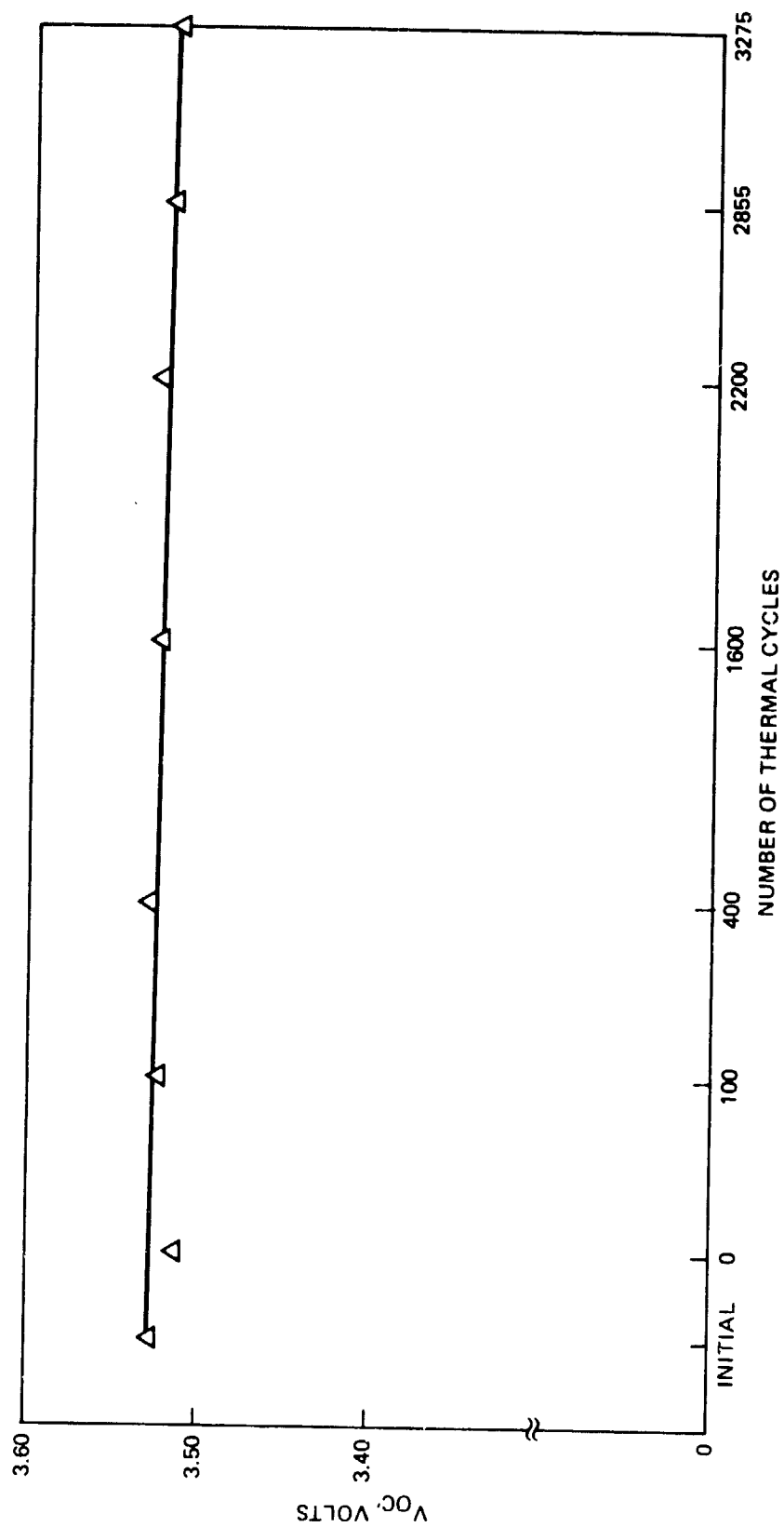(1) DENOTES DIFFERENT CALIBRATION CELL

NUMBER OF THERMAL CYCLES

MAX POWER, WATTS

A-14

Figure 5. Voltage versus Number of Thermal Cycles
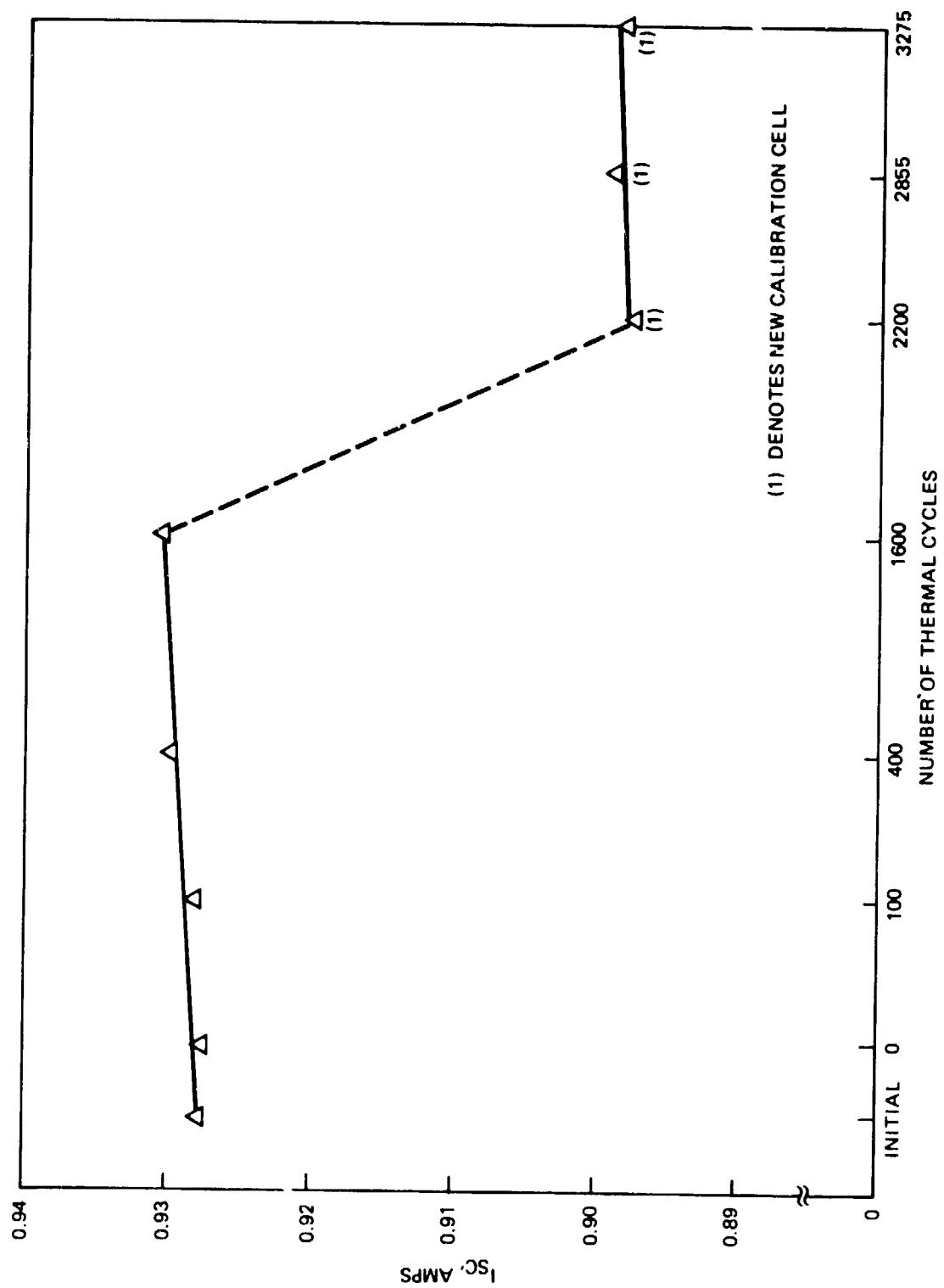
Figure 6. Current versus Number of Thermal Cycles
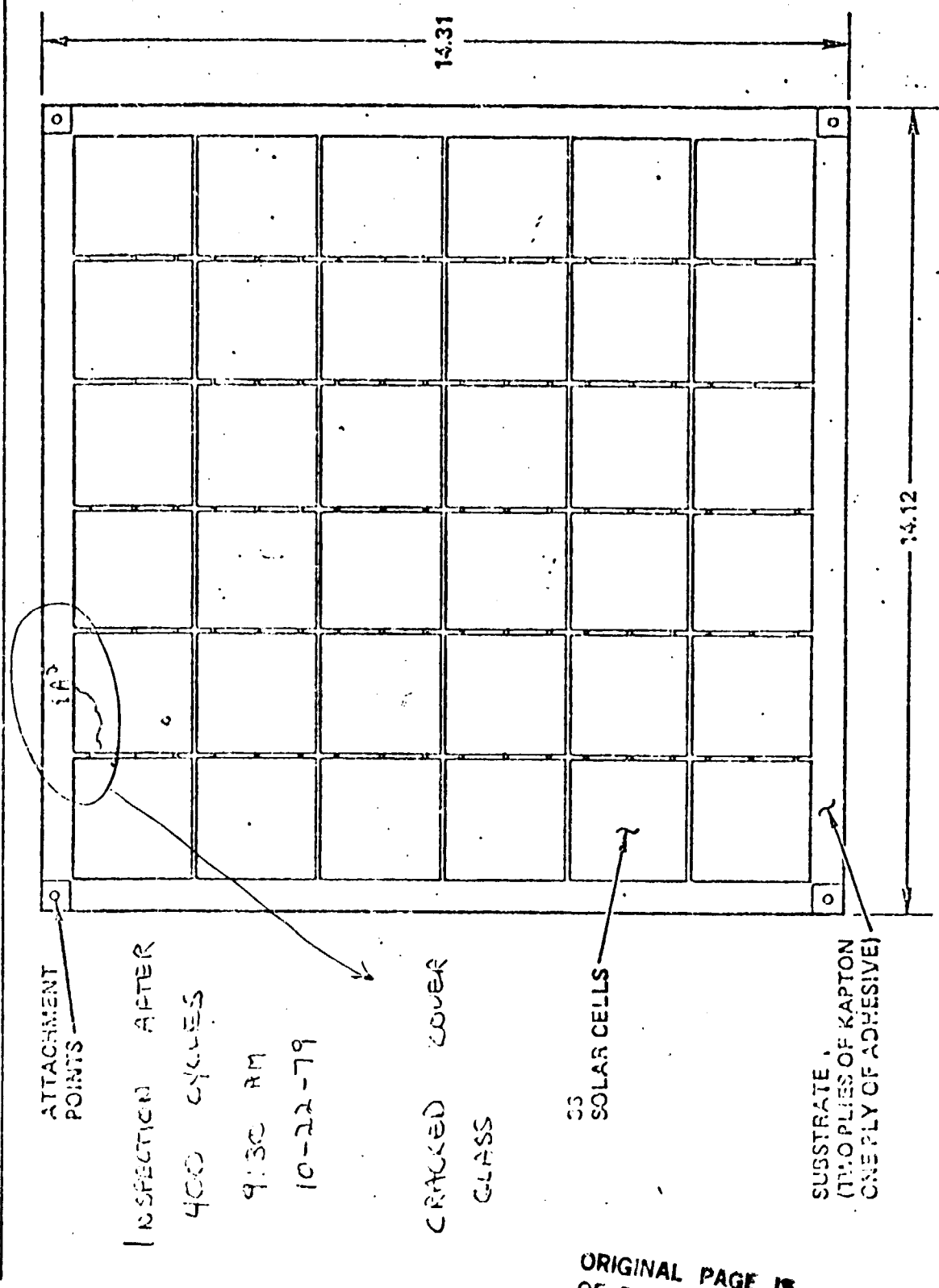
A-16

FIGURE 7. INSPECTION RECORD AT 100 CYCLES
5.0 x 5.0 CM SOLAR CELL
SAMPLE TEST
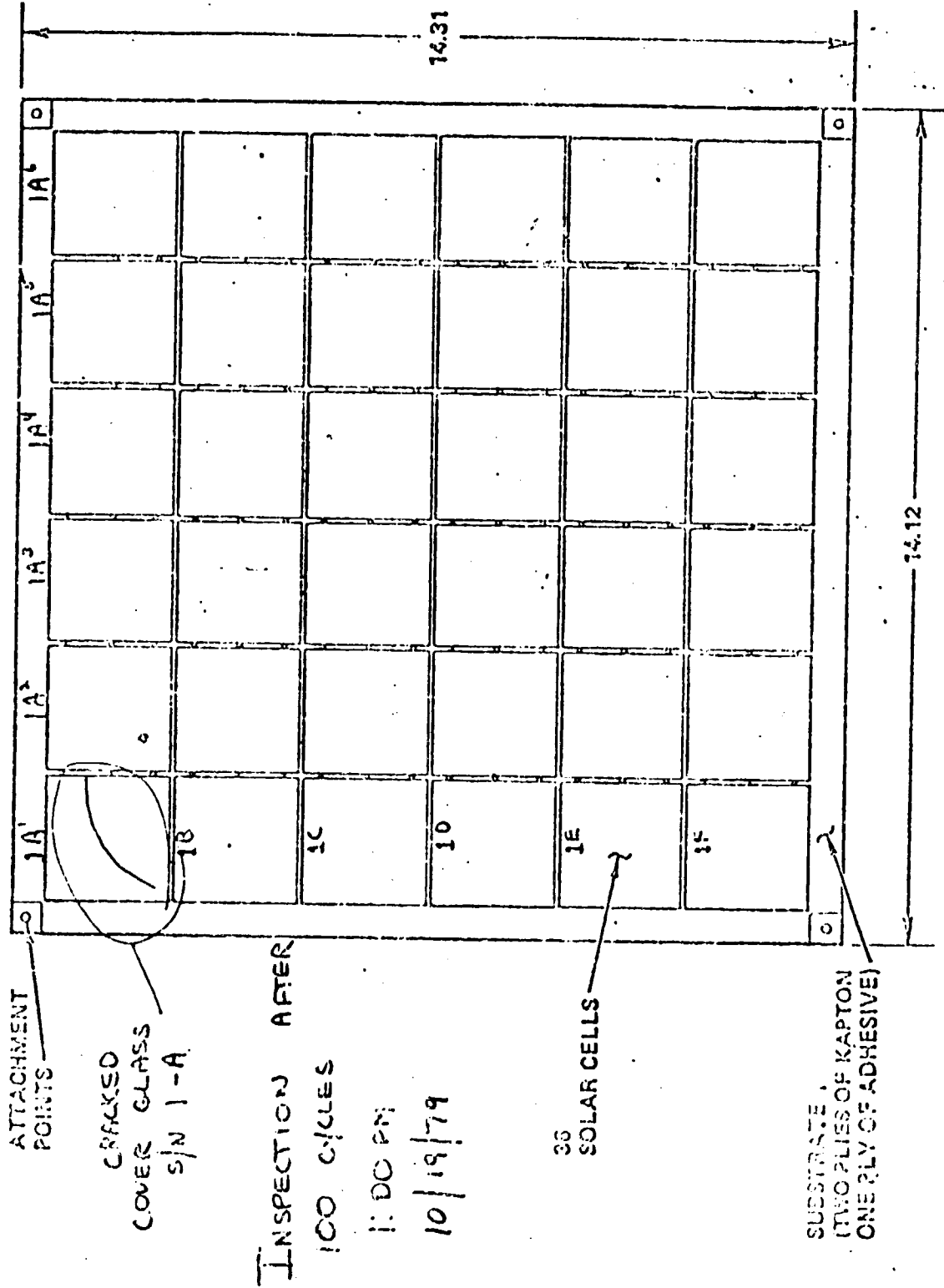
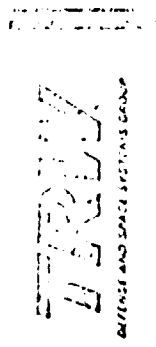FIGURE 8. INSPECTION RECORD AT 400 CYCLES
5.0 x 5.0 CM SOLAR CELL
SAMPLE TEST

TRW
DEFENSE AND SPACE SYSTEMS GROUP

ATTACHMENT POINTS

INSPECTION AFTER
400 CYCLES
9:30 AM
10-22-79

CRACKED COVER
GLASS

33
SOLAR CELLS

SUBSTRATE
(TWO PLIES OF KAPTON
ONE PLY OF ADHESIVE)

14.31

14.12

FIGURE 9. INSPECTION RECORD AT 1600 CYCLES
5.0 x 5.0 CM SOLAR CELL
SAMPLE TEST

TRW
DEFENSE AND SPACE SYSTEMS GROUP

ATTACHMENT POINTS

INSPECTION AFTER
1600 CYCLES

9:30 AM
11/5/79

CRACKED COVER
GLASS
S/N 1F4

36
SOLAR CELLS

SUBSTRATE:
(TWO PLIES OF KAPTON
ONE PLY OF ADHESIVE)

14.31

14.12
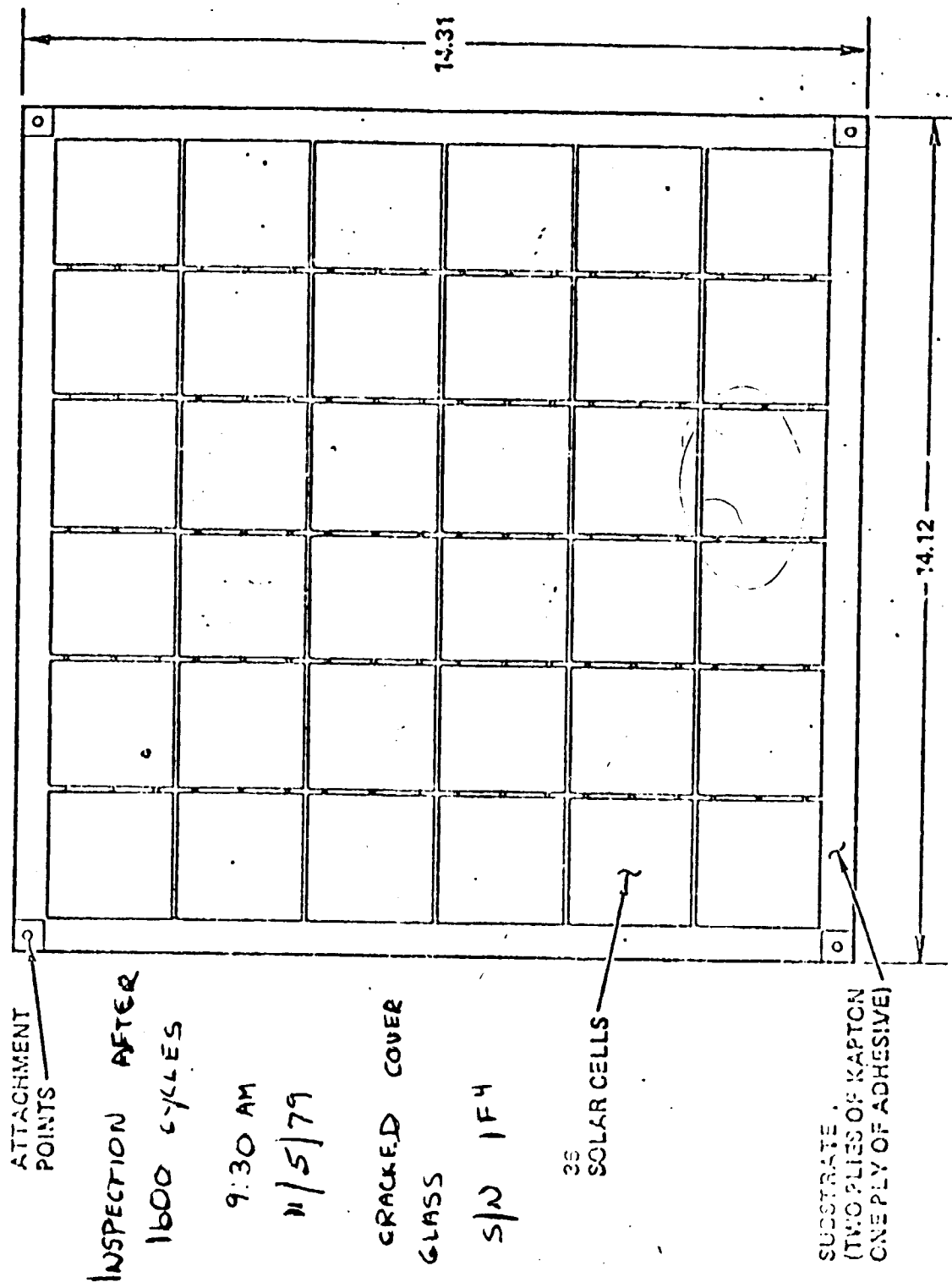
FIGURE 10. INSPECTION RECORD AT 2200 CYCLES
5.0 x 5.0 CM SOLAR CELL
SAMPLE TEST
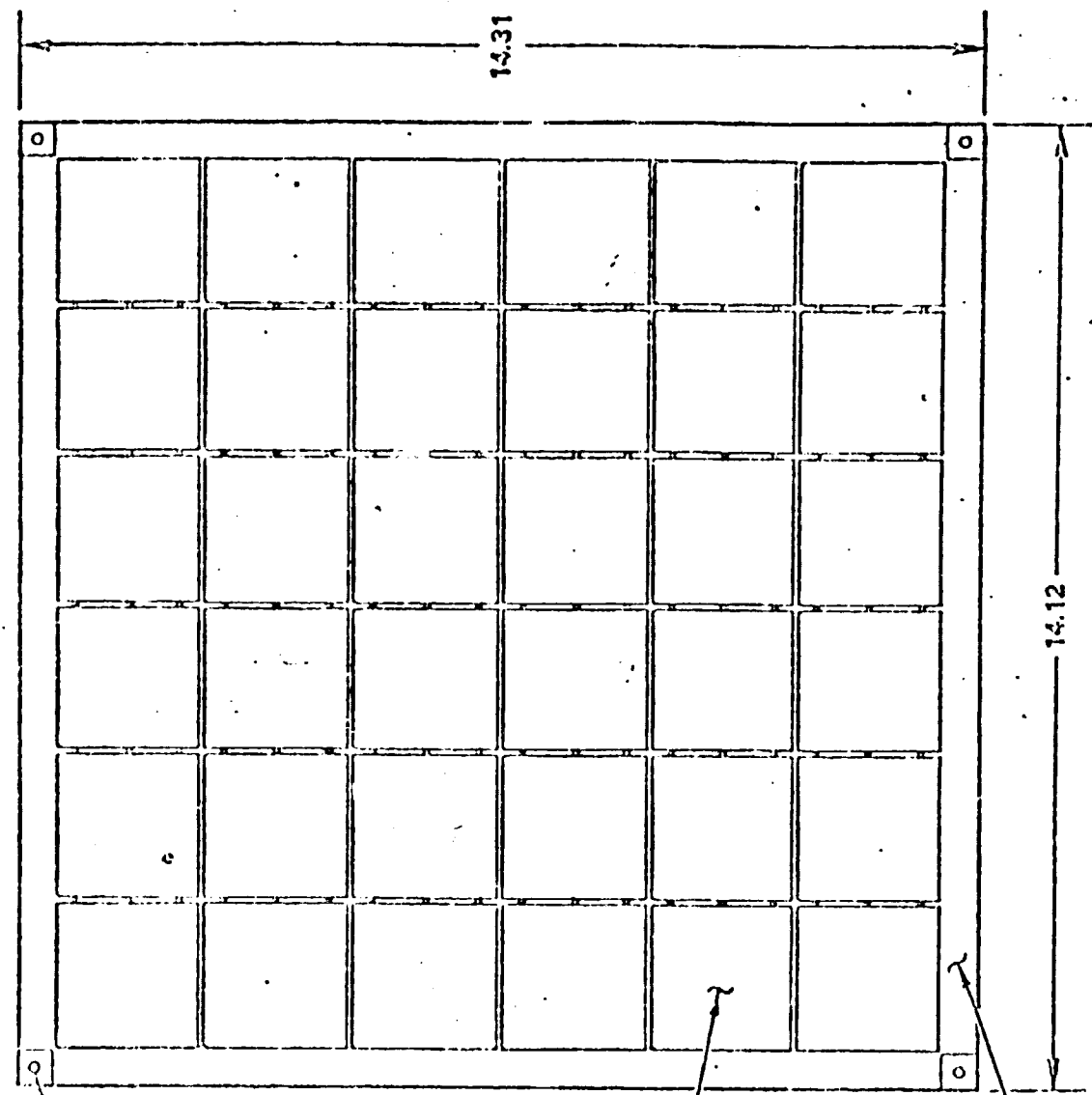
FIGURE 11. INSPECTION RECORD AT 2855 CYCLES
5.0 x 5.0 CM SOLAR CELL
SAMPLE TEST

TRW
DEFENSE AND SPACE SYSTEMS GROUP
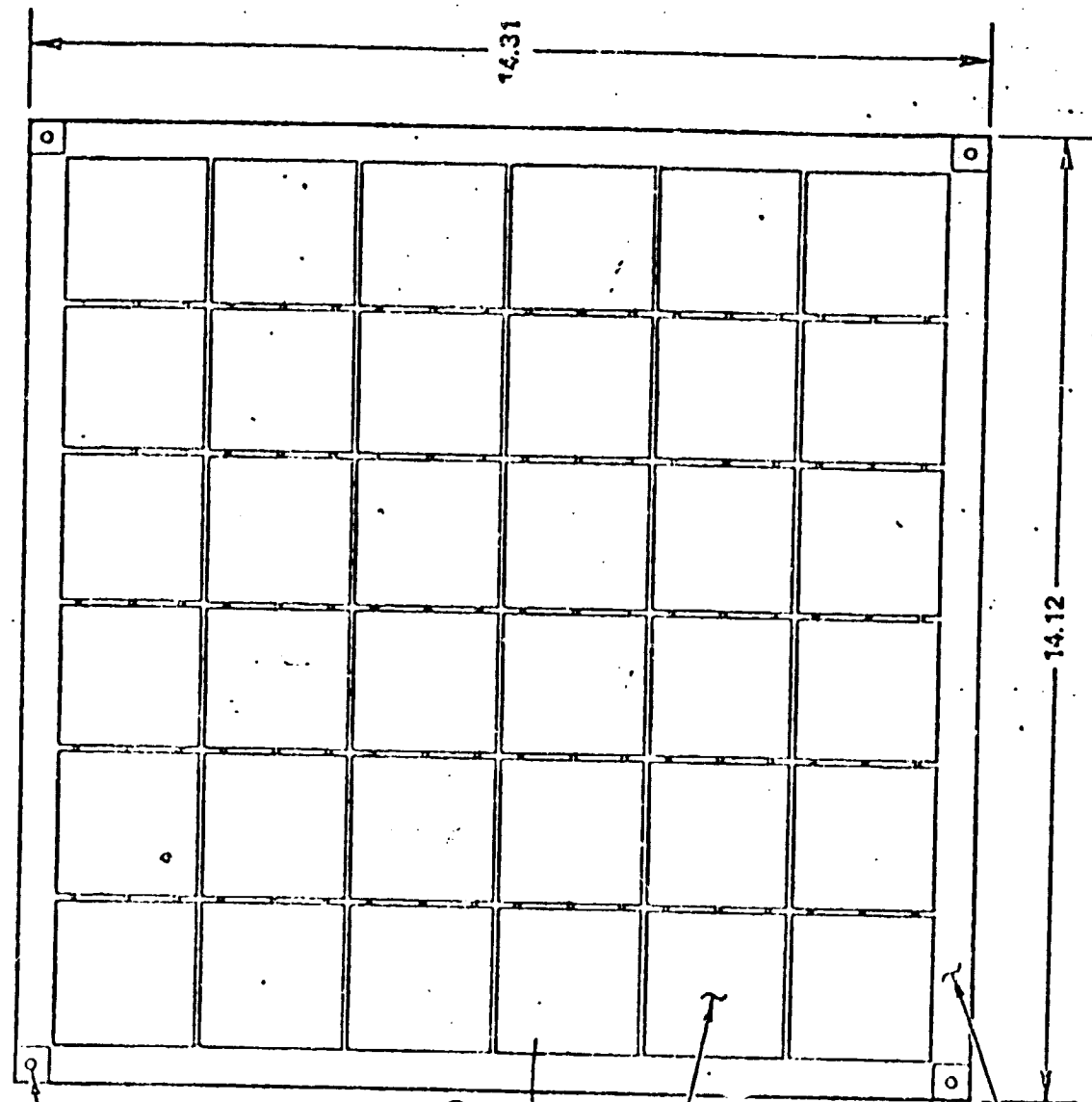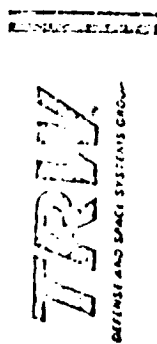
ATTACHMENT POINTS

INSPECTION AFTER
2855 CYCLES
9:30 AM
11-19-79

No ADDITIONAL
DEFECTS NOTICED

3275 CYCLES
10:30 AM
36
SOLAR CELLS
11-29-79

NO ADDITIONAL
DEFECTS NOTICED

SUBSTRATE
(TWO PLIES OF KAPTON
ONE PLY OF ADHESIVE)

14.31

14.12

A-21